Catalysts design for higher alcohols synthesis by CO2 hydrogenation: Trends and future perspectives

Zeng, Feng; Mebrahtu, Chalachew; Xi, Xiaoying; Liao, Longfei; Ren, Jie; Xie, Jingxiu; Heeres, Hero Jan; Palkovits, Regina

Published in:
Applied Catalysis B: Environmental

DOI:
10.1016/j.apcatb.2021.120073

Publication date:
2021

Applied Catalysis B: Environmental 291 (2021) 120073

Contents lists available at ScienceDirect

Applied Catalysis B: Environmental

journal homepage: www.elsevier.com/locate/apcatb

Review

Catalysts design for higher alcohols synthesis by CO_2 hydrogenation: Trends and future perspectives

Feng Zeng [a,1], Chalachew Mebrahtu [a,1], Xiaoying Xi [b], Longfei Liao [a], Jie Ren [a], Jingxiu Xie [b], Hero Jan Heeres [b,*], Regina Palkovits [a,*]

[a] Chair of Heterogeneous Catalysis and Chemical Technology, ITMC, RWTH Aachen University, Worringerweg 2, 52074, Aachen, Germany
[b] Green Chemical Reaction Engineering, Engineering and Technology Institute Groningen, University of Groningen, Nijenborgh 4, 9747 AG, Groningen, The Netherlands

ARTICLE INFO

Keywords:
Carbon dioxide
Higher alcohol
Catalyst design
Reaction condition
Reaction mechanism

ABSTRACT

Global warming due to the accumulation of atmospheric CO_2 has received great attention in recent years. Hence, it is urgent to reduce CO_2 emissions into the atmosphere and develop sustainable technologies for a circular carbon economy. In this regard, CO_2 capture coupled with the conversion into chemicals and fuels provides a promising solution to reduce CO_2 emissions as well as to store and utilize renewable energy. Among the many possible CO_2 conversion pathways, CO_2 hydrogenation to higher alcohols is considered an important strategy for the synthesis of carbon-based fuels and feedstock and holds great promise for the chemical industry. Thus, this review provides an overview of advances in CO_2 hydrogenation to higher alcohols that have been achieved recently in terms of catalyst design, catalytic performance, and insight into the reaction mechanism under different experimental conditions. First, the limitations provided by reaction thermodynamics and the indispensability of catalysts for CO_2 hydrogenation to higher alcohols are discussed. Then, four main categories of catalysts will be introduced and discussed (*i.e.* Rh-, Cu-, Mo-, and Co-based catalysts). Moreover, important factors significantly influencing the efficiency of the catalytic transformation such as alkali/alkaline earth metal promoters, transition metal promoters, catalyst supports, catalyst precursors, and reaction conditions, as well as the reaction mechanism are explained. Finally, the review discusses emerging methodologies yet to be explored and future directions to achieve a high efficiency for the hydrogenation of CO_2 to higher alcohols.

1. Introduction

Every day, huge amounts of greenhouse gases (GHG) are emitted and accumulate in the atmosphere which in turn causes global warming. Notably, carbon dioxide (CO_2) contributes to 72 % of the GHG emissions, mainly due to the combustion of large amounts of fossil resources, and its emission keeps rising in recent years (Fig. 1) [1,2]. Therefore, CO_2 fixation has attracted broad interest, and intensive efforts have been dedicated to develop various technologies for CO_2 capture, sequestration, and utilization.

In this context, using CO_2 as feedstock for chemical processes has attracted great attention since it can reduce the cost and increase the profit for reducing CO_2 emissions [3]. Additionally, the use of CO_2 as a feedstock allows the introduction of overall closed carbon cycles, which is a key for the vision of a circular carbon economy. Thus, together with the generation of renewable H_2 (*i.e.* produced by water electrolysis), CO_2 capture and conversion provide a sustainable way for the synthesis of fuels and chemicals including CO, CH_4, light olefins, dimethyl ether,

Abbreviations: ASF, anderson-schultz-flory; DRIFT, diffuse reflectance infrared fourier transform spectroscopy; EXAFS, extended X-ray absorption fine structure; FFT, fast fourier transform; FTIR, fourier transform infrared spectroscopy; FTS, Fischer-Tropsch synthesis; GHG, greenhouse gas; GHSV, gas hourly space velocity; $\Delta G_{298\ K}$, standard gibbs free energy change; HAADF-STEM, high-angle annular dark-field scanning transmission electron microscopy; HAS, higher alcohols synthesis; HR, high resolution; $\Delta H_{298\ K}$, standard enthalpy change; IR, infrared spectroscopy; $K_{298\ K}$, standard equilibrium constant; MS, methanol synthesis; RWGS, reverse water gas shift; SEM, scanning electron microscopy; SMSI, strong metal-support interaction; STY, space time yield; TEM, transmission electron microscopy; TOF, turnover frequency; WHSV, weight hourly space velocity; XAS, X-ray absorption spectroscopy; XPS, X-ray photoelectron spectroscopy; XRD, X-ray powder diffraction.

* Corresponding authors.
E-mail addresses: h.j.heeres@rug.nl (H.J. Heeres), palkovits@itmc.rwth-aachen.de (R. Palkovits).
[1] These authors have contributed equally to this work.

https://doi.org/10.1016/j.apcatb.2021.120073
Received 23 December 2020; Received in revised form 23 February 2021; Accepted 25 February 2021
Available online 4 March 2021

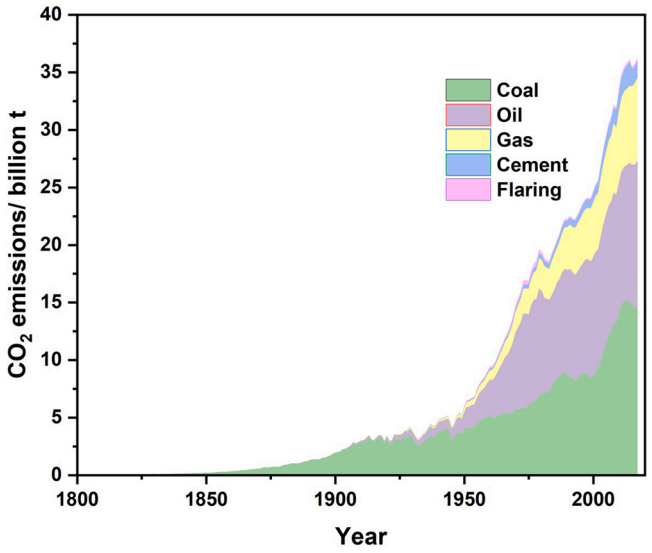

Fig. 1. Annual CO_2 emissions from different sources. Adapted from Ref. [2] licensed under Creative Commons BY.

formates/formic acid, and alcohols [3–21]. Among these chemicals, alcohols such as methanol are very prospective as they have many versatile applications and are prepared on large scale with high market demands. For instance, methanol is currently produced industrially through CO hydrogenation at a production level of 5 ktons per day [22,23]. Compared to methanol, higher alcohols (C_{2-4} alcohols) have some advantages such as higher energy density, lower vapor pressure, and lower affinity to water, and as such are considered alternatives for methanol for fuel and fuel additives [24,25]. Moreover, higher alcohols can be used as solvents for resins, fats, waxes, ethers, gums, *etc.* Besides, they can also be used as feedstock and intermediates for the production of various chemicals, pharmaceuticals, detergents, cosmetics, antiseptics, *etc* [26]. However, C_{2-4} alcohols are currently produced mainly by fertilization of corn and sugar cane, which is considered non-ethical (food *versus* fuel discussions), and the hydration of alkenes [27–31], which is typically done using fossil-based feeds.

Therefore, sustainable methods to produce higher alcohols using renewable energy and resources are of great importance. Renewable energy generation (such as solar PV and wind power) has boomed worldwide, though adaptable storage technologies are required due to the intermittent nature of renewable energy supply. Chemical energy storage could be a solution, and several possibilities have been proposed involving the use of electrochemically generated hydrogen and renewable sources like CO, CO_2, and N_2 (methanol, ammonia, *etc*). An alternative is a conversion of CO_2 to higher alcohols (Fig. 2). In principle, it involves three steps: (i) the generation of renewable electricity, (ii) H_2 production *via* electrochemical water conversion, and (iii) hydrogenation of CO_2 to higher alcohols using renewable H_2. Alternatively, higher alcohols can be synthesized through electrochemical reduction of CO_2; however, ethanol is the main product [32,33]. Thus, CO_2 hydrogenation through thermal catalysis which enables the synthesis of C_3-C_4 alcohols with a relatively high selectivity, remains more interesting.

The synthesis of higher alcohols from syngas has been known since the early 19th century, and several categories of catalysts such as Rh- and Mo-based, modified Fischer–Tropsch synthesis (FTS), and modified methanol synthesis (MS) catalysts have been developed. Meanwhile, the nature of the active species, the structure-performance correlation, and the reaction mechanism have been intensively studied [34]. Furthermore, several bench- to pilot-scale plants were built [35]. However, studies on the synthesis of higher alcohols from CO_2 and H_2 have received less attention, since CO_2 is chemically rather inert and a considerable amount of energy is required to drive the conversion. However, the urgency to reduce CO_2 emissions and the amounts of CO_2 in the atmosphere, the need to develop efficient strategies for the storage of renewable electricity in combination with the demand for clean fuels has vivified research activities on this reaction. Systematic studies date back to the 1980s, focusing mainly on catalyst development as well as uncovering the nature of active species and elucidating the reaction mechanism. Catalysts based on modified materials for higher alcohol synthesis (HAS) from syngas have been developed; however, the activity and selectivity are still low, and harsh reaction conditions are required. Moreover, the nature of the active species and the reaction mechanism are still not clear, leaving room for further studies.

Many reviews have been published covering catalytic systems for the hydrogenation of CO to higher alcohols as well as for the hydrogenation of CO_2 to methanol. These reviews have provided insights into CO_2 activation and higher alcohol formation [5,7,18,20,34,36–44]. Recently some review articles on hydrogenation of CO_2 to higher alcohols have been published [45,46]; however, the effects and mechanisms of different promoters, supports, and reaction conditions have not yet been systematically discussed. Therefore, in this review, we provide a comprehensive and systematic discussion of these aspects. First, we start by introducing the thermodynamics of HAS from CO_2 hydrogenation. It is worth mentioning that, under the typical HAS reaction conditions, hydrocarbons are the most thermodynamically stable products.

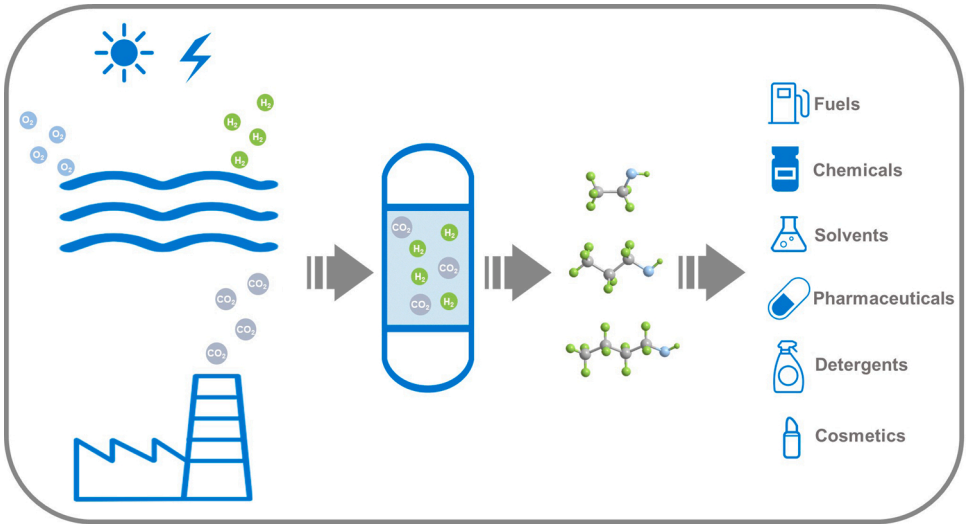

Fig. 2. Scheme for higher alcohol synthesis from renewable energy and CO_2.

Therefore, efficient catalysts are indispensable to suppress the formation of such hydrocarbons and promote alcohol formation. In literature, four types of catalysts are reported for higher alcohol synthesis by CO_2 hydrogenation, namely Rh-, Cu-, Mo-, and Co-based catalysts. Hence, in this review, along with the deep insights into the fundamentals of the reaction and providing an overview of the state of the art catalysts, structure-performance correlations, the effects of reaction parameters, and the reaction mechanisms over those types of catalytic materials will be summarized and discussed. The catalysis part of the review is structured into five sections deal with (i) Rh-based catalysts, (ii) Cu-based catalysts, (iii) Mo-based catalysts, (iv) Co-based catalysts, and (v) other groups of catalysts. Overall, we hope this review will be beneficial to those entering the HAS as well as those already on the topic for future studies on the fundamentals of the reaction and advanced catalyst's design.

2. Thermodynamics

Thermodynamics of chemical reactions provide essential information on the equilibrium conversion and selectivity as a function of reaction temperatures, (partial) pressures, and feed compositions. Table 1 summarizes the standard Gibbs free energy change ($\Delta G_{298\ K}$), the standard enthalpy change ($\Delta H_{298\ K}$), and the standard equilibrium constant ($K_{298\ K}$) of the main reactions occurring during CO_2 hydrogenation [47]. The equilibrium constants ($K_{298\ K}$) for hydrocarbon formation (Entry 3, 15, and 16) are much larger than that for CO (Entry 1), methanol (Entry 5), and ethanol (Entry 13) formation. For instance, the $K_{298\ K}$ for the methanation reaction (Entry 3) is in the order of 10^{19}, indicating that the reaction is irreversible at these conditions. When considering an equilibrium composition with CO_2, H_2, CO, H_2O, CH_4, CH_3OH, CH_3OCH_3, C_2H_5OH, CH_3COOCH_3, and CH_3CHO under typical reaction conditions (*i.e.* 300 °C, 6.0 MPa, $H_2/CO_2 = 3$), CH_4 is the major component, reaching a selectivity close to 100 %, indicating that CH_4 is the most thermodynamically stable product.

Efficient catalysts for HAS *via* CO_2 hydrogenation thus should possess a high kinetic barrier for CH_4 formation to reduce CH_4 selectivity and increase the selectivity towards alcohols. Thermodynamics studies on CO_2 hydrogenation for HAS without considering CH_4 and other hydrocarbons have been performed and provide important insights into equilibrium conversions and selectivities [48,49]. Stangeland et al. studied the thermodynamics of a CO_2 hydrogenation system containing CO_2, H_2, alcohols, CO, and H_2O under relevant conditions (*i.e.* 100−400 °C, 0.1−10 MPa, H_2/CO_2 = 1−10) [48]. CO_2 conversion and product selectivity for $C_{1-2}OH$ and $C_{1-3}OH$ are presented in Figs. 3 and 4, respectively. It was found that low temperatures favor CO_2 conversion and alcohol formation thermodynamically. CO_2 conversion and alcohol selectivity decrease with increasing temperature, because alcohols formation is an exothermic reaction as indicated by the negative $\Delta H_{298\ K}$ in Table 1, and because the reverse water gas shift (RWGS) reaction is endothermic ($\Delta H_{298\ K} = 41.1$ kJ/mol) leading to higher amounts of CO. Besides, high pressure favors alcohol synthesis because alcohol formation causes volume contraction while the RWGS is isovolumetric. When considering the alcohol equilibrium distribution, it appears that the alcohol with the highest carbon number is the major product, while methanol is hardly present. Therefore, in the absence of hydrocarbons, HAS is thermodynamically favored. Nevertheless, for efficient HAS, optimized catalysts are required to increase the kinetic barrier for hydrocarbons formation and reduce the barrier for alcohol formation and carbon chain propagation. Consequently, careful design and optimization of catalytic systems is required for the selective production of higher alcohols.

Table 1
$\Delta G_{298\ K}$, $\Delta H_{298\ K}$, and $K_{298\ K}$ of the main reactions in CO_2 hydrogenation system [47].

Entry	Reaction Equation	$\triangle G^{a}_{298\ K}$ (kJ/mol)	$\triangle H^{b}_{298\ K}$ (kJ/mol)	$K^{c}_{298\ K}$
(1)	$CO_2 + H_2 \leftrightarrow CO + H_2O$	28.6	41.1	9.67×10^{-6}
(2)	$CO + 3H_2 \leftrightarrow CH_4 + H_2O$	−141.9	−206.0	
(3)	$CO_2 + 4H_2 \leftrightarrow CH_4 + 2H_2O$	−113.5	−165.0	7.79×10^{19}
(4)	$CO + 2H_2 \leftrightarrow CH_3OH$		−90.4	
(5)	$CO_2 + 3H_2 \leftrightarrow CH_3OH + H_2O$	3.5	−49.3	2.45×10^{-1}
(6)	$2CH_3OH \leftrightarrow CH_3OCH_3 + H_2O$		−24.52	
(7)	$CH_3OCH_3 + CO \leftrightarrow CH_3COOCH_3$			
(8)	$CH_3COOCH_3 + 2H_2 \leftrightarrow C_2H_5OH + CH_3OH$			
(9)	$CH_3OH + CO + 2H_2 \leftrightarrow C_2H_5OH + H_2O$	−97.0	−165.1	
(10)	$2CH_4 + H_2O \leftrightarrow C_2H_5OH + 2H_2$			
(11)	$C_2H_5OH \rightarrow CH_3CHO + H_2 \leftrightarrow CH_4 + CO + H_2$			
(12)	$2CO + 4H_2 \leftrightarrow C_2H_5OH + H_2O$	−221.1	−253.6	
(13)	$2CO_2 + 6H_2 \leftrightarrow C_2H_5OH + 3H_2O$	−32.4	−86.7	4.70×10^{5}
(14)	$C_2H_5OH + H_2O \leftrightarrow CH_3COOH + 2H_2$			
(15)	$2CO_2 + 7H_2 \leftrightarrow C_2H_6 + 4H_2O$	−78.7	−132.1	6.26×10^{13}
(16)	$3CO_2 + 10H_2 \leftrightarrow C_3H_8 + 6H_2O$	−70.9	−125.0	2.64×10^{12}
(17)	$CH_4 \leftrightarrow C + 2H_2$		74.9	
(18)	$2CO \leftrightarrow CO_2 + C$		−172.5	

Footnotes: [a]Standard Gibbs free energy change; [b]Standard enthalpy change: [c]Standard equilibrium constant.

3. Catalyst families for CO_2 hydrogenation to higher alcohols

Four major groups of catalysts are reported for HAS by CO_2 hydrogenation, namely, Rh-, Cu-, Mo-, and Co-based materials, though individual studies using catalytic systems based on Pt, Ru, Pd, and Au have also been reported. Before a discussion on the performance of these catalyst families, the proposed reaction pathways will be presented (Fig. 5). In general, the activation and hydrogenation of CO_2 lead to the formation of C_1 intermediates on the catalyst surface and/or in the gas phase such as CO, CO_3, COOH, HCOH, and CH_x. Subsequently, C_2 species may be formed by the coupling of C_1 species, for example, $CO/CO_2/CO_3-CH_x$ coupling, $COOH-CH_x$ coupling, $HCOH-HCOH$ coupling, and CH_x-CH_x coupling. These C_2 species are further hydrogenated to form C_2 hydrocarbons and oxygenates. As illustrated in Fig. 6, higher alcohols may be formed through several routes. i) CO/CO_n* (n = 1, 2, or 3) species couple with CH_x to form CO_nCH_x* followed by hydrogenation to ethanol. ii) CH_x-CH_x* coupling leads to the formation of CH_xCH_x* which is then coupled with CO/CO_n* species and further hydrogenated to propanol. Alternatively, CH_xCH_x* can be hydrogenated to CH_2CH_2 followed by hydration to ethanol. iii) The condensation of HCOH* results in the formation of CHCOH* followed by hydrogenation to ethanol. iv) CH_3COO* formed by CH_x-COOH* coupling can be hydrogenated to ethanol. Besides, the C_2 intermediates can also couple with C_1 intermediates to form C_{3+} products. $CO-CH_x$ coupling mechanism is suggested to occur over all the four categories of catalysts, while CO_2-CH_x and CO_3-CH_x coupling processds over Rh-based catalysts. Besides, a CH_x-CH_x mechanism is suggested for Cu-based catalysts, $HCOH-HCOH$ coupling is suggested for Mo-based catalysts, and $COOH-CH_x$ coupling is observed over Co-based catalysts. Moreover, in a slurry bed reactor, the solvent has been proven to be involved in the reaction. Over a Pt/Co_3O_4 catalyst in the presence of water as a solvent, it was assumed that H_2O protonates methanol, followed by dissociation into CH_3*, OH*, and H* (or H_2O) species on the catalyst surface, and CH_3* participated in the carbon chain propagation.

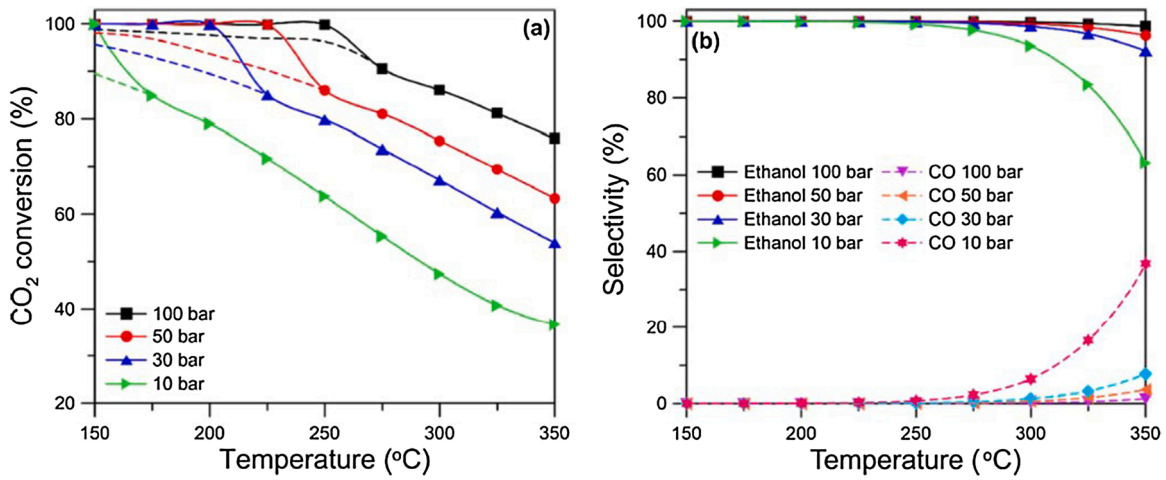

Fig. 3. (a) CO_2 conversion and (b) product selectivity in CO_2 hydrogenation to a mixture of $C_{1-2}OH$ and CO by thermodynamic calculation. $CO_2/H_2 = 1/3$, 150−350 °C, 10−100 bar. Solid and dashed lines represent the chemical equilibrium predicted by liquid-vapor phase and gas phase thermodynamics, respectively. Reproduced with permission from Ref. [48]. Copyright © 2018 American Chemical Society.

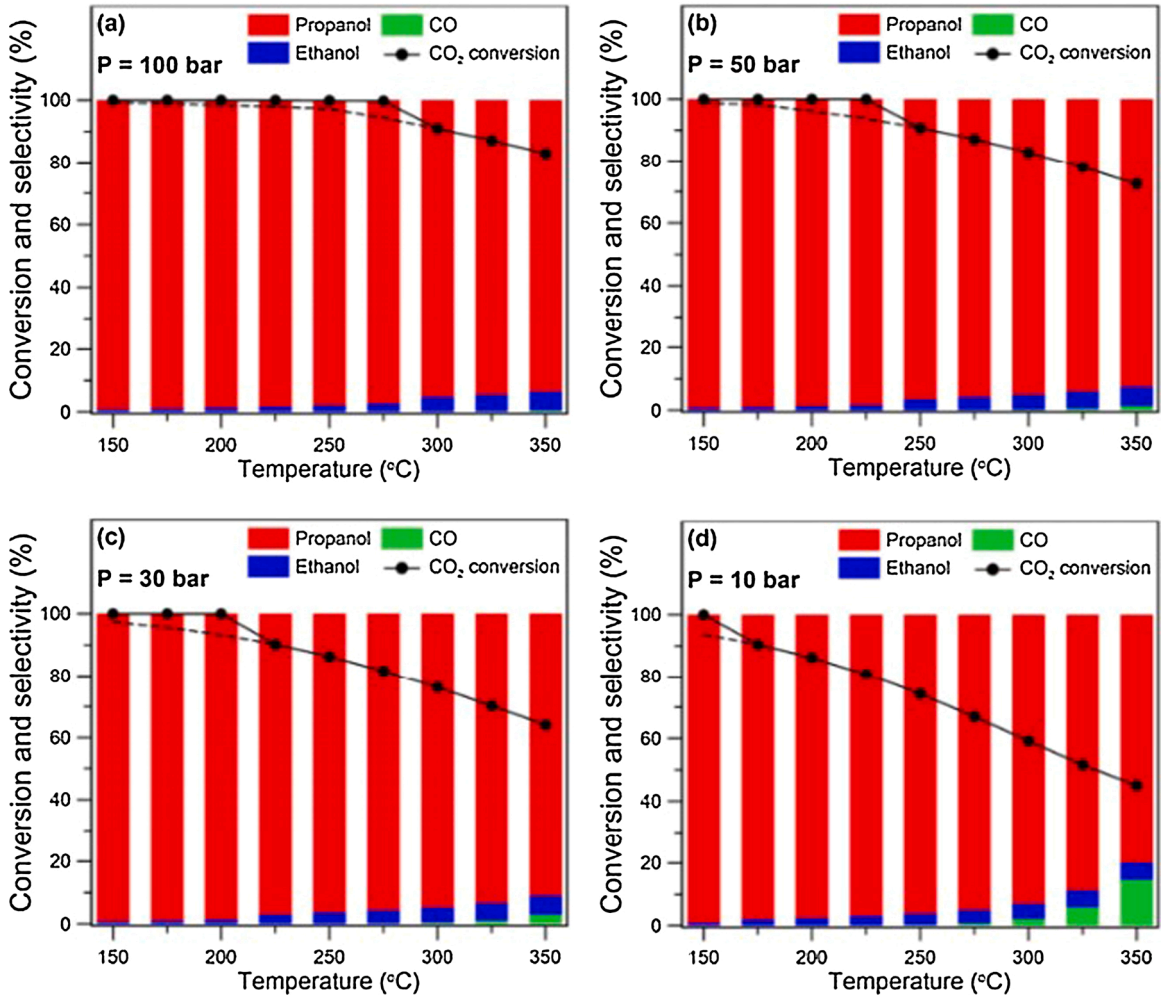

Fig. 4. Conversion and product selectivity in CO_2 hydrogenation to a mixture of $C_{1-3}OH$ and CO by thermodynamic calculations. $CO_2/H_2 = 3/1$, 150−350 °C; (a) 100, (b) 50, (c) 30, and (d) 10 bar. Solid and dashed lines represent the chemical equilibrium predicted by liquid-vapor phase and gas phase thermodynamics, respectively. Reproduced with permission from Ref. [48]. Copyright © 2018 American Chemical Society.

3.1. Rh-based catalysts

Table 2 presents the catalytic performance of representative Rh-based catalysts used for HAS by CO_2 hydrogenation. Typically, HAS over Rh-based materials is performed at 240–270 °C, 2–5 MPa with a gas hourly space velocity (GHSV) of about 7000 $cm^3\ g_{cat}^{-1}\ h^{-1}$ and an H_2/CO_2

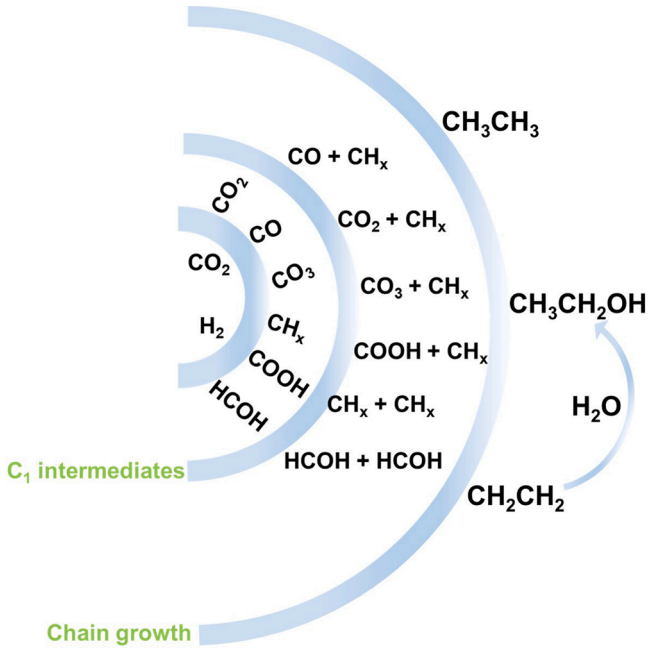

Fig. 5. Schematic representation of pathways in HAS by CO_2 hydrogenation.

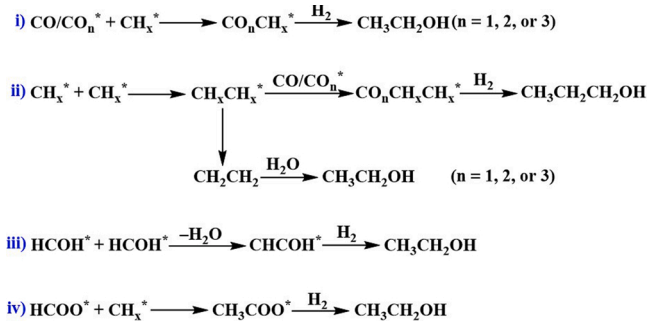

Fig. 6. Schematic representation of carbon chain growth and alcohol formation.

ratio ranging from 1 to 3 in continuous plug flow fixed-bed reactor configurations. Rh-based materials supported on different inorganic supports (TiO_2, SiO_2, CeO_2, and zeolite) and with various promoters (Li, Mn, Fe, and Ce) have been studied. The optimized catalysts show a CO_2 conversion between 7.0–26.7 % and a $C_{2+}OH$ selectivity between 1.2–83 %. Most Rh-based materials result in a low selectivity to methanol (< 10 %). The selectivity of the main side products, CO and hydrocarbons, can be as high as 80 %. Despite optimization, the maximum yield of higher alcohols remains low, and the highest higher alcohol yield of 4.91 % was obtained using a Fe and Li promoted Rh/TiO_2 catalyst. The following sections discuss the effects of alkali metals, transition metals, catalyst support, catalyst precursors, and reaction conditions on HAS by CO_2 hydrogenation over Rh-based materials together with the proposed reaction mechanism.

3.1.1. Monometallic Rh-based materials

Kusama et al. reported the use of SiO_2 supported Rh (Rh/SiO_2) catalysts for CO_2 hydrogenation [52]. Rh/SiO_2 showed a high selectivity of 99.7 % for methane and no ethanol was detected. However, Inui et al. found that Rh supported on a non-metal silicate having an MFI-type structure (Rh/non-metal silicate) partially reduced CO_2 to CO with high selectivity of 99.4 % due to the RWGS [59,60]. A very low concentration of hydrocarbons and no alcohols were detected. It is proposed that the small Rh particles (below ~3 nm) remain oxidized during the reaction, hindering methanation. However, the larger Rh particles possess evident metallic properties that favor methanation [58,61]. Since CO_2 can either be partially reduced to CO or fully reduced to hydrocarbons, these experiments show that it is possible to tailor the electronic state of Rh for alcohol synthesis from CO_2 hydrogenation by controlling the particle size.

The addition of dopants like Se and C on catalyst performance was investigated by Izumi et al. $Rh_{10}Se$ clusters supported on TiO_2 ($Rh_{10}Se/TiO_2$) were found to be active for CO_2 conversion to ethanol at a rate of 1.9×10^{-3} mol h^{-1} g_{cat}^{-1} and selectivity of ~83 % [57,62]. Rh_6C/TiO_2 possessed lower activity (0.4×10^{-3} mol h^{-1} g_{cat}^{-1}) and selectivity (10 %) for CO_2 conversion to ethanol compared to $Rh_{10}Se/TiO_2$. Furthermore, the unpromoted Rh_6/TiO_2 and Rh/TiO_2 produced only methane, suggesting that the presence of an interstitial atom (Se or C) in the Rh cluster framework is important for ethanol synthesis. Among the reported catalysts, $Rh_{10}Se$ supported on TiO_2 and treated at 350 °C showed the highest activity and selectivity for ethanol synthesis. The short Rh–Se distance and strong interaction between Rh_{10} and Se together with considerable electron donation from Se to Rh lead to major changes in the electronic state of Rh. Moreover, it was shown that the electronic state of this catalyst is similar to those of rhodium selenides (Rh_3Se_8 or $RhSe_2$). Thus, a "rhodium selenide"-like electronic state was postulated to inhibit methane formation and to enhance ethanol synthesis by promoting C—C bond formation through CH_x and carbonyl coupling on the surface to form acetate species. Thus, Rh-based catalysts with proper oxidation states were found to be highly active and selective to obtain HA from CO_2. Therefore, the next section focuses on the effects of alkali and transition metal promoters to tailor the electronic state of Rh for HAS.

3.1.2. Effects of alkali and alkaline earth metals on the performance of Rh-based catalysts

Kusama et al. studied more than 30 promoters for CO_2 hydrogenation over Rh/SiO_2 [52]. Ca, V, Mn, and Re led to enhanced CO_2

Table 2
Representative Rh-based catalysts for HAS.

Catalyst	T[a] (°C)	P[b] (MPa)	R[c]	GHSV[d] (cm^3 g_{cat}^{-1} h^{-1})	X_{CO2}^{e} (%)	S_{CO}^{f} (%)	S_{HC}^{g} (%)	S_{MeOH}^{h} (%)	S_{HA}^{i} (%)	Y_{HA}^{j} (%)
$RhFeLi/TiO_2$ [50]	250	3	3	6000[k]	15.7	12.5	53.9	2.2	31.3	4.91
$RhFe/SiO_2$ [51]	260	5	3	6000	26.7	19.7	34.7	29.4	16.0	4.27
$RhMnLi/SiO_2$ [52]	240	5	3	6000	16.1	2.4	88.6	1.3	7.7	1.24
$RhLi/SiO_2$ [52]	240	5	3	6000	7.0	15.7	63.5	5.2	15.5	1.09
$RhCe/SiO_2$ [53]	260	5	3	n.a.	14.0	22.3	64.6	7.3	5.4	0.76
$RhFe/TiO_2$ [54]	270	2	1	8000	9.2	28.4	63.4	1.3	6.4	0.59
Rh/CeO_2-SiO_2 [55]	240	5	3	6000	8.3	33.5	51.4	8.8	6.1	0.51
RhLi/Y [56]	250	3	3	6000	13.1	86.6	8.4	2.3	2.7	0.35
$Rh_{10}Se/TiO_2$ [57]	250	4.7	2	n.a.	n.a.	n.a.	n.a.	n.a.	83.0	0.25[l]
Rh/SiO_2 [58]	260	5	3	6000	n.a.	89.3	3.3	6.0	1.2	0.75[l]

Footnotes: [a]Reaction temperature; [b]Reaction pressure; [c]H_2/CO_2 ratio; [d]Gas hourly space velocity; [e]CO_2 conversion; [f]Selectivity to CO; [g]Selectivity to hydrocarbons; [h]Selectivity to methanol; [i]Selectivity to higher alcohols; [j]Yield of higher alcohols; [k]Space velocity in h^{-1}; [l]TOF in min^{-1}.

conversions and the formation of some methanol, while Li, Sr, Fe, and Ag enhanced ethanol formation. Among them, Li promoted Rh/SiO_2 showed the highest ethanol selectivity of 15.5 %, while no ethanol was formed over the Li free catalyst. Bando et al. also showed positive effects of Li addition on HAS for CO_2 hydrogenation over Li promoted zeolite supported Rh [56]. It was demonstrated that the CO_2 conversion decreased with higher Li to Rh ratios (from 0 to 2.0), and the highest selectivity to ethanol (15.5 %) was obtained with a Li/Rh ratio of 1 with an ethanol/methanol selectivity ratio of 3.0. However, CH_4 was still the main product with selectivity higher than 60 % (Fig. 7a). The addition of Sr also fostered the formation of methanol and ethanol with a selectivity of 7.6 % and 2.5 %, respectively. The other alkali and alkaline earth metals including Na, K, Mg, Ca, and Ba didn't show any positive impact on the formation of ethanol. However, Inoue et al. reported that Na is an efficient promoter to enhance ethanol synthesis over $RhNa/Nb_2O_5$ and $RhNa/TiO_2$, reaching an ethanol selectivity (CO free) of 5.0 % and 13.3 %, respectively [63]. As such, conflicting information on Na promotion is present in the literature, which may be ascribed to the different Na precursors used during catalyst preparation. The counter anions of a carbonate-based precursor (used by Inoue et al.) can be removed to form a new alkali metal complex which is uniformly distributed over the surface under reaction conditions [64].

Typically, the positive effect of alkali metals on HAS over Rh-based catalysts is ascribed to several factors including electron donation, poisoning of active sites for hydrogenation, the formation of new active species, and the stabilization of Rh particles [56]. These factors will be discussed in more detail in the following.

(i) **Electron donation**: Alkali metals have relatively low electron negativity and can donate electrons to Rh leading to a higher electron density at the latter. As a consequence, the back donation of electrons from the promoted metal to CO intermediates results in stronger metal—CO bonds. As such, the activation and/or stabilization of CO are enhanced, which was speculated to result in improved catalyst performance. Besides, the adsorption mode of reactants, intermediates, and products may also change. CO adsorption studies provide detailed insights into the effects of alkali promotion on the electron density of Rh. *In-situ* Fourier-transform infrared spectrum (FTIR) of $Rh(Li)/SiO_2$ shows two types of adsorbed CO species, *viz*. linear and bridged CO at 2040 and 1860 cm^{-1}, respectively (Fig. 7b) [52]. The intensity of these two adsorbed species is almost the same over Li free Rh/SiO_2. However, for $RhLi/SiO_2$, the intensity of the bridged CO adsorption is higher than that of linear CO [52]. The authors propose that this has a strong effect on the reactivity of the Rh catalyst. Bridged CO appears to adsorb stronger to Rh than linear CO. Besides, the bridged CO occupies two Rh atoms, leaving less unoccupied sites for H_2 adsorption and suppressing the hydrogenation ability of the catalyst. Thus, it is hypothesized that with the addition of Li as a promoter, hydrogenation to CH_4 is suppressed and CO species can be inserted into the Rh—CH_3 bond more easily followed by further hydrogenation to alcohols.

(ii) **Active site blockage:** The addition of alkali metals can also block some of the active sites for H_2 activation leading to decreased hydrogenation activity. This may have a positive impact on oxygenate selectivity.

(iii) **New active species:** The addition of alkali metals may lead to the formation of new active species participating in the reaction [65]. Based on IR studies for unpromoted and Li promoted Rh/Y, Bando et al. proposed that a new Rh-Li phase is formed on the surface [56]. Li atoms may participate by coordination/activation of oxygen in adsorbed CO_2.

(iv) **Stabilization of Rh particles:** It has been established that Li promotion can lead to stabilization of Rh particles. For instance, Bando et al. studied the average Rh particle size for Rh/Y in the absence and presence of Li [66,67]. The Rh particles, located in the zeolite cages, in freshly reduced Rh/Y show an average particle size of ~1.3 nm. Under CO_2 hydrogenation conditions, atomically dispersed Rh species are formed due to the exposure of Rh particles to CO intermediates and the reaction with surface OH groups (HO—Si) (Eq. 1) as illustrated in Fig. 7**c**. As a result, the CO concentration on the surface of Rh particles is low and the hydrogenation of CO with the activated H on Rh particles leads to the formation of CH_4 as the main product. In the presence of Li, (LiOS—i) groups are formed and it is suggested that these reduce the rate of the formation of atomic Rh. RhLi/Y shows a bimodal distribution for Rh nanoparticles with maxima at 0.8 and 3 nm. Therefore, the reaction as given in Eq. 1 occurs to a lesser extent than for unpromoted Rh/Y. As a consequence, the selectivity to alcohols is improved.

$$[Rh]_n + 2\ CO + x\ HO\text{–}Si \rightarrow [Rh]_{n-1} + Rh(CO)_2(O)_x + x/2\ H_2 \quad (1)$$

3.1.3. *Effects of transition metal promotion on the performance of Rh-based catalysts*

Transition metals including Fe, Ce, and Mn have been used to

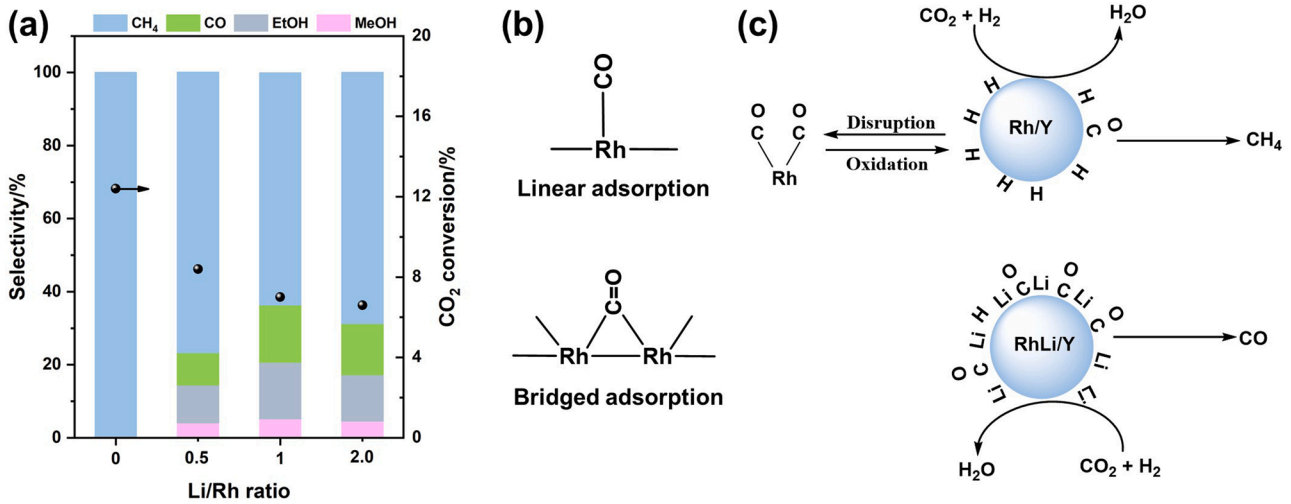

Fig. 7. (a) CO_2 conversion and product selectivity over $RhLi/SiO_2$ with various Li/Rh ratios [52]. (b) Linear and bridged CO adsorption over Rh [68]. (c) Proposed model for Rh particles stabilization by Li. Adapted with permission from Ref. [67]. Copyright © 2000 Elsevier B.V.

promote CO_2 hydrogenation to higher alcohols over Rh-based catalysts. The effects of the individual promoters (Fe, Ce, and Mn) will be discussed and rationalized in the following paragraphs.

(i) **Effects of Fe:** Kusama et al. studied the effects of Fe on the activity and selectivity of ethanol synthesis by CO_2 hydrogenation over Rh/SiO_2 [51]. In the Fe/Rh ratio range of 0–3, CO_2 conversion increased with increasing Fe/Rh ratio reaching a maximum of 26.7 % at a Fe/Rh ratio of 2 and then decreased slightly at higher ratios. Alcohol selectivity showed a similar trend, and the highest ethanol selectivity was about 16 %. The addition of Fe also changes the selectivity of the reaction. The main product over Fe free Rh/SiO_2 was CO, whereas the addition of a small amount of Fe (Fe/Rh = 0.1) leads to high CH_4 selectivity (82.9 %). However, the CH_4 selectivity decreased when the Fe/Rh ratio was further increased. It was found that the percentage of Fe^0 (Fe^0%) is a function of the Fe/Rh ratio, and it decreases with higher Fe/Rh ratios as Fe is more difficult to reduce than Rh. With lower amounts of Fe^0, CH_4 selectivity decreased, while the selectivity to CO, methanol, and ethanol increased (Fig. 8a). This is suggested to be due to the promotional effect of Fe^0 for methanation as well as the dissociation of CO* intermediates. Both linear and bridged CO adsorptions were found over $RhFe/SiO_2$. Furthermore, as Fe^0% decreases, the amount of bridged CO and the ethanol selectivity were found to increase, an indication that non-metallic Fe favors the formation of alcohols.

(ii) **Effects of Ce:** The use of Ce as a promoter in Rh catalysts was shown to enhance both CO_2 conversion and alcohol selectivity [53,55]. Kusama et al. showed that the addition of Ce increases the CO_2 conversion to 14 % and ethanol selectivity to 5.4 %, compared with 3.0 % and 0.3 % over Ce free Rh/SiO_2. Ce, on one hand, was postulated to facilitate CO_2 adsorption. On the other hand, Ce can also increase the dispersion of Rh and the intimate contact between Rh and Ce, resulting in the formation of tilted CO intermediate species (Fig. 8b) as detected by FTIR. As a result, CO dissociation and CO insertion are promoted by a reduced C—O bond order and changes in the electron density in the vicinity of the carbon atom of CO [69,70], leading to higher amounts of CH_4 and ethanol.

(iii) **Effects of Mn:** Kusama et al. used Mn to promote CO_2 hydrogenation over $RhLi/SiO_2$ [52]. At 473 K, both CO_2 conversion and ethanol selectivity first increased and then decreased with increasing Mn/Rh ratios. The highest CO_2 conversion (6.3 %) and the highest ethanol selectivity (16.1 %) were obtained at Mn/Rh ratio of 0.5 and 0.2, respectively. The highest ethanol yield of 0.58 % was obtained at Mn/Rh ratio of 0.2. Mechanistic consequences were not discussed.

3.1.4. *Effects of catalyst supports on the performance Rh-based catalysts*

The performance of Rh-based catalysts is highly dependent on the

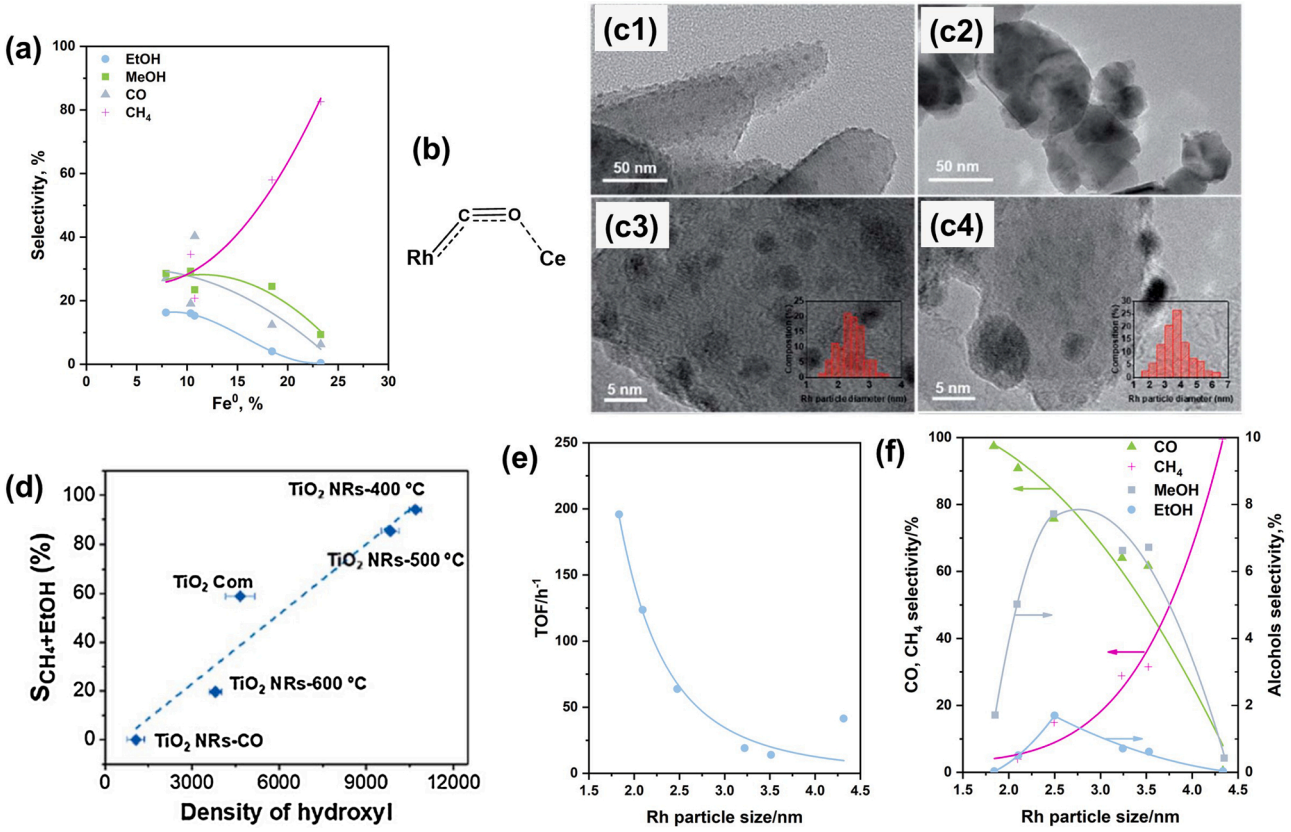

Fig. 8. (a) Correlation between Fe°/Fe and product selectivity. The solid lines are shown for guidance only. Adapted with permission from Ref. [51]. Copyright © 1996 Published by Elsevier Ltd. (b) Tilted CO adsorption [53]. (c) TEM (c1 and c2) and HRTEM (c3 and c4) images, and particle size distributions (inset figures) of RhFeLi supported on TiO_2 nanorods and nanoparticles, respectively. Adapted from Ref. [50] licensed under a Creative Commons Attribution-NonCommercial 3.0 Unported Licence. (d) The summed selectivity to CH_4 and ethanol as a function of the hydroxyl density obtained over RhFeLi supported on different TiO_2 supports. Adapted from Ref. [50] licensed under a Creative Commons Attribution-NonCommercial 3.0 Unported Licence. (e) Correlation between TOF and the size of Rh supported on SiO_2. The solid lines are shown for guidance only. Adapted with permission from Ref. [78]. Copyright © The Japan Petroleum Institute. (f) Correlation between product selectivity and the size of Rh supported on SiO_2. The solid lines are shown for guidance only. Adapted with permission from Ref. [78]. Copyright © The Japan Petroleum Institute.

nature of the support. Studies revealed that for CO hydrogenation, the main product for acidic supports are hydrocarbons, whereas weakly basic or neutral supports are best to obtain C_{2+} oxygenates [63,71]. Inoue et al. investigated the influence of catalyst supports (Nb_2O_5, ZrO_2, MgO, and TiO_2) on CO_2 hydrogenation over supported Rh catalysts [63]. The main product over Rh/MgO and Rh/ZrO_2 was methane, while methanol and a small amount of ethanol were formed over Rh/Nb_2O_5 and Rh/TiO_2. The latter was explained by assuming that strong metal-support interactions (SMSI) due to the interaction of Rh with easily reduced Nb_2O_5 and TiO_2 favor methanol selectivity. Unlike for CO hydrogenation, the strong basic support (MgO) did not enhance methanol formation for CO_2 hydrogenation, indicating a different mechanism for methanol formation for CO and CO_2 hydrogenation. Further promotion of Rh/Nb_2O_5 and Rh/TiO_2 with Na leads to higher amounts of ethanol, as already illustrated in Section 3.1.2. Yang et al. studied the effects of the number of hydroxyl groups on TiO_2 on catalyst performance for CO_2 hydrogenation using Li promoted RhFe particles supported on TiO_2 (*i.e.* RhFeLi/TiO_2) [50]. Both commercial TiO_2 and TiO_2 nanorods were used. The RhFeLi/TiO_2 nano-rods gave a higher CO_2 conversion (~15 %) and higher ethanol selectivity (32 %) than the commercial TiO_2. These results were explained by the higher surface area of TiO_2 nanorods in comparison to the commercial TiO_2, leading to a higher Rh dispersion (Fig. 8c). It was found that the selectivity to methane and ethanol (the total selectivity to CH_x*) increases with increasing hydroxyl density on the surface-treated TiO_2 nanorods (Fig. 8d). *In-situ* FTIR experiments showed the presence of an additional band at 1746 cm^{-1} ascribed to the adsorbed formyl species (CHO*) for the RhFeLi/TiO_2 nanorods. The formation of such CHO* species is suggested to be the rate-limiting step for ethanol synthesis [72]. Thermodynamically, dissociation of CHO* into CH_x* is favored above CO formation [73–76]. Besides, the abundant hydroxyl facilitates the scission of the C—O bond in CH_3O* to produce CH_3*. Subsequently, a CO intermediate can be inserted into CH_3* followed by further hydrogenation to form ethanol. Bando et al. also studied ion-exchanged Y-type zeolite supported Rh (Rh/Y) for CO_2 hydrogenation [66,67,77]. According to the experimental results, Rh/Y showed a 10 times higher turnover frequency than the conventional impregnated Rh/SiO_2. This high activity of the Rh/Y catalyst was rationalized by the authors considering the size of the zeolite cage, which is important in condensing and supplying CO_2 to the Rh sites outside the cage, thus promoting CO_2 conversion. Further promoting Rh/Y with Li enhances the formation of methanol and ethanol as illustrated in Section 3.1.2. Moreover, when using CeO_2 as catalyst support higher CO_2 conversion and ethanol selectivity was obtained compared with SiO_2 [55]. These positive effects of CeO_2 may be similar to Ce promotion as previously illustrated in Section 3.1.3.

3.1.5. Effects of catalyst precursors on the performance Rh-based catalysts

The precursors used during catalyst preparation are known to influence the morphology and size of Rh particles and as such catalyst performance. A study by Kusama et al. showed the effects of the use of different catalyst precursors for Rh-based catalysts on the performance of CO_2 hydrogenation [58]. For this purpose, Rh/SiO_2 catalysts were prepared with different Rh precursors (acetate (Rh-Ac/SiO_2), nitrate (Rh-Nitr/SiO_2), and chloride (Rh-Cl/SiO_2)). The turnover frequency (TOF) of the reaction with CO_2 and hydrogen was found to increase in the order of Rh-Nitr/SiO_2 < Rh-Ac/SiO_2 < Rh-Cl/SiO_2. The main product over Rh-Ac/SiO_2 and Rh-Nitr/SiO_2 was CO, while Rh-Cl/SiO_2 produces mainly CH_4 (with 99.8 % selectivity). A small number of alcohols were obtained over Rh-Ac/SiO_2 (selectivity, 6.0 % methanol and 1.2 % ethanol) and Rh-Nitr/SiO_2 (selectivity, 5.4 % methanol and 0.5 % ethanol). These differences in activity and selectivity were ascribed to the differences in the average Rh particle size (Rh-Ac/SiO_2 (2.82 nm) < Rh-Nitr/SiO_2 (3.27 nm) < Rh-Cl/SiO_2 (5.50)). The effects of Rh particle size on the catalytic performance of CO_2 hydrogenation were further studied by Kusama et al. using an Rh/SiO_2 catalyst [78]. A series of Rh/SiO_2 with a particle size ranging from 1.84 to 4.33 nm were prepared and tested. It was shown that the TOF decreased with increasing particle size (Fig. 8e). Catalysts with small Rh particle sizes produce mainly CO, whereas the CO selectivity decreased and the CH_4 selectivity increased when using catalysts with larger particle sizes (Fig. 8f). Alcohols selectivity *versus* particle size showed a volcano-like trend reaching the highest selectivity to methanol (~8 %) and ethanol (~2 %) at a particle size of 2.5 nm. To explain this trend, the amount of absorbed H_2 was considered by the authors. It was found that higher amounts of H_2 are adsorbed on larger Rh particles than on smaller ones. The chemisorption of H in the form of $Rh^{+\delta}$–$H^{-\delta}$ leads to a lowering of electron density of Rh at higher amounts of H_2 adsorbed. As a consequence, the hydrogenation activity of the catalyst is promoted. Bando et al. investigated the structure of Rh/SiO_2 catalysts prepared using acetate (Rh-Ac/SiO_2) and chloride (Rh-Cl/SiO_2) precursors by *in-situ* extended X-ray absorption fine structure (EXAFS) [61]. Rh-Cl/SiO_2 possesses spherical Rh particles while the Rh particles in Rh-Ac/SiO_2 have different shapes such as disk-like ones. The latter was shown to be more easily oxidized when exposed to air, indicating a higher affinity to oxygen. It may also imply a high-affinity for CO_2 which in turn may explain the differences in product selectivity.

3.1.6. Effects of reaction conditions on the performance of Rh-based catalysts

Reaction conditions are known to strongly affect the rate and selectivity of HAS from CO_2 hydrogenation over Rh-based catalysts. Kusama et al. studied the effects of temperature, pressure, and H_2/CO_2 ratio for a RhLi/SiO_2 catalyst [52]. They observed that the CO_2 conversion increased from 3.7 % to 7.0 % when increasing the pressure from 0.1 to 5 MPa. Besides, the formation of ethanol started to become evident at a pressure higher than 1 MPa. The selectivity to alcohols (methanol and ethanol) increased and methane selectivity decreased monotonously with increasing pressure reaching a maximum alcohol selectivity of 20.7 % with an ethanol/methanol ratio of 3.0 at 5 MPa. The latter was explained based on thermodynamic considerations, dictating that selectivity to alcohols is improved at higher pressures. A study by Gogate et al. also found similar effects of reaction pressure on CO_2 hydrogenation and ethanol selectivity over RhFe/TiO_2 [54]. The effect of reaction temperature was also investigated. With increasing reaction temperature from 200 to 260 °C, the CO_2 conversion increased from 1.4 % to 15.7 % [52]. Besides, the selectivity to alcohols showed an optimum, with the highest ethanol selectivity at 240 °C (15.5 %). However, CO was shown to be the main product at low temperatures whereas CH_4 was formed in the highest amounts at high temperatures. Kinetic modeling was used to determine the activation energies for relevant reactions. The activation energy for the overall CO_2 conversion to alcohols, CO, and methane was estimated to be 87 kJ/mol and 121 kJ/mol for CH_4 formation, respectively, indicating that high temperature kinetically favors CH_4 formation. As a result, ethanol selectivity decreased at high temperatures. Similar effects of temperature on catalyst performance were also reported for RhFe/TiO_2 and $Rh_{10}Se$/-TiO_2 [54,62]. Besides, the effect of the H_2/CO_2 ratio on reaction performance was explored. It was found that CO_2 conversion increased from 1.7 % to 13.4 % when increasing the H_2/CO_2 ratio from 0.6 to 9.0. Also, methanol and methane selectivity increased, while ethanol and CO selectivity decreased with increasing H_2/CO_2 ratio. The highest ethanol yield of 0.7 % (with CO_2 conversion of 13.4 % and 5.5 % ethanol selectivity) was obtained at an H_2/CO_2 ratio of 9 [52]. The effect of weight hourly space velocity (WHSV) over Rh/TiO_2 (270 °C, 2 MPa, $H_2/CO_2 = 1$) was explored by Gogate et al. [54]. The experimental results showed that CO_2 conversion increased with decreasing WHSV, and the product selectivity was fairly independent of conversion level.

3.1.7. Proposed reaction mechanism over Rh-based catalysts

Several reaction mechanisms have been proposed for HAS over Rh-based catalysts and debate is ongoing. The proposed mechanisms can

mainly be categorized into two classes, namely i) higher alcohols formed *via* direct CO_2 hydrogenation without CO as an intermediate and ii) higher alcohols formed through CO (either from the bulk gas phase or an adsorbed form generated by the RWGS) hydrogenation.

Kusama et al. employed FTIR experiments under a CO_2-H_2 atmosphere to gain insights into the mechanism of HAS. Adsorbed CO species were observed on the surface of $RhLi/SiO_2$ [52]. Besides, CO was also detected as a byproduct, and based on these findings, it was concluded that CO plays a role. Inoue et al. compared the performance of several Rh-based catalysts for CO and CO_2 hydrogenation [63]. The obtained products from CO_2 hydrogenation were mostly methane and methanol, whereas C_{2+} hydrocarbons and ethanol from C—C bond-forming reactions were hardly detected. However, higher amounts of C_{2+} hydrocarbons and ethanol were formed over the same catalysts when CO_2 was replaced by CO. Besides, similar intermediates were observed on the surface of the alkali metal promoted Rh catalysts giving ethanol for both CO and CO_2 hydrogenations. Based on these findings, the authors propose that, under the experimental conditions reported, CO_2 is hydrogenated to methanol and ethanol with CO as a clear intermediate, formed *e.g.* by the RWGS [51,53,56,57,67,78].

As stated above, one of the mechanistic proposals assumes that CO is a key intermediate and may be formed by the RWGS. Since the rate of C—C bond formation in CO_2 hydrogenation is typically lower than in CO hydrogenation over Rh-based catalysts [79–81], gas-phase CO seems to be important for C—C bond formation. However, Bando et al. excluded an effect of gas-phase CO on ethanol formation by adding CO in the feed gas over Rh/Y and RhLi/Y catalysts [56]. They expected that ethanol formation would be enhanced for Rh/Y due to the existence of high amounts of methyl species. However, it was found that ethanol formation was enhanced significantly over the RhLi/Y after CO addition, whereas the product distribution was hardly affected. Thus, the authors excluded an *ex-situ* insertion of CO from the gas-phase to methyl species. Moreover, Kusama et al. proposed a mechanism for HAS through adsorbed CO intermediates (Fig. 9a) [52]. They suggested that adsorbed CO species form on the surface of the catalyst through the RWGS. Then, the adsorbed CO species are either desorbed to form gaseous CO or hydrogenated to methanol. Besides, adsorbed CO can also be hydrogenated to form methyl species on the catalyst surface, leading to the formation of CH_4 upon hydrogenation, while the insertion of adsorbed CO into the methyl species results in the formation of acyl species. Finally, ethanol is formed by further hydrogenation of the acyl groups.

Bando et al. further proposed a dual-site mechanism for ethanol synthesis over $RhLi/SiO_2$ (Fig. 9b) [56]. They proposed that Li promotion creates two types of active sites (*i.e.* Li free and Li modified sites). A Li free Rh_a site is responsible for the rapid conversion of CO_2 to methyl (Rh_a—CH_3) species with a reactive terminal CO species (Rh_a—CO) as the intermediate. Likewise, Li modified Rh_b is responsible for CO_2 adsorption in the form of a η^2-type (Rh_b—CO_2) and stabilization of adsorbed CO (Rh_b—CO). FTIR study proved that CO_2 activation on the Rh_b surface is preferable to Rh_a. Besides, the insertion of CO* into CH_3* led to the formation of acyl species which finally desorb as ethanol. CO added in the CO_2-H_2 feed works as a source for methyl formation (Rh_a—CH_3) instead of CO insertion. Yang et al. were able to observe the formation of adsorbed CHO* and CH_3O* over the $RhFeLi/TiO_2$ catalyst and suggested that CH_x* may be formed by CHO* and CH_3O* dissociation [50].

Izumi et al. proposed another possible mechanism for ethanol synthesis from CO_2 hydrogenation over $RhSe_{10}/TiO_2$ which does not proceed *via* CO as an intermediate (Fig. 9c) [57,62,82]. They found that adsorbed bidentate carbonate species were formed on both $RhSe_{10}/TiO_2$ and TiO_2. The study also showed acetate species on the surface of $Rh_{10}Se/TiO_2$. Besides, from the *in-situ* FTIR studies, the intensities of CH_3* and CH_2* signals were proportional to the rate of ethanol formation, while the intensities of the CO* stretching bands were weak suggesting that CO* was not present in large numbers on the surface of $RhSe_{10}/TiO_2$. Based on these findings, it is postulated that adsorbed CO_2* on $Rh_{10}Se$ particles can be hydrogenated to CO* and CH_x*; though the rate of the conversion to CO is very low. The CH_3* or CH_2* on $Rh_{10}Se$ may first react with CO_3* formed on the TiO_2 support or with CO_2* forming acetate followed by hydrogenation to ethanol on Rh sites. This suggests that CO_2 hydrogenation to HAS occurred at the metal/support interface, which hypothesis is increasingly investigated in the recent literature of CO_2 hydrogenation [83,84].

3.2. Cu-based catalysts

Cu-based materials are known to be efficient catalysts for methanol synthesis [5,85–100] and the RWGS [101–110]. Table 3 summarizes the catalytic performance of representative Cu-based catalysts for CO_2 conversion to higher alcohols. Typical reaction conditions used are 300–350 °C, 3.0–8.0 MPa, 3600–20,000 h^{-1}, and an H_2/CO_2 ratio of 3.0 in continuous setups. Cu-based materials promoted by Zn, Fe, K, Pa, Ga, and Co were also reported as potential catalysts for HAS from CO_2.

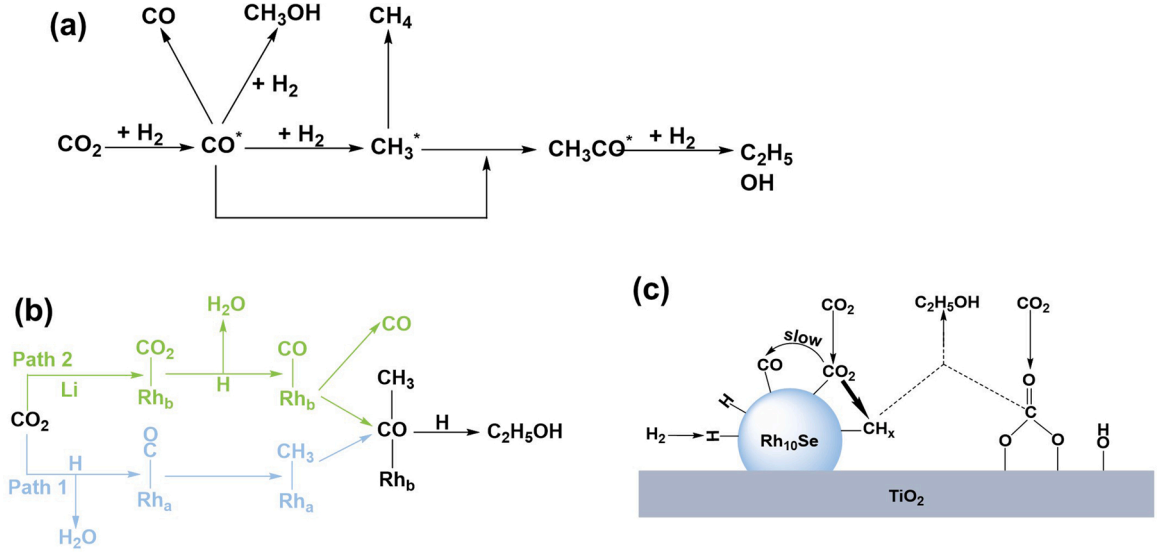

Fig. 9. (a) CO insertion mechanism for ethanol synthesis. Adapted with permission from Ref. [52]. Copyright © 1996 Published by Elsevier B.V. (b) CO insertion mechanism for ethanol synthesis over dual Rh site. Adapted with permission from Ref. [56]. Copyright © 1998 Elsevier Science B.V. (c) CH_x—CO_3/ CO_2 coupling mechanism for ethanol synthesis over $Rh_{10}Se/TiO_2$. Adapted with permission from Ref. [82] licensed under Creative Commons.

Table 3
Representative Cu-based catalysts for HAS.

Catalyst	T[a] (°C)	P[b] (MPa)	R[c]	GHSV[d] (h^{-1})	X^{e}_{CO2} (%)	S^{f}_{CO} (%)	S^{g}_{HC} (%)	S^{h}_{MeOH} (%)	S^{i}_{HA} (%)	Y^{j}_{HA} (%)
CuZnFeK [111]	300	6.0	3.0	5000	42.3	6.9	56.4	4.7	31.9	13.51
CuZnFeK [112]	300	7.0	3.0	5000	44.2	5.9	46.1	2.0	26.9[k]	11.89
Pd-GaCuZnAlK-CuFeAlK [113]	330	8.0	3.0	20000	54.5	9.7	64.5	5.2	17.0	9.27
PdGaCuZnAlK-CuFeAlK [59]	330	8.0	3.0	20000	47.0	12.3	62.8	5.84	19.1[k]	8.98
CuZnFeZrK [114]	320	3.0	3.0	3600	25.5	53.1	23.6	14.3	8.9	2.27
CuZnK/CuFeCoK [115]	350	6.0	3.0	5000	32.4	45.3	42.9[l]	5.3	6.5	2.11
CuZnK [111]	300	6.0	3.0	5000	25.1	80.4	8.7	6.9	4.0	1.0
CuFeCoK [115]	350	6.0	3.0	5000	19.98	71.38	22.2[l]	2.4	4.0	0.80
CuZnK [115]	350	6.0	3.0	5000	27.2	84.3	8.2[l]	6.2	1.33	0.36
$CuZnFeZrO_2K$ [114]	320	3.0	3.0	3600	24.2	29.6	50.3	17.9	2.2	0.53
Zr_{12}-bpdc-CuCs [116]	100	4	3.0	-[m]	52	n.a.	n.a.	n.a.	> 99	>40.04
Zr_{12}-bpdc-CuCs [116]	85	35	0.17	-[m]	2.7	n.a.	n.a.	n.a.	> 99	>2.67

Footnotes: [a]Reaction temperature; [b]Reaction pressure; [c]H_2/CO_2 ratio; [d]Gas hourly space velocity; [e]CO_2 conversion; [f]Selectivity to CO; [g]Selectivity to hydrocarbons; [h]Selectivity to methanol; [i]Selectivity to higher alcohols; [j]Yield of higher alcohols; [k]C_{2+} oxygenates are included; [l]Oxygenates are included; [m]10 mg catalyst in 10 ml THF for 10 h.

However, these materials possess a high selectivity to either CO or hydrocarbons. When considering the entries in Table 3, it is evident that the selectivity to (CO + hydrocarbons) is the highest for all catalysts and ranges from 52.0 % to 93.6 %. The selectivity to methanol is below 18 %, while that to C_{2+} alcohols ranges from 1.3 % to 31.9 %. The C_{2+}OH yield is between 0.36 % and 13.51 %, with a CuZnFeK catalyst giving the best results. Some studies have reported the use of an anhydrous THF solvent in combination with a Zr_{12}-bpdc-CuCs catalyst (CuCs nanocrystals supported on metal-organic framework, UiO-66) at low temperature (< 100 °C) in a slurry batch reactor and in this case, an impressive ethanol selectivity of 99 % and yield of 40.04 % were observed. In the following sections, the effect of alkali metals, transition metals, and reaction conditions, as well as the reaction mechanism when using Cu-based catalysts will be discussed.

3.2.1. *Effects of alkali metals on the performance of Cu-based catalysts*

Takagawa et al. found that CO_2 hydrogenation over a CuZn catalyst without alkali metal promotion produces mainly CO and methanol, and C_{2+} oxygenates or hydrocarbons were not detected [112]. Guo et al. observed a very small amount of the C_{2+} alcohols (selectivity, 0.37 %) in CO_2 hydrogenation over a similar CuZn catalyst; however, the main products were still CO and methanol [115]. Promotion of CuZn with K was shown to enhance the formation of C_{2+} alcohols (Fig. 10a). When increasing the K/Cu ratio from 0 to 0.3, CO_2 conversion was increased first but then decreased and reached a maximum of 27.6 % at a K/Cu ratio of 0.23 with CO as the main product. A similar trend was found for mixed alcohols (incl. methanol), with a maximum at a K/Cu ratio of 0.15. The formation of ethanol was also enhanced by the addition of K, and the $C_{2+}OH/C_1OH$ ratio over the optimized K promoted catalyst was much higher (0.39) than that for the K free catalyst (0.067). The experimentally observed best catalytic performance for HAS when using a K/Cu ratio of 0.15, is thus likely due to i) an optimum deposition and dispersion of CuO on ZnO, ii) an easier reduction of Cu, and iii) enhanced interaction between CuO and ZnO. However, too high amounts of K may cover the Cu surface and weaken the synergetic effects between ZnO and CuO, thus resulting in lower CO_2 conversion. In addition to the advantages discussed above, K was also suggested to neutralize the catalyst surface acidity for CuZnFeZrO catalysts. This will lead to a higher number of catalytic centers for HAS and lower amounts of H* on the surface, and as such lead to reduced amounts of hydrocarbons [114].

Moreover, An et al. described a metal-organic framework (MOF) with cooperative Cu sites on a Zr_{12} cluster for selective CO_2 hydrogenation to ethanol [116]. They propose that an intimate Cu-Cu pair forms an active site and is responsible for ethanol synthesis (Fig. 11). The addition of an alkali metal was found to further enhance ethanol formation. The promotional effect on ethanol selectivity increases in the order of Li < Na < K < Cs (from 66.3 % to > 99 %). This trend was

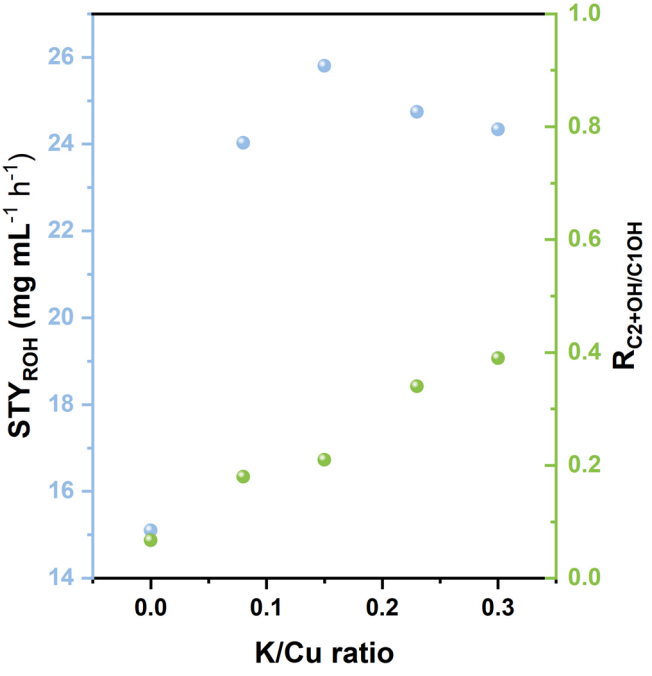

Fig. 10. STY of alcohols and $C_{2+}OH/C_1OH$ ratio over K promoted CuZn [115].

rationalized by considering the effect of the cation on the oxidation state of Cu. Cs^+ is considered a much better electron-donor than Li^+ leading to an electron-richer Cu center in the presence of Cs. Such an electron-rich Cu site was proposed to be beneficial for HAS as it promotes the oxidative addition of hydrogen, forming a Cu^{II}–H^-. Besides, electron-rich Cu centers are expected to facilitate formyl formation from a CH_2O_2 intermediate due to the increasing basicity of an oxygen atom coordinated on Cu. These intermediate formyl species are thought to be key intermediates for the coupling with methanol to form a C—C bond, ultimately leading to ethanol.

3.2.2. *Effects of the addition of transition metals on the performance of Cu-based catalysts*

The effects of transition metals including Zn, Fe, Cr, Co, Mo, Pd, and Ga on Cu-based catalysts for CO_2 hydrogenation to higher alcohols were studied by different research groups. The results for the individual promoters will be discussed separately in the following paragraphs.

(i) **Effects of Zn:** Guo et al. investigated the effects of ZnO promotion over a CuK catalyst for CO_2 hydrogenation [115]. An optimum

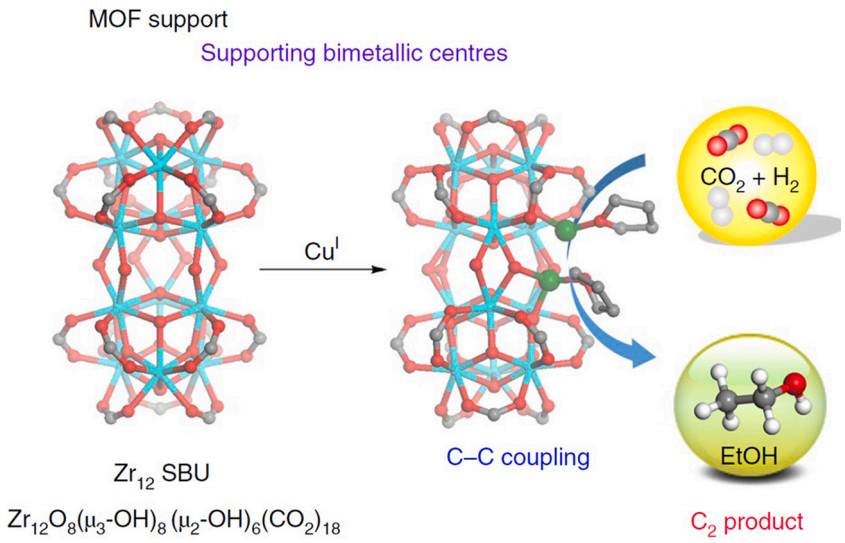

Fig. 11. Schema of ethanol formation over Cu-Cu dual-site. Reproduced with permission from Ref. [116]. Copyright © 2019, Springer Nature.

Zn/Cu ratio in the range 0.5–2.0 was observed concerning CO_2 conversion, though with CO as the main product (selectivity > 73 %). The selectivity to mixed alcohols (incl. methanol) was independent of the Zn/Cu ratio (*i.e.* 6.23–7.56 %); however, the $C_{2+}OH/C_1OH$ ratio increased significantly from 0.19 to 0.8. This promotional effect of Zn was ascribed to a change in the dispersion of Cu species. High dispersion of Cu leads to an increase in surface area of Cu and facilitates intimate contact between Cu and Zn, thus enhancing the required change in the oxidation state of the Cu surface ($Cu^0 \leftrightarrow Cu^I$) for CO_2 activation [117].

(ii) **Effects of Fe:** Fe-based catalysts are known to be efficient for CO_2 conversion and C—C bond formation [63,118–132,16]. For instance, FeK oxides used in Fischer-Tropsch synthesis are known to convert CO_2 to hydrocarbons, CO, and alcohols. Thus, the addition of Fe to a CuZnK catalyst should be beneficial for HAS [111]. As shown in Fig. 12, the CuZnK catalyst without Fe mainly produces CO with high selectivity of 80.4 %. The selectivity to alcohols was only 10.91 % with a low $C_{2+}OH/C_1OH$ ratio of 0.57. Upon the incorporation of Fe in the catalyst formulation, the selectivity to CO was lowered, and the selectivity to alcohols and hydrocarbons significantly increased. The highest alcohol selectivity (36.67 %) and $C_{2+}OH/C_1OH$ ratio (6.76) were obtained at a Fe/Cu ratio of 0.5. Moreover, higher levels of Fe promotion lead to a decrease in both alcohol selectivity and the $C_{2+}OH/C_1OH$ ratio. Such positive effects of Fe addition to CuZnK catalysts were also reported by Takagawa et al. [112]. Several explanations have been put forward to explain this effect. For instance, it has been proposed that Fe facilitates the reduction of CuO and $CuFe_2O_4$. Also, it was shown by N_2 physisorption and XRD that the presence of Fe enhances the dispersion of Cu species on ZnO, which is known to promote CO formation through the RWGS reaction. Besides, evidence was provided that Fe forms a strong bond with Zn which facilitates the dispersion and reduction of $ZnFe_2O_4$ spinels to iron carbides, which are known to promote CO conversion and carbon chain growth.

(iii) **Effects of Pd and Ga:** Pd and Ga were also used as promoters to enhance HA yields over CuFeAlK-CuZnAlK catalysts [59,60,113]. The Pd and Ga free CuFeAlK-CuZnAlK were shown to give an ethanol selectivity of 15.8 % and an ethanol space-time yield (STY) of 321 g L_{cat}^{-1} h^{-1}. Upon Pd promotion, the selectivity and STY for ethanol increased (selectivity, 17.4 %, and a STY of 420 g L_{cat}^{-1} h^{-1}). For Ga, the selectivity was increased to 17.0 %, and a STY of 476 g L_{cat}^{-1} h^{-1} was reported. These promotional effects of Pd and Ga are ascribed to hydrogen spillover and inverse spillover of Pd and Ga, respectively. By changing the particle size of Pd to tailor its metallic properties and changing the loading of Ga, the level of (inverse) hydrogen spillover can be controlled. Accordingly, the catalyst allows for optimum performance with high ethanol selectivity and STY because the desired reduced state of the catalyst can be obtained.

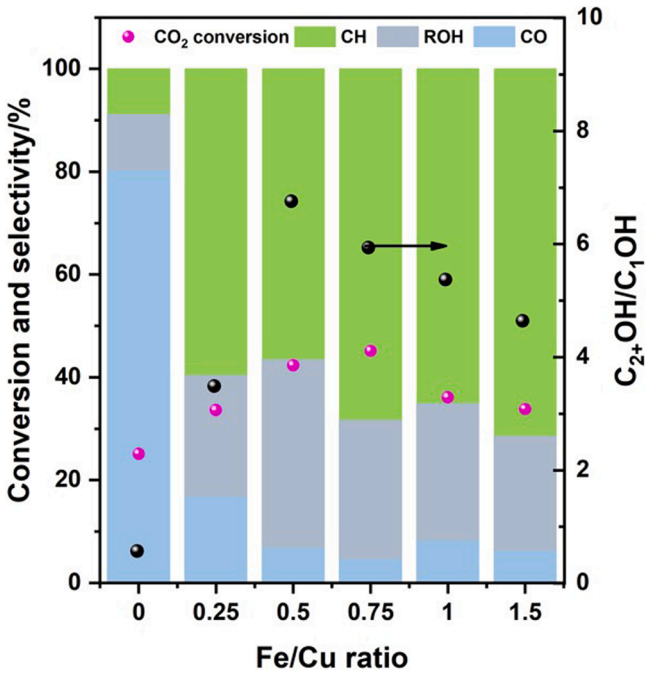

Fig. 12. CO_2 conversion, product selectivity, and $C_{2+}OH/C_1OH$ ratio over Fe promoted CuZnK catalysts [111].

(iv) **Effects of Co and Mo:** Kieffer et al. prepared a copper-rare earth oxide (*i.e.* Cu-$La_2Zr_2O_7$) catalyst with a cubic pyrochlore structure for alcohol synthesis from CO_2 [133]. CO_2 was mainly converted to methanol and CO when using this catalyst. The addition of Co and Mo led to a reduction in the formation of methanol and CO, giving methane as the main product together with some C_{2+} hydrocarbons and alcohols. It was hypothesized that Co is essential for carbon chain growth whereas Mo addition increases the rate of hydrogenation reactions [134].

(v) **Effects of Cr:** Cr was shown to enhance the stability of CuZnFeK catalysts and stable operation was achieved in a continuous set-up for more than 150 h on stream [135]. In contrast, though CuZnFeK is active for CO_2 conversion to ethanol, the activity of this catalyst decreases fast under reaction conditions due to the segregation of active spinel components to $FeCO_3$, ZnO, and Cu. It was proposed that Cr stabilizes the catalytically active spinel structure and prevents segregation leading to a longer catalyst life.

3.2.3. *Mixtures with Cu as one of the catalyst components for HAS*

Several studies have been reported on the use of reactor configurations with either a well-mixed blend of catalysts or two spatially separated (Cu- and Fe-) based catalyst for HAS by CO_2 hydrogenation [59,60,113,115]. This has been reported to have a marked influence on activity and selectivity [16,136–138]. For instance, Inui et al. used a combination of Pd and Ga modified CuZnAlK and CuFeAlK catalysts [59,60,113]. The former is a commonly used catalyst for methanol synthesis giving mainly CO and methanol when using CO_2 as the feed. The Fe-based catalyst CuFeAlK is known to convert CO_2 to mainly hydrocarbons (with selectivity up to 64.9 %) as well as considerable amounts of ethanol and methanol. Reactions were carried out with Pd and Ga modified CuZnAlK (PdGaCuZnAlK) and CuFeAlK, either as a blend or in a dual catalytic bed. As presented in Fig. 13, the well-mixed blend of catalysts showed a high CO_2 conversion of 47.0 % with hydrocarbons as the main product (selectivity of 62.8 %) as well as a high ethanol selectivity of 17.4 %. Using a dual bed system, a lower CO_2 conversion and ethanol selectivity were obtained compared to the blend. Unfortunately, a clear explanation to explain this phenomenon was not reported.

Other studies using this concept have been reported as well. For instance, the use of a well-mixed blend of CuZnK and CuFeCoK [115] lead to a thermal coupling effect between the RWGS and CO hydrogenation [139]. This coupling between the endothermic RWGS (over CuZnK or PdGaCuZnAlK) and exothermic CO hydrogenation (CuFeCoK or CuFeAlK) leads to a peculiar temperature profile in the reactor (*e.g.* an isothermal reaction zone) which may influence the activity, selectivity, and stability of the catalyst. On the other hand, the proximity of both catalysts may benefit the conversion of CO and methanol produced over CuZnK and PdGaCuZnAlK to the surface of CuFeCoK and CuFeAlK, leading to enhanced formation of C_{2+} hydrocarbons and alcohols.

3.2.4. *Effects of reaction conditions on the performance of Cu-based catalysts*

The effects of reaction conditions on CO_2 hydrogenation over Cu-based catalysts were examined by different research groups. The CO_2 conversion was found to increase with increasing temperature (200–350 °C) when using a CuZnFeK catalyst [112]. The product distribution was also temperature-dependent. Below 250 °C, CO was the main oxygenated product whereas CO formation was suppressed above 250 °C, and ethanol formation became dominant. At 300 °C, the highest ethanol selectivity of ~20 % was obtained. Higher temperatures led to lower ethanol selectivity. Besides, methanol selectivity was found to be lower than 5 % in the investigated temperature range. The effect of GHSV was also studied over the same catalyst and it was observed that when increasing GHSV from 2000 to 20,000 h^{-1}, CO_2 conversion decreased slightly, while the selectivity to CO and ethanol remained almost constant. Consequently, the STY of ethanol was increased at higher GHSV and reached a maximum of 290 g L_{cat}^{-1} h^{-1} at a GHSV of 20,000 h^{-1}. Moreover, the methanol selectivity was very low in the reported range of GHSVs. Likewise, Yamamoto et al. also studied the effects of GHSV on the conversion of CO_2 to alcohols over Pd and Ga modified Cu/Fe- based catalysts (*i.e.* Pd-FeCuAlK-GaCuZnAlK) [59,113]. Based on their experimental results, an increase in the GHSV from 10,000 to 70,000 h^{-1} results in a decrease in the conversion of CO_2 to hydrocarbons and alcohols, while the CO selectivity increases. The possible reason for this trend is that at high GHSV values (low residence time) further hydrogenation of the intermediate CO to hydrocarbons and alcohols is occurring to a lesser extent. The effect of GHSV on the STY for ethanol was also investigated using PdGaCuZnFeAlK, GaCuZnFeAlK, and PdCuZnFeAlK catalysts (Fig. 14). When increasing the GHSV for

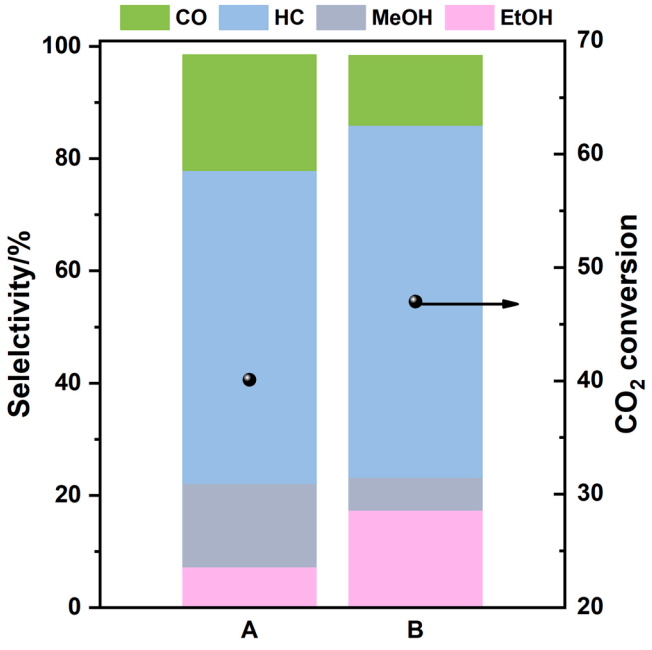

Fig. 13. CO_2 conversion and product selectivity using dual Cu- and Fe- based catalysts. A: PdGaCuZnAlK and CuFeAlK spatially separated in a dual-bed, B: A well-mixed blend of PdGaCuZnAlK and CuFeAlK [59].

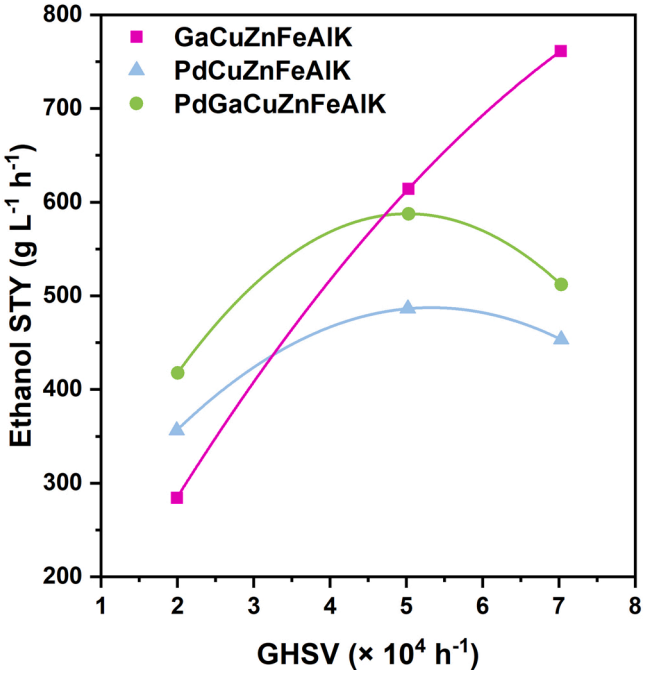

Fig. 14. The effects of GHSV on ethanol STY over PdGaCuZnFeAlK, GaCuZnFeAlK, and PdCuZnFeAlK. Adapted with permission from Ref. [59]. Copyright © 1999 Elsevier Science B.V.

PdGaCuZnFeAlK and PdCuZnFeAlK from 20,000 to 70,000 h^{-1}, the STY for ethanol showed a maximum at a GHSV of about 50,000 h^{-1}. The Ga doped catalyst performed slightly better than the unpromoted one. A different profile was found for the Pd free GaCuZnFeAlK catalyst. For this catalyst, a close to linear relation was found between the GHSV and STY. At low GHSV, the catalyst shows the lowest STY of all catalysts, though the highest STY at the highest GHSV in the range. A possible explanation is given by the authors and they propose that when using PdGaCuZnFeAlK and PdCuZnFeAlK at high GHSV values, thus at a low conversions, relatively high amounts of hydrogen are present in the gas phase. This leads to more effective hydrogen spillover through Pd. Accordingly, the catalyst surface becomes more reductive and this will retard alcohol formation.

3.2.5. *Proposed reaction mechanism for Cu-based catalysts*

Several reaction mechanisms have been proposed for alcohol synthesis from CO_2 hydrogenation over Cu-based materials. However, dedicated mechanistic studies involving reaction intermediates and active sites have not been provided yet. There is an indication that ethanol may be formed directly from CO_2 as well as from CO, and that CO is more reactive than CO_2 (Fig. 15). For example, Takagawa et al.

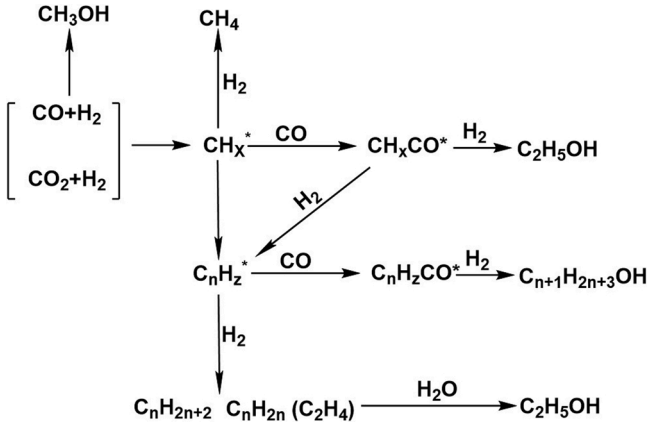

Fig. 15. Mechanism of HAS over Cu-based catalysts [38,111,133].

[112] found that methanol selectivity is low and independent of the GHSV in CO_2 hydrogenation over CuZnFeAl, indicating that methanol is likely not the intermediate product for ethanol formation. Moreover, partial replacement of CO_2 by CO in the feed gas did not change the selectivity to methanol, ethanol, and hydrocarbons (C_1–C_5). However, the total yield of the products increased at higher CO contents in the feed gas. Besides, CO selectivity remained very low in the GHSV range of 2000–20,000 h^{-1} during CO_2 hydrogenation. A study by Guo et al. also suggested that CO is an intermediate for HAS when using CuZnK-CuZnFeK [115]. Furthermore, Yamamoto et al. [59,113] found that CO selectivity increased with higher GHSV over Pd-CuFeAlK-GaCuZnAlK. They also observed that the selectivity to methanol, ethanol, and hydrocarbons decreased, suggesting that CO is an intermediate for both alcohols and hydrocarbons. Longer contact times (shorter GHSVs) were found to be beneficial for CO conversion. Besides, a significant decrease in ethylene in the C_2 hydrocarbons fraction combined with high ethanol formation rates suggests that ethanol is formed by the hydration of ethylene (Fig. 15).

Li et al. also proposed a reaction mechanism when using CuZnFeK catalysts [111]. They assume that CuZnFeK is active for the RWGS reaction producing CO while Cu and Fe carbides, formed from $CuFe_2O_4$ and $ZnFe_2O_4$ solid solutions, respectively, are active for CO_2 hydrogenation. Specifically, Fe carbides were reported to be the active sites for CO dissociation, carbon-chain propagation, and hydrogenation, while Cu sites were responsible for associative CO adsorption and alcohol formation. As presented in Fig. 15, carbon chain growth was proposed to occur through CH_x* addition forming a metal-alkyl group (C_nH_z*), which upon further hydrogenation results in the formation of hydrocarbons. Besides, adsorbed CO* can insert into a metal—nCnHz bond *via* surface migration over a short distance between Fe and Cu sites followed by further hydrogenation leading to the formation of $C_{n+1}OH$ [38]. A similar reaction mechanism for alcohols and hydrocarbons formation from CO_2 hydrogenation over Co-Mo promoted $CuLa_2Zr_2O_7$ was also proposed by Kieffer et al. [133].

Furthermore, An et al. also proposed a mechanism for ethanol synthesis over an alkali metal-doped Cu-based metal-organic framework catalyst (Zr_{12}-bpdc-Cu) by tracking reaction intermediates [116]. Alkali metal-doped Zr_{12}-bpdc-Cu was shown to be highly active when using a solvent (THF) and combined reasonable CO_2 conversion (52 %) with high ethanol selectivity (> 99 %, see Table 3). A Li promoted catalyst

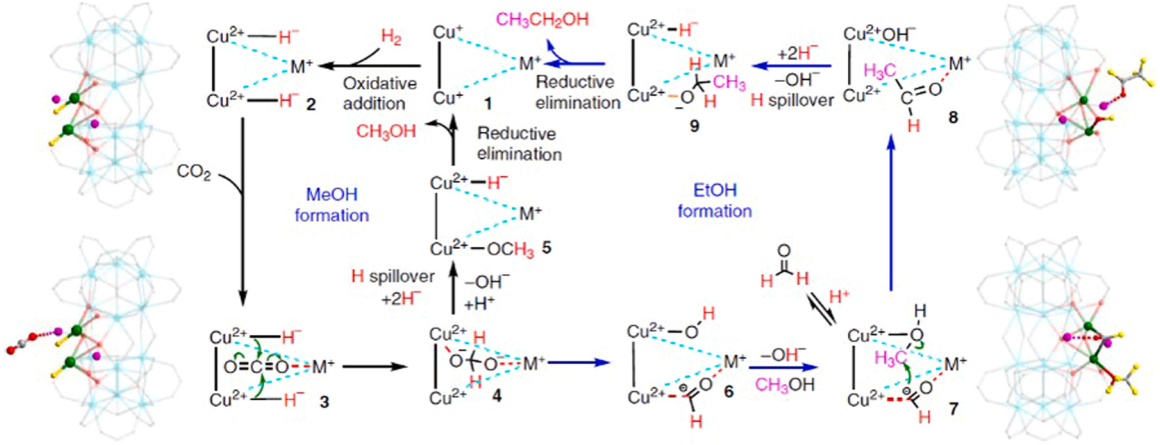

Fig. 16. Mechanism of alcohol formation over a Cu-Cu dual-site. Reproduced with permission from Ref. [116]. Copyright © 2019, Springer Nature.

(Zr_{12}-bpdc-CuLi) was used to study the mechanism. Cu^{I} centers appeared to be the active sites for ethanol synthesis, while Cu^{II} was inactive. It appears that the presence of intimate Cu^{I}–Cu^{I} centers which are stabilized by the MOF framework, are crucial for catalytic activity.

Ethanol was the main product from formaldehyde hydrogenation, indicating that formyl species are involved in ethanol formation, which was also proven by CH_3I trapping experiments. Besides, the catalyst is inactive for the hydrogenation of methanol in THF, excluding the formation of ethanol through methanol homologation. However, when $CO_2 + H_2 + {}^{13}CH_3OH$ were used as substrates, the ^{13}C label was present in the ethanol ($^{13}CH_3^{12}CH_2OH$) formed, indicating that methanol participates in ethanol formation. Kinetic studies revealed that the apparent activation energies for methanol (90.6 kJ mol^{-1}) and ethanol (91.4 kJ mol^{-1}) are similar, implying that the rate-determining step in the catalytic cycle occurs before C—C bond formation. Moreover, characterization of the used catalysts proved that Cu is mainly in the Cu^{I} form and not as Cu^{II}–$H^{-}\cdot$ This suggests that H_2 activation is the rate-determining step in the catalytic cycle (Fig. 16). The reaction probably starts with H_2 activation on Cu^{I}–Cu^{I} sites forming $(Cu^{2+}–H^{-})_2$ followed by CO_2 hydrogenation to methanol and formyl species. Then, carbon chains grow through a nucleophilic attack on the carbon of methanol by a formyl which might be stabilized by the alkali cation, resulting in CH_3CHO formation. Finally, reductive elimination leads to the formation of methanol, ethanol, and H_2O as well as the regeneration of Cu^{I}–Cu^{I}. The hydrogen required for the reaction can be supplied by either H spillover from adjacent Cu sites or the transfer of intermediates among different catalytic sites.

3.3. Mo-based catalysts

Mo-based catalysts in the form of sulfides, oxides, and carbides and promoted by K, Na, Co, Fe, and Ir have been studied for HAS under typical reaction conditions of 200–340 °C, 2.0–10.4 MPa, an H_2/CO_2 ratio of 1–5, and GHSVs between 1200–9000 $cm^3\ g_{cat}^{-1}\ h^{-1}$ in continuous plug flow fixed-bed reactor configurations (Table 4). CO_2 conversions were found in the range from 3 % to 32 %, whereas CO and hydrocarbons are typically the main products. The reported selectivity towards alcohols is relatively low and for example, ethanol selectivity over Mo-based catalysts is below 6.0 %. The highest $C_{2+}OH$ yield reported so far is only 1.92 % by using CoMoS. Besides gas-phase reactions, CO_2 hydrogenation in the presence of 1,4-dioxane as solvent was also studied in a slurry batch reactor (Table 4), showing a relatively high alcohol selectivity (25 % for ethanol). This suggests the potential of a more engineering approach to tune product selectivity. The effects of alkali metals, transition metals, catalyst support, and reaction conditions on alcohol synthesis from CO_2 hydrogenation over Mo-based catalysts will be discussed in the following sections.

3.3.1. Monometallic Mo-based catalysts

Mo-based materials are known to be active for both higher alcohol synthesis from syngas and the RWGS reaction [34,146–159], therefore, they are considered also as suitable catalysts for HAS from CO_2. Calafat et al. tested MoO_3 for CO_2 hydrogenation and only detected hydrocarbons (*i.e.* mainly methane) [143]. Moreover, Kishida et al. found that Mo/SiO_2 (reduced at 400 °C in H_2) gave a low CO_2 conversion of only about 0.5 %, with methanol as the main product (selectivity, 65.7 %), together with hydrocarbons (selectivity, 13.3 %), and CO (selectivity, 19.2 %), while no ethanol was formed [141]. On the other hand, Mo/SiO_2 activated in a CO/H_2 mixture showed a selectivity (CO free) to hydrocarbons of 75.2 %, 22.1 % for methanol, and 2.8 % for $C_{2+}OH$ [160]. Mo_2C was also investigated and a CO_2 conversion of 4.6 % was obtained with hydrocarbons and CO as the main products, though some methanol (selectivity of 17.7 %) and ethanol (selectivity 0.8 %) were formed [161]. Similar results were also found over α-MoC_{1-x} and β-MoC_y under comparable reaction conditions [144]. Chen et al. further studied CO_2 hydrogenation over Mo_2C using 1,4-dioxane as the solvent in a slurry batch reactor [145]. At these conditions, relatively high selectivity to methanol (about 53 %) and ethanol (16 %) was obtained. Additionally, MoS_2/AC mainly produced CO and hydrocarbons with a low amount of C_{2+} alcohols [142]. Thus, it can be concluded that Mo-based materials alone are not efficient for HAS. Improvements were reported by promotion with (alkali) metals, the use of supports, and process conditions, and these strategies are discussed in the following sections.

3.3.2. Effects of alkali metals on the performance of Mo-based catalysts

The promotional effect of alkali metals on Mo-based catalysts for HAS by CO_2 hydrogenation was investigated in detail by several research groups. Among these studies, Tatsumi et al. focused on the effects of different alkali metals (K_2CO_3, KF, KCl, LiCl, and NaCl) on alcohol synthesis over Mo/SiO_2 (activated in a CO/H_2 mixture at 250 °C) [160]. Based on the results obtained, KCl was shown to be the most effective promoter. The addition of KCl was found to increase the rate of alcohol and hydrocarbon formation from 26.4 to 34.1 $\times\ 10^{-2}$ mmol $g_{cat}^{-1}\ h^{-1}$ (carbon-based) with the selectivity to C_{2+} alcohols (CO free) increasing from 2.8 % to 64.9 %. Furthermore, the positive effects of K as promoter were also observed for Co-Mo oxide and Co-Mo sulfide systems [142,143,162]. The addition of K to β-$CoMoO_4$ and α-$CoMoO_4$ by mechanically mixing led to a decrease in CO_2 conversion, though enhanced production of alcohols together with a higher ethanol selectivity (CO free) compared to catalyst without K addition (Fig. 17). Besides, the addition of K to (Co)Mo sulfide shifts the main products from hydrocarbons to CO and alcohols resulting in a higher selectivity (CO free) to alcohols and C_{2+} alcohols [142,162].

Generally, the effect of alkali metals is attributed to several factors. These include:

Table 4
Representative Mo-based catalysts for HAS.

Catalyst	T[a] (°C)	P[b] (MPa)	R[c]	GHSV[d] ($cm^3\ g_{cat}^{-1}\ h^{-1}$)	X^{e}_{CO2} (%)	S^{f}_{CO} (%)	S^{g}_{HC} (%)	S^{h}_{MeOH} (%)	S^{i}_{HA} (%)	Y^{j}_{HA} (%)
CoMoS [140]	340	10.4	3	0.43[k]	32	57.5	16.5	20.0	6.0	1.92
CoMoS [140]	310	10.4	3	0.43[k]	28	58.5	6.1	31	4.4	1.23
$IrMo/SiO_2$ [141]	200	4.9	2	2000[l]	11.9	15.9	67.8	9.6	6.1	0.73
KMoCoS-AC [142]	320	5.0	3	3000	8.1	69.8	12.2	13.2	4.8	0.39
α-$CoMoO_4$/K [143]	250	3	1	1200	7.2	27.8	31.6	35.7	4.8	0.35
β-MoC_y [144]	200	2	5	~9000	6	39	36	21	3[m]	0.18
α-MoC_{1-x} [144]	200	2	5	~9000	3	52	14	28	4[m]	0.12
Co/Mo_2C [145]	200	4	3	-[n]	35[o]	9.5	17.1	46	25	n.a.
Fe/Mo_2C [145]	200	4	3	-[n]	38[o]	6.8	18.6	58	16	n.a.
Mo_2C [145]	200	4	3	-[n]	20[o]	4.9	25.8	53	16	n.a.

Footnotes: [a]Reaction temperature; [b]Reaction pressure; [c]H_2/CO_2 ratio; [d]Gas hourly space velocity; [e]CO_2 conversion; [f]Selectivity to CO; [g]Selectivity to hydrocarbons; [h]Selectivity to methanol; [i]Selectivity to higher alcohols; [j]Yield of higher alcohols; [k]GHSV in the unit of g $g_{cat}^{-1}\ h^{-1}$; [l]GHSV in the unit of h^{-1}; [m]C_{2+} oxygenates are included; [n]200 mg catalyst in 37.5 ml 1,4-dioxane for 2 h; [o]TOF of CO_2 conversion in the unit of $s^{-1} \times 10^4$.

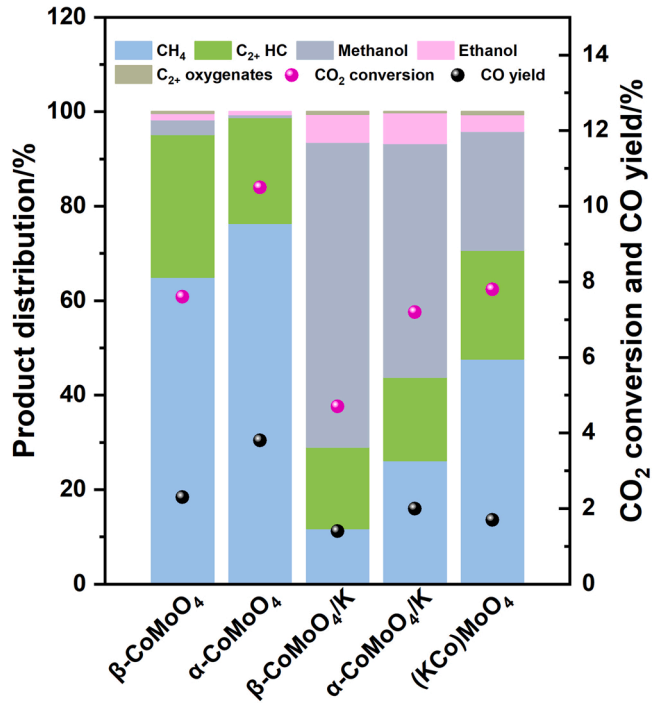

Fig. 17. CO_2 conversion, CO yield, and product distribution over $CoMoO_4$-based catalysts [143].

(i) **Poisoning of acid sites:** the addition of K by mechanical mixing is proposed to result in either an alkali overlayer in the case of α-$CoMoO_4$/K or a new phase (K_2MoO_4) in the case of β-$CoMoO_4$/K, which leads to poisoning of acid sites and thus inhibits the formation of hydrocarbons.

(ii) **Tailoring the reducibility:** incorporation of K favors the reduction of Co or Co-molybdate phases, while it inhibits the reduction of Mo-oxide phases to metallic Mo. The latter is known to favor hydrocarbon formation [163].

(iii) **Formation of active species:** K may also be part of the active centers directly involved in the reaction. Though less effective than mechanical mixing, the addition of K by coprecipitation together with Co and Mo (*i.e.* to form $K_2Co_2(MoO_4)_3$) also enhances alcohol formation (Fig. 17). It is proposed that the coprecipitation method is less effective due to the formation of $K_2Co_2(MoO_4)_3$, which reduces the accessibility of K containing active centers and is less active for HAS. Besides, additions of K to Mo sulfide-based materials lead to the formation of KMoS phases which favor CO (generated *via* RWGS) insertion promoting the formation of C_{2+} alcohols [154].

3.3.3. *Effects of transition metals on the performance of Mo-based catalysts*

Co and Fe-based catalysts are known to be effective for FTS, and thus enable carbon chain growth [164–173]. As such, both metals have been considered as a promoter to enhance HAS over Mo-based catalysts. Even though the monometallic MoO_3 system produced only hydrocarbons, alcohols were detected over Co molybdate (α-$CoMoO_4$ and β-$CoMoO_4$). However, alcohol selectivity was still very low (< 5 %, CO free) as shown in Fig. 17 [143]. α-$CoMoO_4$ gave a higher CO_2 conversion, while β-$CoMoO_4$ provided a better selectivity to alcohols. The differences in activity and selectivity for CO_2 conversion was ascribed to the reducibility of Mo^{6+} species. It has been proposed that the activity for hydrocarbons over Mo-based catalysts increases when the Mo center has a higher reduction state [163]. Under mild reaction conditions, the reduction of Mo in the α-phase is easier than that in the β-phase and thus leads to higher CO_2 conversion and hydrocarbon selectivity.

Furthermore, Co has also been used to promote HAS over Mo sulfide-based materials [140,142,162]. The addition of Co was shown to enhance the formation of alcohols in general and C_{2+} alcohols in particular. Co was hypothesized to modify the electronic state of Mo and to enhance carbon chain growth. Co was also supported on Mo_2C [145], and both the CO_2 conversion TOF and ethanol selectivity increased to 35 $\times 10^{-4}$ s^{-1} and 25 %, respectively, compared with 20 $\times 10^{-4}$ s^{-1} and 16 % over Co free Mo_2C. Besides, the Co/Mo_2C system gave a higher carbon chain growth probability. A further improvement in CO_2 conversion was found by the addition of a second promoter in the form of Fe. Though ethanol selectivity did not change, the selectivity to C_{2+} hydrocarbons increased. It is proposed that RWGS reaction occurred on Mo_2C producing CO which is subsequently hydrogenated on the surface of the Co and Fe particles as well as Mo_2C. Co and Fe are known to be effective for FTS and a higher CO surface coverage on Co/Mo_2C and Fe/Mo_2C leads to enhanced CO_2 conversion activity and carbon chain growth. Besides, Mo_2C catalysts can adsorb CO both dissociatively and associatively, while the latter is responsible for chain growth. Therefore, it is proposed that the addition of Fe promotes associative CO adsorption resulting in enhanced rates for carbon chain propagation.

Other potential promoters such as Ir were also used to promote HAS by CO_2 hydrogenation over Mo/SiO_2 (reduced in H_2 at 400 °C) [141]. Mo/SiO_2 produced mainly methanol, while Ir/SiO_2 produced only hydrocarbons. C_{2+} alcohols were not formed for both catalysts. However, Ir doped Mo/SiO_2 resulted in a higher CO_2 conversion compared to Mo/SiO_2 and Ir/SiO_2 with the formation of ethanol and propanol achieving the highest C_{2+}OH selectivity of 6.3 % at a Mo/Ir ratio of 0.33.

3.3.4. *Effects of additives and supports on the performance of Mo-based catalysts*

The type of supports and additives used for Mo-based catalysts play a crucial role for HAS by CO_2 hydrogenation. SiO_2, Al_2O_3, TiO_2, and activated carbon have been used as additives or supports for KCoMoS in CO_2 hydrogenation to higher alcohols [142,162]. The addition of inorganic supports such as SiO_2, Al_2O_3, and TiO_2 to KCoMoS influenced the CO_2 conversion slightly. On the other hand, CO selectivity increased after the incorporation of additives though the CO-free selectivity to hydrocarbons, methanol, and C_{2+} alcohols only changed slightly (Fig. 18). However, the addition of activated carbon reduced CO_2 conversion significantly to 8.5 % and decreased the CO selectivity to 64.4 %. Besides, activated carbon increased the selectivity (CO free) to hydrocarbons and C_{2+} alcohols (15.5 %), while that to methanol decreased (Fig. 18). A more isolated MoS_2 phase is postulated to be formed on the surface of activated carbon that possesses a high methanation activity [174] and low (R)WGS activity [175], resulting in lower CO selectivity

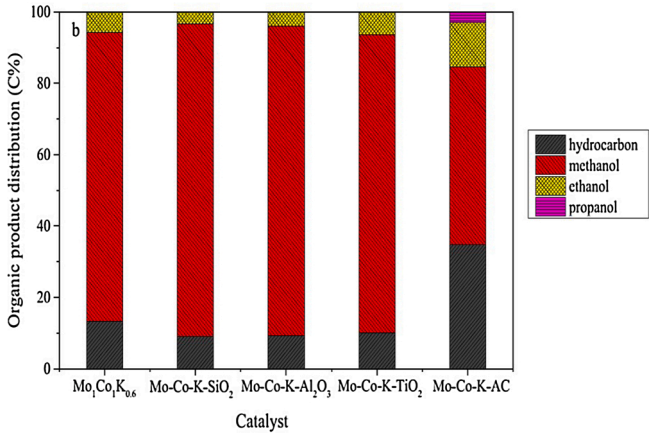

Fig. 18. Product distribution of CoMoS supported on different supports. Reproduced with permission from Ref. [162]. Copyright © 2017, Elsevier.

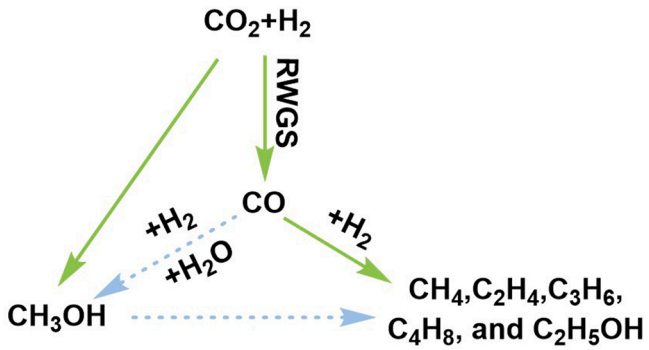

Fig. 19. Reaction pathways to produce alcohols and hydrocarbons by CO_2 hydrogenation. The solid arrows denote major pathways and the dashed arrows denote minor pathways. Adapted with permission from Ref. [145]. Copyright © 2016 Elsevier Inc.

and higher hydrocarbon (*i.e.* mainly methane) selectivity over such activated carbon-supported catalysts. Therefore, the positive effects of activated carbon on the formation of higher alcohols are ascribed to enhanced Co-Mo interactions leading to higher levels of Mo^{4+} species, which are postulated to be responsible for carbon chain propagation [176]. Support for this hypothesis was obtained by controlling the pretreatment conditions for KCoMoS/AC synthesis, where catalyst with a high Mo^{4+} content were shown to give an increased $C_{2+}OH/C_1OH$ ratio [177].

3.3.5. *Effects of reaction conditions on the performance of Mo-based catalysts*

The effects of reaction conditions on HAS by CO_2 hydrogenation over Mo-based materials have been explored in detail. Liu et al. studied the effects of temperature, pressure, and GHSV on mixed alcohol synthesis over KCoMoS catalysts [162]. As the temperature increases from 280 to 340 °C, CO_2 conversion increased from 20.7 % to 27.7 %. The CO selectivity also increased due to the endothermic nature of the RWGS reaction. Besides, the selectivity to hydrocarbons (CO free) increased with higher reaction temperatures due to enhanced hydrogenation, leading to lower alcohols selectivity (CO free). This negative effect on alcohol formation at higher reaction temperature over Mo-based catalyst was observed by various researchers [140,143–145,161,162]. Besides, it is suggested that ethanol formed by HAS may be dehydrated at 300 °C over Co molybdate-based catalysts leading to lower ethanol selectivity [143]. However, the $C_{2+}OH/C_1OH$ ratio was found to increase with increasing temperature indicating that higher reaction temperatures favor carbon chain growth. Thus, an intermediate temperature of 320 °C is preferred to achieve a relatively high $C_{2+}OH$ yield.

The effect of pressure for KCoMoS catalysts has also been investigated. CO_2 conversion increased at higher pressures in the range from 3.0 to 12.0 MPa [162]. Unfortunately, the alcohol selectivity (CO free) decreased with higher pressure, though the $C_{2+}OH/C_1OH$ ratio in the alcohol fraction increased. At 12.0 MPa, CO_2 conversion reached 28.8 % with an alcohol selectivity (CO free) of 81.8 % and C_{2+} alcohols selectivity (CO free) of 10.9 % [162]. Similar effects of pressure were also observed over KCoMoS/AC catalysts [142]. The effect of GHSV has also been explored for KCoMoS and it was shown that when increasing the GHSV from 750 to 6000 ml g_{cat}^{-1} h^{-1}, the CO_2 conversion remained about constant (25.0 %–26.1 %). The alcohol selectivity increased, as well as the CO selectivity (from 71.9 % to 78.0 %) [162]. Besides, the hydrocarbon selectivity (CO free) decreased. This trend was explained by assuming that the WGS/RWGS reactions consist of a series of fast elementary reactions that reach thermodynamic equilibrium relatively fast [178], while the consecutive CO hydrogenation is kinetically-controlled. Additionally, the effect of feed composition was also studied [140]. The authors observed an increase in CO_2 conversion, a decrease in CO selectivity, and increased alcohol and alkene selectivity when the H_2/CO_2 ratio increased from 1 to 3.

3.3.6. *Proposed reaction mechanism over Mo-based catalysts*

The commonly accepted mechanism for HAS using Mo-based catalysts involves CO_2 conversion to CO through the RWGS followed by CO hydrogenation to produce alcohols [140–142,160,162]. This is supported by experiments using $IrMo/SiO_2$ catalysts, where the selectivity to $C_{2+}OH$ for CO_2 hydrogenation was lower than for CO hydrogenation, indicating that the C_{2+} alcohols are preferentially formed *via* CO hydrogenation [141]. Tatsumi et al. also employed $KCl\text{-}Mo/SiO_2$ and suggested that the formation of alcohols proceeds *via* CO as the intermediate, though they observed enhanced alcohol formation from CO_2/H_2 compared to CO/H_2 [160]. This finding was explained by considering the ability of CO_2 to oxidize Mo species into an intermediate oxidation state that stabilizes the required active sites for alcohols synthesis.

A more complicated reaction mechanism, in which methanol and higher alcohols are formed from CO_2 by different routes, was proposed by Chen et al. using Fe/Mo_2C and Cu/Mo_2C (Fig. 19) [145]. The authors observed that when CO_2 is replaced by CO in the feed, CH_3OH formation from CO hydrogenation is by far lower than that produced by CO_2 hydrogenation, *viz.* 7.7 % over Cu/Mo_2C and 3.2 % over Fe/Mo_2C. The results indicate that most CH_3OH is formed *via* direct CO_2 hydrogenation with formates and aldehydes as the major intermediates [179,180]. However, neither formic acid nor aldehydes were detected as products, likely due to the rapid conversion of these intermediate species. Moreover, separate experiments with methanol were to determine whether this is an intermediate product. However, the methanol consumption rate was 3 %–5 % of the methanol production rate during CO_2 hydrogenation. This implies that methanol is not the major intermediate for the C_{2-4} hydrocarbons formation. It is postulated that carbon chain growth involves methoxy species (−CHO) on the surface, formed by hydrogenation of associatively adsorbed CO (Fig. 20) [181,182].

Studies have also been performed to identify which of the Mo_2C phases (α-MoC_{1-x} or β-Mo_2C) is the active phase. It was found that the α-MoC_{1-x} phase is primarily responsible for the CH_3OH formation, while CO and perhaps C_{1-4} hydrocarbons are formed mainly on the β-Mo_2C phases. Also, it is assumed that Fe is essential for carbon-chain growth and ethanol formation [181,182]. Here, associative CO adsorption, a prerequisite for carbon chain propagation occurs on Fe-Mo_2C.

3.4. *Co-based catalysts*

Co and Co-promoted by K, Ga, Pt, Ni, Fe, and Ir are among the active catalysts reported for CO_2 hydrogenation to higher alcohols (Table 5). Typical reaction conditions used for CO_2 hydrogenation to higher alcohols over Co-based materials are 200−250 °C, 1.2−5.0 MPa, 3000−6000 cm^3 g_{cat}^{-1} h^{-1}, and an H_2/CO_2 ratio of 3 in continuous plug flow fixed-bed reactor configurations.Generally, CO_2 conversion reached between 7.6 % and 28.9 %. Considerable amounts of alcohols

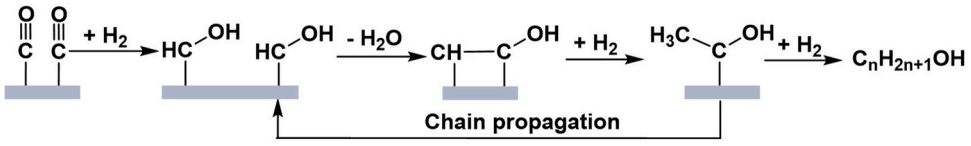

Fig. 20. CHO condensation mechanism for carbon chain growth and alcohols formation. Adapted with permission from Ref. [182].

Table 5
Representative Co-based catalysts for HAS.

Catalyst	T[a] (°C)	P[b] (MPa)	R[c]	GHSV[d] ($cm^3\ g_{cat}^{-1}\ h^{-1}$)	X^e_{CO2} (%)	S^f_{CO} (%)	S^g_{HC} (%)	S^h_{MeOH} (%)	S^i_{HA} (%)	Y^j_{HA} (%)
LaCoGaO [183]	240	3	3	3000	9.8	0	25.3	12.1	62.6	6.13
Co_3O_4 [184]	200	2	3	6000	28.9	0	~80.8	10.2	9.0	2.60
Pt/Co_3O_4 [184]	200	2	3	6000	10.7	28.3	~24.5	23.6	23.6	2.53
$NaCo/SiO_2$ [185]	250	5	3	4000[k]	18.8	29.1	61.4	1.8	7.7	1.45
Pt/Co_3O_4-p [186]	200	2	3	3000	27.3	0	80.1	15.7	4.2	1.15
KFeCo [187]	240	1	3	1.5[l]	14.5	45.5	47.2	0.7	6.6	0.96
$NaIrCo/SiO_2$ [188]	220	2	3	2000[k]	7.6	38.5	45.3	7.8	7.9	0.60
$CoNiAlO_x$ [189]	200	4	3	-[m]	n.a.	n.a.	n.a.	n.a.	>85.7	1.32[n]
$CoAlO_x$-600 [190]	140	4	3	-[o]	n.a.	n.a.	n.a.	n.a.	>92.1	>0.44[n]
Pt/Co_3O_4 [191]	200	8	3	-[p]	n.a.	n.a.	n.a.	n.a	82.5	0.42[n]

Footnotes: [a]Reaction temperature; [b]Reaction pressure; [c]H_2/CO_2 ratio; [d]Gas hourly space velocity; [e]CO_2 conversion; [f]Selectivity to CO; [g]Selectivity to hydrocarbons; [h]Selectivity to methanol; [i]Selectivity to higher alcohols; [j]Yield of higher alcohols; [k]Space velocity in h^{-1}; [l]Space velocity in nL h^{-1} $g^{-1}_{metal\ oxalates}$; [m]25 mg catalyst in 2 ml H_2O for 12 h; [n]STY based on carbon in mmol $g^{-1}_{cat}\ h^{-1}$; [o]20 mg catalyst in 2 ml H_2O for 15 h; [p]20 mg catalyst in 1 ml solvent (1,3-dimethyl-2-imidazolidinone /water) for 15 h.

are formed with methanol selectivities ranging from 0.7 % to 28.9 % and higher alcohol selectivities ranging from 4.2 % to 62.6 %, corresponding to a higher alcohol yield between 0.60 % and 6.13 %. CO selectivity ranged from negligible to 45.5 % and hydrocarbons selectivity ranged from 24.5 %–80.8 %. CO_2 hydrogenation in the presence of a solvent in slurry batch reactors has also been reported. Very high C_{2+}OH selectivities (> 82.5 %) and yield (0.42 mmol $g^{-1}_{cat}\ h^{-1}$, C-based) are reported. In the following section, the effect of alkali/alkaline earth metal and transition metal promoters, catalyst supports, reaction conditions, as well as the reaction mechanism, will be discussed.

3.4.1. *Monometallic Co-based catalysts*

The catalytic performance of CO_2 hydrogenation over monometallic Co-based catalyst is highly dependent on the electron density of the Co

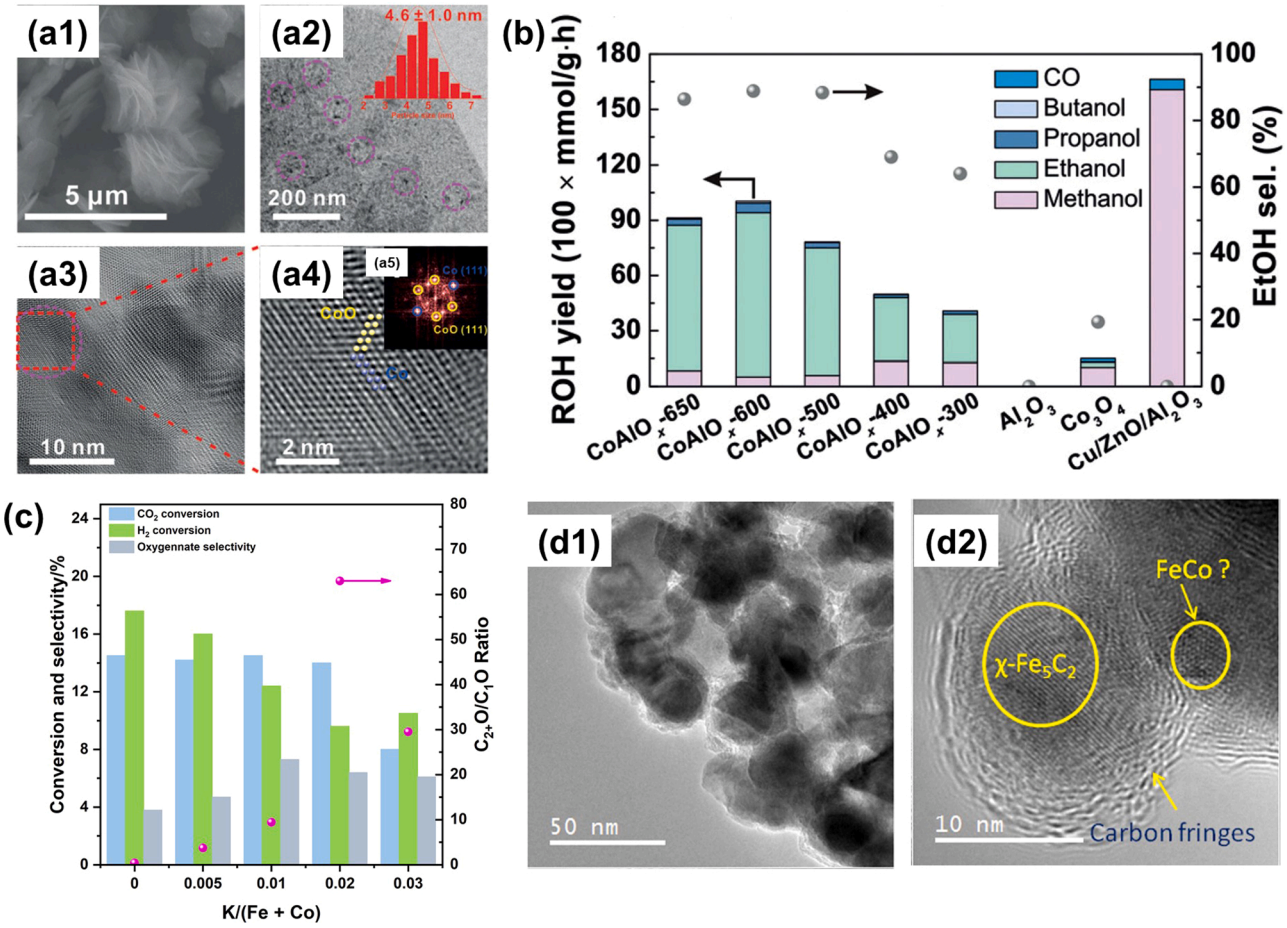

Fig. 21. (a) Electron microscopy characterization of $CoAlO_x$-600. (a1) Scanning electron microscopy (SEM) image; (a2) Transmission electron microscopy (TEM) image (inset: size distribution of the Co nanoparticles); (a3) High resolution (HR) TEM image; and (a4) Fast Fourier transform (FFT) image of the Co nanoparticles corresponding to the HRTEM image in (a3). Reproduced with permission from Ref. [190]. Copyright © 2018 Wiley-VCH Verlag GmbH & Co. KGaA. (b) Alcohols yield and ethanol selectivity over various catalysts. Reproduced with permission from Ref. [190]. Copyright © 2018 Wiley-VCH Verlag GmbH & Co. KGaA. (c) Conversion, oxygenates selectivity, and the ratio of C_{2+} to C_1 oxygenate over K-FeCo [187]. (d) HRTEM images of carburized K-FeCo. Reproduced with permission from Ref. [187]. Copyright © 2017 Wiley-VCH Verlag GmbH & Co. KGaA.

center and considerable differences were found for Co_3O_4, CoO_x, Co_2C, and metallic Co. Among them, Co_3O_4 showed a relatively low activity for CO_2 conversion and alcohol formation [191]. For a Co/SiO_2 catalyst, a strong dependence on the type of precursor used in the synthesis of the catalyst was observed [188]. The $Co(N)/SiO_2$ catalyst obtained from a nitrate precursor showed relatively high activity (~9 % CO_2 conversion) with methane as the main product. However, catalyst $Co(A)/SiO_2$, synthesized from an acetate precursor, showed low CO_2 conversion of 0.5 %. A possible explanation is the difference in amounts of metallic Co (Co^0), which is hypothesized to be the active species for methane formation, in both catalysts. Indeed X-ray photoelectron spectroscopy (XPS) confirmed this hypothesis and proved that Co in $Co(N)/SiO_2$ is more easily reduced to the metallic state than Co in $Co(A)/SiO_2$ [192–194].

Interestingly, partially reduced Co_3O_4 (CoO_x) was found to be active for CO_2 hydrogenation, ultimately leading to higher alcohol formation. Wang et al. studied the conversion of CO_2 to ethanol over $CoAlO_x$ in a slurry batch reactor. The $CoAlO_x$ catalyst was reduced at 600 °C in H_2 and shown to contain both Co^0 and CoO (Fig. 21a). The co-existence of Co^0 and CoO_x in the catalyst favors ethanol formation [190]. An impressive ethanol selectivity of 92.1 % and a STY of 0.444 mmol g^{-1} h^{-1} were obtained (Fig. 21b). Methanol, n-propanol, and n-butanol were also detected, and remarkably the most common products of CO_2 hydrogenation (CO, methane, and higher hydrocarbons) were not formed. When performing the reduction at lower temperatures (*i.e.* 300 and 400 °C), the activity and ethanol selectivity decreased considerably due to the absence of metallic Co.

Similar findings were also reported by Liu et al. when using partially reduced mesoporous Co_3O_4 [184]. Of interest was the observation of confinement effects in the mesopores. For instance, when comparing the performance of a mesoporous Co_3O_4 precursor (Co_3O_4-m) and a Co_3O_4 nanoparticle precursor (Co_3O_4-np) with similar phase composition (*i.e.* Co^0 and CoO) after reduction at 250 °C, not only the STY of alcohols for Co_3O_4-m was about 5 times higher (3.4 mmol g_{cat}^{-1} h^{-1}) but also the STY for $C_{2+}OH$ was about 40 times higher (1.6 mmol g_{cat}^{-1} h^{-1}). A possible explanation is that interactions between the CH_x species formed by CO_2 hydrogenation in the mesoporous channels lead to enhanced rates for carbon chain propagation instead of hydrogenation to form CH_4. Besides, Co_3O_4-m was stable for 50 h times on stream, while the activity of Co_3O_4-np decreased monotonously with time on stream. The mesoporous structure together with the high surface area of Co_3O_4-m was suggested to contribute to the good stability of the former catalyst.

Zheng et al. also investigated Co-oxide catalysts promoted with La for CO_2 hydrogenation [183]. CO_2 conversion over $LaCoO_3$ was found to be high (30.4 %); however, the main products were methane (with a selectivity of 97.8 %), and very low amounts of alcohols (0.5 %) were formed. The chemoselectivity was explained by considering synergistic effects between Co^0 and Co_2C species, formed by reduction and carbonization of $LaCoO_3$ during the reaction [183]. Such mixtures are known to be active for the CO_2 hydrogenation, though give methane as the main product and only minor amounts of oxygenates [195].

3.4.2. *Effects of alkali and alkaline earth metals on the performance of Co-based catalysts*

Alkali and alkaline earth metals have been used as promoters for HAS by CO_2 hydrogenation over Co-based materials. Alkali and alkaline earth metal promotion has been shown to suppress hydrogenation and enhancing carbon chain growth. For instance, Okabe et al. explored the effect of Li_2O, Na_2O, K_2O, MgO, CaO, and SrO on $IrCo/SiO_2$ catalyst for CO_2 hydrogenation [188]. For all, the formation of methane was reduced while CO formation was enhanced. It was found that the observed effects were stronger for the most basic alkali or alkaline earth metals. Besides, CaO was shown to promote (mainly) methanol formation (selectivity of 35.2 %), while alkali metal (Li_2O, Na_2O, and K_2O) additives also enhanced ethanol formation, giving a maximum ethanol selectivity of 7.9 % with Na_2O promotion.

Moreover, K has been used to promote C_{2+} oxygenates formation over FeCo-based catalysts [187]. H_2 conversion decreased with increasing K/(Fe + Co) ratio indicating that the hydrogenation activity is reduced at higher ratios (Fig. 21c). A possible explanation is the deposition of higher amounts of carbon on the surface of Fe with K promotion causing lower hydrogenation activity. Besides, K addition may weaken the Fe—H bond leading to a lower rate of H_2 dissociation. As a consequence, K addition inhibits hydrocarbons formation (with selectivity, from 81.0 %to to 35.7 %–69.1 %), while promoting C_{2+} oxygenates formation (with selectivity, from 1.1 % to 3.7 %–6.6 %)

It has also been proposed that alkali and alkaline earth metal promotion of Co catalysts leads to stabilization of carbide species and inhibition of the formation of Co^0, which is negative for HAS. For instance, Gnanamani et al. found that $NaCo/SiO_2$ activated in CO contained both CoO and Co_2C and was an active and stable catalyst for HAS [196]. The CO activated Na free Co/SiO_2 catalyst showed a low HAS selectivity while methane selectivity was high. Although the catalyst was shown to contain both CoO and Co_2C phases before reaction, it was shown that the Co species can be reduced easily to Co^0, which is known to be an active component for CO_2 methanation. Another study by Gnanamani et al. showed that K promotion of FeCo-based catalysts facilitates the dissociative adsorption of CO and CO_2, which increases the extent of carbon deposition on Fe in a stable semicrystalline form and as such stabilizes the surface carbides (Fig. 21d) [187].

3.4.3. *Effects of transition metal on the performance of Co-based catalysts*

Transition metals including Ga, Fe, Ni, and Pt have been used to promote Co-based catalysts for CO_2 hydrogenation to higher alcohols.

(i) **Effect of Ga:** Ga was studied as a promoter for alcohol synthesis over $LaCo_{(1-x)}Ga_xO_3$ catalysts [183]. It was observed that the Ga free $LaCoO_3$ produces mainly methane with a very low alcohol selectivity of 0.5 %. Ga promotion decreased CO_2 conversion and shifted the product selectivity to alcohols, particularly ethanol. Using $LaCo_{0.7}Ga_{0.3}O_3$ as a catalyst, an alcohol selectivity of 74.7 % with an ethanol weight fraction of 88.1 % was obtained at a CO_2 conversion of 9.8 %. Enhanced alcohol formation can be ascribed to the presence of a Co-Ga interaction, which leads to a slightly positive charged Co center ($Co^{\delta+}$) on the catalyst surface, as was shown by XPS. Synergic effects between Co^0 and $Co^{\delta+}$ centers are postulated to reduce the hydrogenation ability of metallic Co, inhibiting CH_4 formation by hydrogenation, and thus enhance ethanol synthesis [197,198].

(ii) **Effect of Ir:** the effects of Ir promotion on alcohol synthesis by CO_2 hydrogenation over a Co/SiO_2 catalysts prepared from nitrate (N) and acetate (A) precursors was investigated [188]. The addition of Ir to $Co(A)/SiO_2$ gave a very positive effect and led to higher CO_2 conversions (from 0.5 % to 10.0 %) accompanied by enhanced methanol formation [199–204].

(iii) **Effect of Fe:** carburized FeCo-based catalysts were reported to be active materials for CO_2 hydrogenation [195]. It is observed that the hydrogenation activity and methane selectivity were decreased with increasing Fe/Co ratio. However, the selectivity to C_{2-4} hydrocarbons and CO were increased. With higher Fe/Co ratios, the selectivity to oxygenates was increased first then decreased and the optimum selectivity of 4.5 % was reached using $Co_{50}Fe_{50}$. It was also shown by Mössbauer spectroscopy that oxygenate selectivity and CO_2 conversion increased with higher Fe carbide content in the catalysts ($Fe_{100} < Co_{25}Fe_{75} < Co_{50}Fe_{50}$). This is in line with a previous study that suggested that the active sites of carburized CoFe are associated with the Fe carbide species [187].

(iv) **Effects of Ni:** Ni has also been used as a promoter to enhance alcohol formation over $CoAlO_x$ catalysts for CO_2 hydrogenation [189]. Ni free $CoAlO_x$ containing metallic Co and CoO showed ethanol productivity of 0.88 mmol g_{cat}^{-1} h^{-1}. Ni promotion of

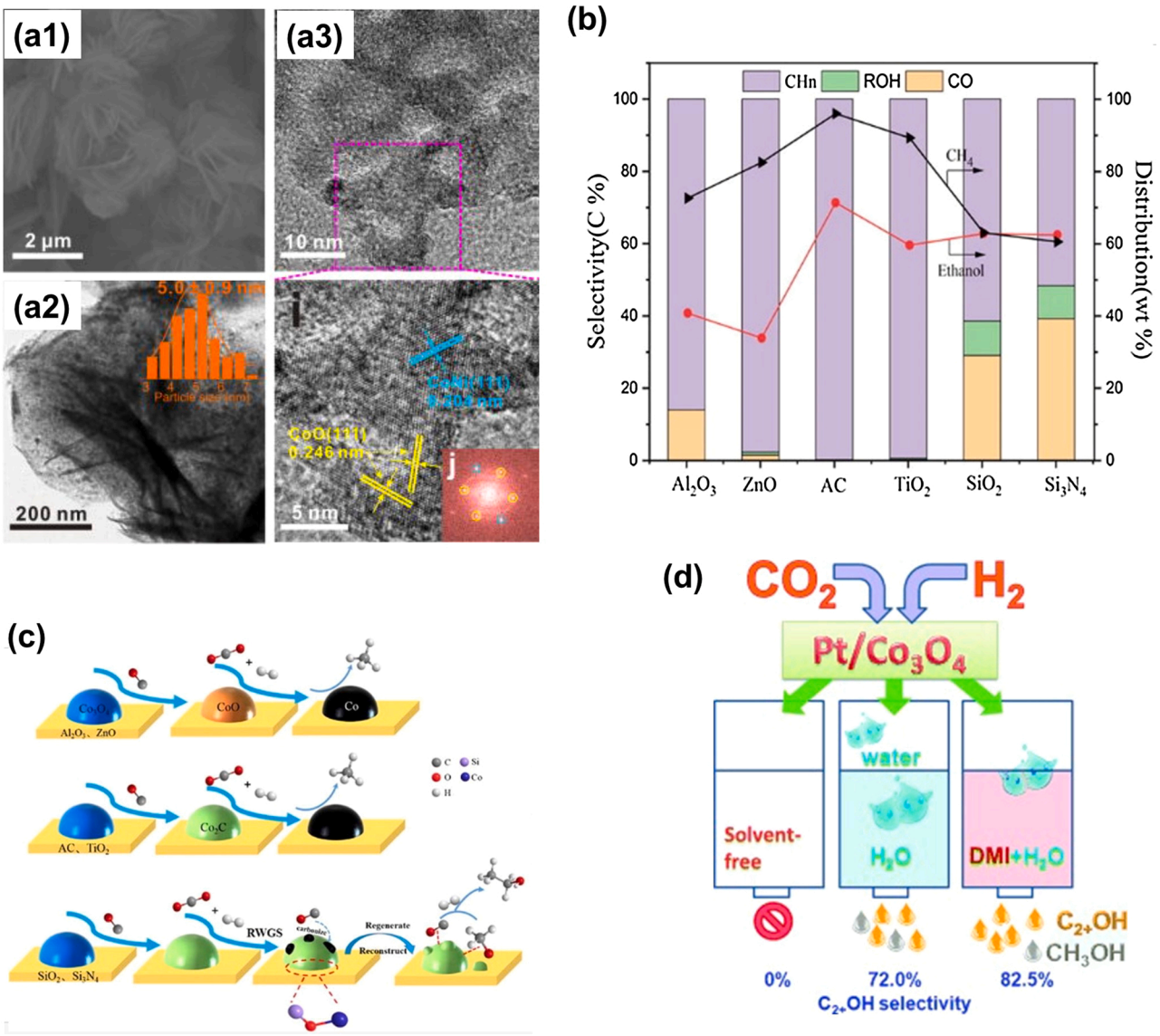

Fig. 22. (a) Electron microscopy characterization of $Co_{0.52}Ni_{0.48}AlO_x$. (a1) SEM image. (a2, a3) TEM images (inset in a2: nanoparticle size distribution). Reproduced with permission from Ref. [189]. Copyright © 2019 American Chemical Society. (b) Product selectivity and distribution of Na promoted Co supported on various supports. Reproduced with permission from Ref. [185]. Copyright © 2019 Elsevier Inc. (c) Schema of Co phase transformation supported on various supports for CO_2 hydrogenation. Reproduced with permission from Ref. [185]. Copyright © 2019 Elsevier Inc. (d) The selectivity of ethanol over Pt/Co_3O_4 in various solvents. Reproduced with permission from Ref. [191]. Copyright © 2016 WILEY-VCH Verlag GmbH & Co. KGaA.

$Co_{0.52}Ni_{0.48}AlO_x$ which contains a Co-Ni alloy and CoO phases (Fig. 22a) is more active and ethanol productivity is increased to 1.32 mmol g_{cat}^{-1} h^{-1} with a selectivity of 85.7 %. In contrast, the Co free Ni catalyst ($NiAlO_x$) showed very low ethanol productivity (0.10 mmol g_{cat}^{-1} h^{-1}) with methanol as the major product. The positive effects of Ni are speculated to be related to the presence of the Co-Ni alloy. On this alloy, the absorbed CH_x* is stabilized and shows a lower rate of reaction to methane.

(v) **Effects of Pt:** the promotional effect of Pt on HAS from CO_2 was studied for Co_3O_4 catalysts with different morphologies (nanoplates and nanorods) [186]. Co_3O_4 nanoplates (Co_3O_4-p) were found to be more easily reduced than the nanorods (Co_3O_4-r). The addition of Pt was found to lead to higher levels of reduction of Co_3O_4 due to hydrogen spillover from Pt to Co_3O_4 [205]. Significant differences in reduction levels were observed for the two types of catalysts (nanorods and nanoplates). The Co in Pt/Co_3O_4-p was fully reduced to metallic Co at 250 °C, while the reduction was less facile for Pt/Co_3O_4-r and Co was mainly present as CoO. CO_2 hydrogenation experiments, with both catalysts, showed a high selectivity to hydrocarbons, while the alcohols selectivity was < 2 % over Pt/Co_3O_4-p and < 4 % over Pt/Co_3O_4-r. The reduction temperature was shown to affect the chemoselectivity of the reaction considerably. When reduced at 200 °C, Pt/Co_3O_4-p showed a much higher selectivity to alcohols (26.7 %) than at 250 °C, with methanol as the main product. Enhanced alcohol formation over this catalyst was assigned to the coexistence of CoO and metallic Co phases.

Liu et al. also showed a similar trend for Pt promotion when using mesoporous Co_3O_4. The addition of Pt was found to decrease the methane selectivity and to increase the selectivity to alcohols and CO [184]. For alcohols, the selectivity reached 47.2 % with a $C_{2+}OH$ STY of 1.5 mmol g_{cat}^{-1} h^{-1} over Pt promoted mesoporous Co_3O_4.

3.4.4. *Effects of support on the performance of Co-based catalysts*

Support effects for Co-based catalysts for CO_2 hydrogenation to

higher alcohols have been investigated. Zhang et al. explored this effect using Na-promoted Co-based catalysts [185]. These included $NaCo/Al_2O_3$, NaCo/ZnO, NaCo/AC (activated carbon), $NaCo/TiO_2$, $NaCo/SiO_2$, and $NaCo/Si_3N$, activated in a CO atmosphere prior to CO_2 hydrogenation. Among the prepared catalysts, only $NaCo/SiO_2$ and $NaCo/Si_3N_4$ produced alcohols, with selectivities of 9.54 % (87.50 % $C_{2+}OH$) and 9.19 % (88.48 % $C_{2+}OH$), respectively (Fig. 22b). Alcohol selectivity was shown to be related to the amount of Co_2C present in the catalyst formulation. As shown in Fig. 22c, Co_3O_4 and/or CoO species are present on Al_2O_3 and ZnO, while Co_2C and CoO species coexist on AC, TiO_2, SiO_2, and Si_3N_4 supported Co-based catalyst after pre-treatment by CO. After the reaction, metallic Co was present when using the ZnO, Al_2O_3, AC, and TiO_2 support while Co_2C was predominant on SiO_2 and Si_3N, and is proof that the latter phases are active for HAS [206,207].

3.4.5. Effects of reaction conditions on the performance of Co-based catalysts

Reaction conditions significantly influence the catalytic performance of CO_2 conversion to higher alcohols over Co-based materials. The effect of temperature was studied for $LaCo_{1-x}Ga_xO_3$, Co_3O_4, and Pt/Co_3O_4 [183,184,186]. In all cases, CO_2 conversion increased and total alcohol selectivity decreased at higher temperatures. Also, the STY for $C_{2+}OH$ alcohols and the fraction of $C_{2+}OH$ in the alcohols increased at higher temperatures. This trend was explained by considering that a positive of temperature on the rate of CO_2 conversion, and a preference for $C_{2+}OH$ due to favorable thermodynamics at a higher temperature [184,186]. However, the trend is not observed for all catalysts and a decrease of the $C_{2+}OH$ fraction in the alcohol mixture at higher temperatures occurred over $LaCo_{0.7}Ga_{0.3}O_3$. This might be due to a higher level of oxidation of metallic Co by CO_2 during the reaction [183].

The effect of temperature on HAS by CO_2 hydrogenation over $CoNiAlO_x$, Co_3O_4, and Pt/Co_3O_4 catalysts has also been investigated in the presence of solvents [189–191]. At higher temperatures, the STY for alcohols increased whereas the $C_{2+}OH$ selectivity and STY increased first and then leveled off at higher temperatures. The effect of solvents on ethanol formation was also studied by He et al. over Pt/Co_3O_4 [191]. As presented in Fig. 22d, alcohols were not formed at solvent-free conditions. When using water, a significant increase in CO_2 conversion and $C_{2+}OH$ selectivity was found and the $C_{2+}OH$ selectivity reached 72.0 %. Solvents such as 1,3-dimethyl-2-imidazolidinone (DMI) and N-methyl-2-pyrrolidone (NMP) led to higher STY for alcohols, though the $C_{2+}OH$ selectivity was much lower *i.e.* 29.0 % and 9.8 %, respectively. Hydrocarbon-based solvents such as cyclohexane and n-decane have poor performance and a low STY for alcohols and $C_{2+}OH$ selectivity was found. The best results were obtained with a combination of DMI and water as the solvent. A mixture with 15 vol% H_2O gave the highest selectivity to $C_{2+}OH$ (82.5 %) and alcohol yield. It was assumed that H_2O protonates methanol, followed by dissociation into CH_3*, OH*, and H* (or H_2O) species on the catalyst surface. Then, these absorbed CH_3* species react with CO to form absorbed CH_3CO*, which is subsequently hydrogenated to ethanol.

3.4.6. Proposed reaction mechanisms for HAS using Co-based catalysts

Several mechanisms have been proposed for alcohol synthesis by CO_2 hydrogenation over Co-based catalysts. Zheng et al. proposed a mechanism for ethanol synthesis over $LaCo_{1-x}Ga_xO_3$ [183]. They propose that ethanol is formed over Co^0 and $Co^{\delta+}$ sites, stabilized by LaGa oxide. In the first steps H_2 is dissociated on Co^0 sites [186,208], whereas CO_2 is adsorbed dissociatively and subsequently hydrogenated to CH_3* species on Co^0 sites [190]. Besides, non-dissociative CO_2 adsorption may also occur on $Co^{\delta+}$ sites and the reaction with H* leads to the formation of absorbed HCOO*· This species may decompose at the surface to form absorbed CO*. Finally, the coupling of CO* and CH_3* led to the formation of CH_3CO* which then can be converted to ethanol by further hydrogenation.

Gnanamani et al. proposed a similar CO insertion mechanism for alcohol synthesis over carburized $NaCo/SiO_2$ [196]. However, it was suggested that the carbon chain may also grow through a carbene type insertion mechanism (Fig. 6 ii).

The CO insertion mechanism for higher alcohols formation *via* CO_2 hydrogenation was studied by *in-situ* diffuse reflectance infrared Fourier transform spectroscopy (DRIFT) over carburized $NaCo/SiO_2$ [185]. In a CO_2/H_2 atmosphere, bands for CO_3^{2-}, $HCOO^-$, O—C—O (stretching), CH_4, chemisorbed and gas-phase CO, adsorbed CHO*, unsaturated C—H (CH_x*), methoxy (CH_3O*) were observed. Similar intermediates were found for CO_2 hydrogenation, indicating a similar reaction mechanism for CO_2 and CO hydrogenation over $NaCo/SiO_2$. It was suggested that CO* is generated by the RWGS reaction and that it is subsequently hydrogenated to CH_x*. Finally, the insertion of CO* and the subsequent hydrogenation resulted in the formation of ethanol.

He et al. found that the use of water as a solvent promotes ethanol formation through CH_x—CO coupling over Pt/Co_3O_4 [191]. It was speculated that water protonates methanol followed by dissociation into CH_3*, OH*, and H* (or H_2O) species. Subsequently, CH_3CO* can be formed through CH_3*—CO coupling, and hydrogenation finally leads to the formation of ethanol. Using deuterium and ^{13}C labeling this mechanism was proven by showing that parts of the C and H in ethanol were derived from methanol and water.

Gnanamani et al. proposed that the presence of K has an impact on the mechanism for oxygenates formation over carburized CoFe (Fig. 23a) [195]. As presented in Cycle A, in the presence of K, the RWGS reaction is promoted over carburized CoFe and generates CO from CO_2. The insertion of absorbed CO into an M—CH_3 bond (*i.e.* M is the active metal) results in the formation of an acyl group which is converted in the presence of K to a K stabilized carboxylate. The latter can be converted to either acetic acid by reaction with water or to acetaldehyde by reaction with H_2. The relative rate of both reactions, thus the chemoselectivity will depend on reaction parameters such as temperature. A competing route to ethanol does not involve K and is represented as Cycle B in Fig. 23a.

Higher alcohol formation by a COOH—CH_x coupling mechanism (Fig. 6 iv) was proposed by Wang et al. [190]. Operando FTIR was performed to study the mechanism of ethanol synthesis by CO_2 hydrogenation over $CoAlO_x$ in a continuous CO_2 flow with pulsed hydrogen. In a CO_2 atmosphere, the formation of $CO_2^{\delta-}$, CO_3^{2-}, and $HCO_3^{\delta-}$ species was observed due to the initial adsorption and activation of CO_2. After pulsing H_2, CH_x*, and $HCOO^-$ were formed. Among the intermediates, $HCOO^-$ was considered to be relatively stable and thus difficult to be hydrogenated [209], and thereby inhibiting the formation of methanol. Upon the introduction of additional H_2, $HCOO^-$ and CH_x* were consumed, while acetate species were formed by CH_x* and $HCOO^-$ coupling, hindering the undesired hydrogenation of CH_x* to methane [190,210,211]. Compared to formate, the C═O bond in the acetate species is weaker facilitating further hydrogenation to form ethoxy species and ethanol [212].

CO_2 hydrogenation was also studied using a Ni promoted $CoAlO_x$ catalyst by *in-situ* FTIR spectroscopy in CO_2/H_2 atmosphere [189]. It was found that HCOO* may be formed through the reaction between chemically adsorbed CO_3^{2-} and H*, which is then converted to CH_x*. The intensities of the peaks arising from CH_x* are much lower than those of HCOO*, indicating CH_x* formation as the rate-determining step.

3.5. Miscellaneous catalysts

In addition to the catalyst groups discussed above, other types of catalysts have also been reported for CO_2 hydrogenation to higher alcohols and the most relevant ones are discussed below.

(i) **PtRu/Fe_2O_3catalyst:** He et al. studied the synthesis of higher alcohols by CO_2 hydrogenation over $PtRu/Fe_2O_3$ in a slurry batch reactor [213]. The incorporation of Pt and Ru was found to

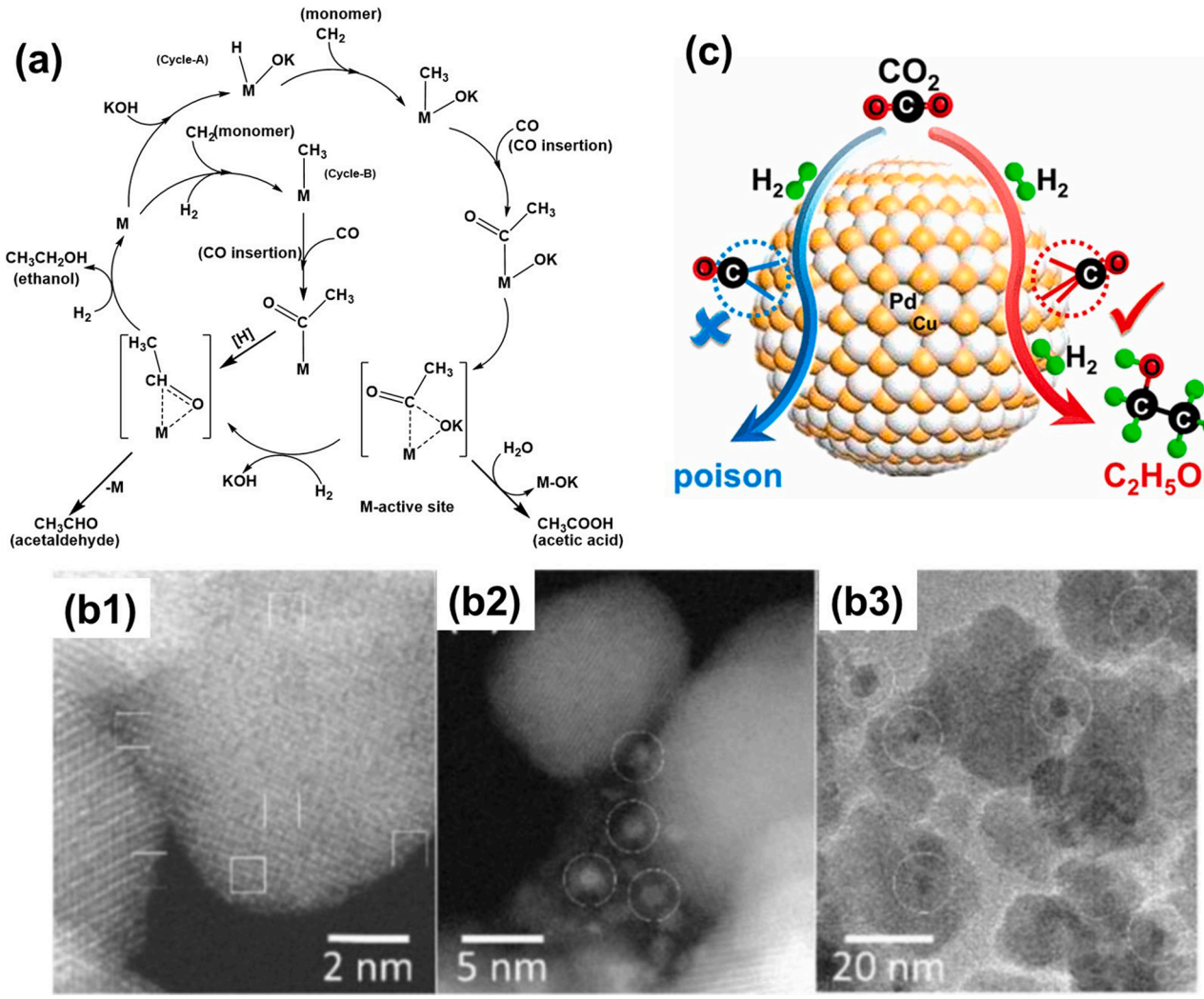

Fig. 23. (a) A plausible mechanism for the formation of C_{2+} oxygenates over alkalized metal surfaces. Adapted with permission from Ref. [195]. Copyright © 2016, American Chemical Society. (b) Representative aberration-corrected high-angle annular dark-field scanning transmission electron microscopy (HAADF-STEM) images of Pd/Fe_3O_4. (b1) SA-Pd/Fe_3O_4; (b2) CL-Pd/Fe_3O_4; and (b3) NP-Pd/Fe_3O_4. Reproduced with permission from Ref. [214]. Copyright © 2018 Wiley-VCH Verlag GmbH & Co. KGaA. (c) Schema for ethanol formation over PdCu catalyst. Reproduced with permission from Ref. [216]. Copyright © 2017 American Chemical Society.

facilitate the reduction of Fe_2O_3 due to the interaction between Pt, Ru, PtRu, and Fe_2O_3. After the reduction, the Fe_2O_3 support was partly reduced to Fe_3O_4 and Fe^0. Unpromoted Fe_2O_3 was not very active for CO_2 conversion (0.1 mmol CO_2 g_{cat}^{-1} h^{-1}) and only produced hydrocarbons. On the other hand, the Pt/Ru modified catalysts showed much higher activity (1.9–2.6 mmol CO_2 g_{cat}^{-1} h^{-1}) and alcohols were also formed, though the main products were still hydrocarbons. The chemoselectivity was highly dependent on the composition of the catalysts. Pt/Fe_2O_3 and Ru/Fe_2O_3 gave mainly methanol and low amounts of $C_{2+}OH$. Catalysts with a Pt/Ru ratio of 1/2 showed the best performance with a CO_2 conversion rate of 2.4 mmol CO_2 g_{cat}^{-1} h^{-1} together with the highest selectivity to alcohols (42.3 %) and $C_{2+}OH$ (36.0 %).

(ii) **Pd/Fe_3O_4catalyst:** Caparrós et al. reported CO_2 hydrogenation to ethanol over Pd/Fe_3O_4 catalysts [214]. Different catalysts *i.e.* Pd single atoms (SA-Pd/Fe_3O_4, 0.1 wt% Pd), clusters (CL-Pd/Fe_3O_4, 0.38 wt% Pd, 1.2 ± 0.2 nm), and nanoparticles (NP-Pd/Fe_3O_4, 3.0 wt% Pd, 4.3 ± 0.4 nm) were supported on Fe_3O_4 (Fig. 23b). CO was found to be the main product over CL-Pd/Fe_3O_4 and NP-Pd/Fe_3O_4 (selectivity > 80 %), while the $C_{2+}OH$ selectivity ranged from 2.5 % to 19.8 % (300–400 °C). For the SA-Pd/Fe_3O_4 catalyst, only alcohols were formed with ethanol productivity of 413 mmol EtOH g_{Pd}^{-1} h^{-1} and selectivity of 97.5 % at 300 °C. The Pd nanoparticle size was shown to affect catalyst performance. Smaller Pd particles gave higher ethanol selectivity and yield, with Pd single atoms maintained the highest ethanol selectivity and yield. Moreover, a decrease in ethanol selectivity at higher temperatures over SA-Pd/Fe_3O_4 was postulated to the formation of Pd nanoparticles (1.1 ± 0.3 nm) due to the mobility of Pd atoms. At higher temperatures, the CO_2 conversion increased while the ethanol selectivity decreased. However, propanol and trace amounts of butanol were formed at higher temperatures. High pressures were shown to enhance CO_2 conversion (to 1.4 %). An experiment at low temperature and high pressure (*i.e.* 250 °C and 30 bar). gave an ethanol selectivity of 98.0 %, and an ethanol yield of 440 mmol EtOH g_{Pd}^{-1} h^{-1}.

Similar results were obtained by using CO/H_2 as a feed gas, indicating CO as an intermediate for alcohol formation over the SA-Pd/Fe_3O_4 catalyst. This might be due to the presence of Fe_3O_4 which is known to be active for the RWGS reaction generating CO for the further hydrogenation step [215].

(iii) **Pd-Cu nanoparticles:** Bai et al. investigated ethanol synthesis by CO_2 hydrogenation over bimetallic Pd-Cu catalysts with P25 TiO_2 as the support in the presence of water solvent in a slurry batch reactor [216]. A methanol yield of 8.9 mmol g^{-1} h^{-1} and an ethanol yield of 9.1 mmol g^{-1} h^{-1} were obtained using the Pd/P25 catalyst. The incorporation of Cu resulted in a higher ethanol yield (1.5 mmol g^{-1} h^{-1}) over Pd_2Cu/P25 (Pd/Cu = 2); however, a further increase in the Cu content leads to a lower ethanol yield. The interaction between Pd and Cu was supposed to enhance the reducibility of surface oxides to a metallic state, which is regarded as the active site for CO_2 activation with these types of catalysts. Furthermore, support effects were studied by using bimetallic Pd_2Cu catalysts supported on SiO_2, CeO_2, and Al_2O_3. Among all, Pd_2Cu/P25 exhibited the highest TOF_{Pd} and ethanol selectivity, which was ascribed to oxygen vacancies on P25 that facilitate CO_2 hydrogenation. It was also observed, methanol yield was independent of the temperature, while the yield and selectivity to ethanol were increased. This was rationalized by considering the activation energies for the relevant reactions. Ethanol formation was shown to have a high apparent activation energy (~161.3 kJ mol^{-1}) favoring a high reaction temperature. By *in-situ* DRIFT experiments, intermediates including carboxylate ($CO_2^{\delta-}$), bidentate carbonate, unidentate carbonate, alkoxy species, formate species ($HCOO^-$), CH, and 3-fold bridge-bonded CO species (CO*) were observed over Pd_2Cu/P25. Therefore, it was proposed that ethanol is most likely formed through the insertion of CO* into CH_3*. As presented in Fig. 23c, the presence of too high amounts of Cu in the catalyst formulation leads to the formation of a stable 2-fold bridge-bonded CO* with a higher surface coverage of Pd sites, which can be a catalyst poison. Therefore, the rate-determining step for ethanol formation was hypothesized to be the hydrogenation of CO* to HCO* [72].

(iv) **Au/TiO_2catalysts:** Wang et al. investigated ethanol synthesis *via* CO_2 hydrogenation over supported Au-based catalysts in a slurry batch reactor [217]. It was found that smaller particles and a higher Au dispersion lead to improved catalytic performance. Au nano-clusters (1.0 ± 0.1 nm) supported on TiO_2 gave the highest ethanol yield of 635.4 mmol g_{Au}^{-1} h^{-1}. Moreover, among the different titania polymorphs tested including anatase (a), rutile (r), brookite (b), and amorphous (am), a-TiO_2 was the most suitable support for ethanol synthesis and an ethanol selectivity > 99 % and activity of 942.8 mmol g_{Au}^{-1} h^{-1} were reported. These findings were rationalized by considering the number of oxygen vacancies in the support, which is highest for the a-TiO_2 support. The effect of different solvents such as N-methyl-2-pyrrolidone, cyclohexane, tetrahydrofuran, water, and *N,N*-dimethylformamide on the performance of the Au/a-TiO_2 was also studied and *N,N*-dimethylformamide gave the best results. Furthermore, 240 °C is optimal, and higher reaction temperatures led to a decreased ethanol selectivity and yield, possibly due to the enhanced CO formation by the RWGS reaction.

In general, Fe, Co, and Cu can work as both active sites and additives. As active sites, Fe, Co, and Cu participate in CO_2 activation, carbon-chain propagation, and hydrogenation, while they tailor the electronic structure of the catalyst when working as an additive. For example, as an active site, Fe is responsible for methanation, RWGS, and the formation of hydrocarbons, while Fe can tailor the electronic structure of Rh to enhance higher alcohol synthesis working as an additive in a FeRh-based catalyst. Cu is the active site for the formation of alcohols, while it works as an additive in a CuPd-based catalyst facilitating the reduction of surface oxides through Cu-Pd interaction. Co is the active site for methanation, hydrocarbon formation, and alcohol formation, while it tailors the reducibility of Mo as an additive in a CoMo-based catalyst.

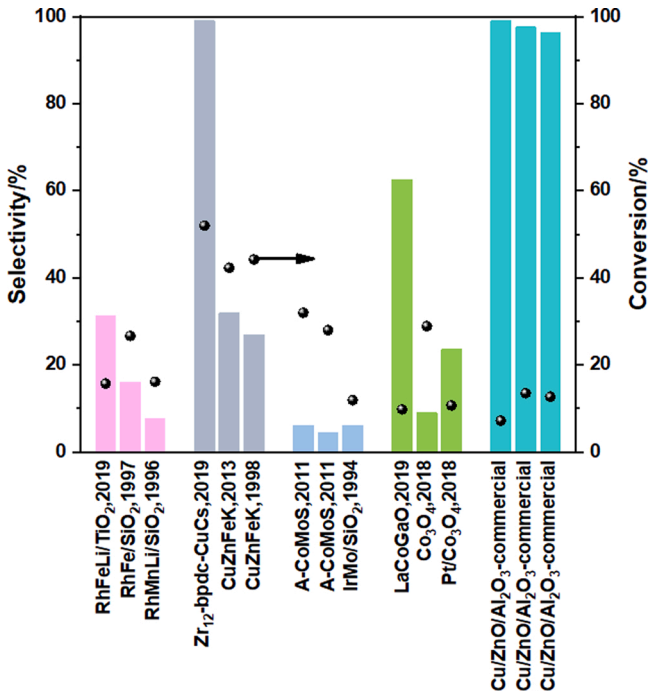

Fig. 24. Comparison of high-performance HAS catalysts with MS catalyst [218–220]. The selectivity for HAS catalysts is only for higher alcohols (C_nOH, n ≥ 2), while that of the MS catalyst includes only methanol.

3.6. Potential of HAS by CO_2 hydrogenation

As we discussed in the introduction, the societal demand to decrease CO_2 emissions has opened new directions to create sustainable solutions for chemicals and fuel production using CO_2 as a carbon feedstock. Besides, there are potential cost savings from carbon tax. In this respect, CO_2 valorization by thermocatalytic processes to HAS presents an interesting opportunity. The industrial implementation of HAS greatly depends on both the cost of renewable H_2 production and catalysts. Though further improvements are still required, and hydrogen prices need to be reduced, renewable H_2 production by water electrolysis using renewable electricity generated from solar PV or wind turbines is considered an established technology. Thus, currently, the techno-economic feasibility of HAS using CO_2 as the feed will heavily depend on the advancement of the catalytic hydrogenation step.

Substantial progress has been made in the field of exploratory catalyst development and suitable catalyst families for HAS have been identified and tested on lab scale. To illustrate the progress achieved over the past years, the performance of state-of-the-art HAS catalysts were compared with methanol synthesis (MS) catalysts. The results are provided in Fig. 24. It can be seen that HAS catalysts generally possesses a higher conversion due to the favorable thermodynamics. However, compared with MS catalysts, the selectivity of most HAS catalysts is usually much lower producing a mixture of alcohols and resulting in higher cost for downstream processing. Thus, HAS would be more favorable if the selectivity to a certain $C_{2+}OH$ is high enough for simple downstream separations because of the higher value of HA. Even though a high selectivity was obtained by Zr_{12}-bpdc-CuCs, the main product is ethanol, and direct synthesis of C_{3+} alcohols would further enhance the economic advantage of this process.

4. Summary and future perspectives

CO_2 hydrogenation to higher alcohols is considered an attractive technology for the conversion of CO_2 to value-added chemicals and fuels and has been studied extensively in the past decades. Several promising

categories of catalysts, including Rh-, Cu-, Mo-, and Co-based catalysts, have been developed. The effects of catalyst's structure, promoters, supports, catalyst precursors and reaction conditions on the catalytic performance have been studied. Also, structure-performance correlations and reaction mechanisms have been proposed.

The catalytic performance of the four categories of catalysts are comparable with each other, thus it is difficult to suggest which category of catalyst is more likely to achieve industrial applications in the future. However, several issues should be considered for further catalyst development.

(i) Selectivity to higher alcohols: is one of the most important concerns. The selectivity to higher alcohols over most of the reported catalysts tested in a fixed bed reactor is relatively low, and the highest selectivity to higher alcohol of 83 % was obtained by $Rh_{10}Se/TiO_2$. Some catalysts possess high selectivity to higher alcohols in a slurry bed reactor (*e.g.* > 99 % over CuCs and > 92.1 % over $CoAlO_x$-600). However, the selectivity is only 25 % over Mo-based catalysts. Further study should aim for improving the selectivity to higher alcohols for reactions in a fixed bed reactor.
(ii) Cost of the catalyst: is one of the critical issues for a successful catalyst development. Compared to Cu-, Mo-, and Co-based materials, Rh is scarcer and more expensive, so Cu-, Mo-, and Co-based catalysts are more favorable for industrial applications.
(iii) Stability of the catalyst: is also important during catalysts design. One of the possible CO_2 sources is an emission from the power plants which also contains S, a poison for many catalysts. Rh- [221,222], Cu- [223], and Co-based [224] catalysts are sensitive to S poisoning and may possess a shorter lifetime. Mo-based catalysts such as MoS_2 and MoC are sulfur tolerant [225,226], which may possess a longer life in the presence of S in the feed. Even though a pretreatment is possible to remove S from the feed, the deep desulfurization of the feed is an expensive process.

Moreover, higher alcohol synthesis by CO_2 hydrogenation produces a mixture of alcohols that needs to be separated for downstream processing. The separation process is energy-consuming, so increasing the selectivity of a certain higher alcohol can ease the separation. Synthesis of a single higher alcohol with high selectivity from CO_2 hydrogenation is a future direction. Furthermore, the main higher alcohol from CO_2 hydrogenation is ethanol, and further studies to enhance the carbon chain propagation to achieve more propanol and butanol are also of great importance.

Concerning the above mentioned issues, we have proposed the following directions for rational catalyst design for higher alcohol synthesis from CO_2 hydrogenation in the future.

(i) **Developing new bifunctional active sites.** Since carbon chain propagation and alcohol formation are two main aspects of higher alcohol synthesis, an efficient catalyst for higher alcohol synthesis should process dual-sites providing both functions. As we discussed above, bifunctional dual sites such as Rh and Li-Rh sites in Rh-based catalysts, Cu and Fe sites in Cu-based catalysts, MoS_2 and K-MoS_2 sites in Mo-based catalysts, and Co^0 and CoO sites in Co-based catalysts work concertedly to form higher alcohols. Recently, many efficient catalysts for CO_2 conversion to methanol, such as Cu-based catalysts [227], Pd-based catalysts [227], ZnO-ZrO_2 catalysts [228], In_2O_3 catalysts [229], and NiGa-based catalysts [230] have been reported. Also, highly active Fe and Co-based catalysts [227] for long-chain hydrocarbons synthesis have been reported. These catalysts possess highly active sites for alcohol synthesis or carbon chain propagation, respectively. Modifying these catalysts to incorporate the other function (carbon chain propagation for methanol synthesis catalysts and alcohol formation function for FT catalysts) would be a fast approach to search for new catalytic systems for higher alcohol synthesis which needs to be further studied.
(ii) **Tailoring the active sites at an atomic scale.** It has been found that atomically dispersing Pd on Fe_3O_4 or tailoring the distance of Cu-Cu site can enhance higher alcohol synthesis. Thus, tailoring the above-mentioned dual-sites at an atomic scale may promote the synergy between alcohol synthesis and carbon chain propagation to enhance higher alcohol synthesis.
(iii) **Understanding the effect of solvent in a slurry bed reactor.** It has been found that when the reaction is performed in a slurry bed reactor, the selectivity to higher alcohols is generally higher than that in a fixed bed reactor. Besides, the selectivity to a certain alcohol is generally very high in a slurry bed reactor. However, a separation, which is energy consuming, is required to separate the product and the catalyst from the solvent. Understanding the effects of the solvent and transfer this knowledge to design catalysts may prompt selective higher alcohol synthesis in a fixed bed reactor.

Structure-performance correlations have been reported, though, most of them are based on the structure of the "catalyst precursor", while the catalyst structure is most likely very different after the often complicated catalyst activation procedures and the harsh reaction conditions usually applied for HAS. Thus, in the future, dedicated studies on the state and structure of the active species under reaction conditions, for example, by *in-situ* X-ray powder diffraction (XRD), *in-situ* X-ray photoelectron spectroscopy (XPS), *in-situ* transmission electron microscopy (TEM), and *in-situ* X-ray absorption spectroscopy (XAS), would be of high importance, not only for a better understanding of the active sites but also to be used as the basis for real structure-performance correlations for rational catalyst design. Besides, various reaction mechanisms have been proposed for HAS, though without reaching a consensus and this topic is still open for discordance. The preferred mechanistic pathways and products appear to be highly dependent on the surface coverages, for instance high H and CH_x would favour methanation and hydrocarbon formation. High HAS selectivity would require a balance of CH_x surface species with CO or formate surface species. Some of the proposed mechanisms are based on the product and byproduct formation as a function of reaction conditions; others are based on intermediates observed by IR experiments. More rigorous experiments, such as $^{13}C/^{2}H$ labeled experiments and *in-situ* IR (high pressure), as well as theoretical calculations, should be performed in the future to get an advanced understanding of the reaction mechanism at the atomic level. We, therefore, believe that with improved synthesis protocols, adequate characterization, and in-depth mechanistic studies, tailored non-noble metals based catalysts could be designed as next-generation catalytic systems for CO_2 hydrogenation for the synthesis of higher alcohols. Beyond rational catalyst design, we also suggest to improve the process from the engineering perspective. Most catalysts were evaluated in continuous plug flow fixed-bed reactors, but interestingly, regardless of HAS catalyst categories, the best catalytic performance were reported using slurry batch reactors in the presence of different solvents. Finally, we hope this review provides useful information for those active in catalyst development for HAS and will stimulate further research activities in the field of HAS by CO_2 hydrogenation.

Declaration of Competing Interest

The authors declare that they have no known competing financial interests or personal relationships that could have appeared to influence the work reported in this paper.

Acknowledgements

Feng Zeng, Xiaoying Xi, Longfei Liao, and Jie Ren acknowledge

China Scholarship Council for financial support. We acknowledge the Clusters of Excellence Fuel Science Center (EXC 2186, ID: 390919832) funded by the Excellence Initiative by the German federal and state governments. The authors acknowledge Qingyun Wu for designing the graphical abstract.

References

[1] J. Olivier, J. Peters, Trends in Global CO_2 and Total Greenhouse Gas Emissions. Summary of the 2019 Report, PBL Netherlands Environmental Assessment Agency, The Hague, 2019.

[2] H. Ritchie, M. Roser, CO_2 and Greenhouse Gas Emissions, Our World Data, 2017 (accessed April 8, 2020), https://ourworldindata.org/co2-and-other-greenhouse-gas-emissions.

[3] C. Hepburn, E. Adlen, J. Beddington, E.A. Carter, S. Fuss, N. Mac Dowell, J. C. Minx, P. Smith, C.K. Williams, The technological and economic prospects for CO_2 utilization and removal, Nature 575 (2019) 87–97, https://doi.org/10.1038/s41586-019-1681-6.

[4] L. Wang, W. Chen, D. Zhang, Y. Du, R. Amal, S. Qiao, J. Wu, Z. Yin, Surface strategies for catalytic CO_2 reduction: from two-dimensional materials to nanoclusters to single atoms, Chem. Soc. Rev. 48 (2019) 5310–5349, https://doi.org/10.1039/C9CS00163H.

[5] J. Zhong, X. Yang, Z. Wu, B. Liang, Y. Huang, T. Zhang, State of the art and perspectives in heterogeneous catalysis of CO_2 hydrogenation to methanol, Chem. Soc. Rev. 49 (2020) 1385, https://doi.org/10.1039/C9CS00614A.

[6] S. Nitopi, E. Bertheussen, S.B. Scott, X. Liu, A.K. Engstfeld, S. Horch, B. Seger, I.E. L. Stephens, K. Chan, C. Hahn, J.K. Nørskov, T.F. Jaramillo, I. Chorkendorff, Progress and perspectives of electrochemical CO_2 reduction on copper in aqueous electrolyte, Chem. Rev. 119 (2019) 7610–7672, https://doi.org/10.1021/acs.chemrev.8b00705.

[7] R. Guil-López, N. Mota, J. Llorente, E. Millán, B. Pawelec, J.L.G. Fierro, R. M. Navarro, Methanol synthesis from CO_2: a review of the latest developments in heterogeneous catalysis, Materials 12 (2019) 3902, https://doi.org/10.3390/ma12233902.

[8] S. Saeidi, N.A.S. Amin, M.R. Rahimpour, Hydrogenation of CO_2 to value-added products—a review and potential future developments, J. CO2 Util. 5 (2014) 66–81, https://doi.org/10.1016/j.jcou.2013.12.005.

[9] U. Ulmer, T. Dingle, P.N. Duchesne, R.H. Morris, A. Tavasoli, T. Wood, G.A. Ozin, Fundamentals and applications of photocatalytic CO_2 methanation, Nat. Commun. 10 (2019) 3169, https://doi.org/10.1038/s41467-019-10996-2.

[10] Q. Lu, F. Jiao, Electrochemical CO_2 reduction: electrocatalyst, reaction mechanism, and process engineering, Nano Energy 29 (2016) 439–456, https://doi.org/10.1016/j.nanoen.2016.04.009.

[11] R. Kas, K. Yang, D. Bohra, R. Kortlever, T. Burdyny, W.A. Smith, Electrochemical CO_2 reduction on nanostructured metal electrodes: fact or defect? Chem. Sci. 11 (2020) 1738–1749, https://doi.org/10.1039/C9SC05375A.

[12] Z. Ma, M.D. Porosoff, Development of tandem catalysts for CO_2 hydrogenation to olefins, ACS Catal. 9 (2019) 2639–2656, https://doi.org/10.1021/acscatal.8b05060.

[13] J. Wu, Y. Huang, W. Ye, Y. Li, CO_2reduction: from the electrochemical to photochemical approach, Adv. Sci. 4 (2017), 1700194, https://doi.org/10.1002/advs.201700194.

[14] X. Chang, T. Wang, J. Gong, CO_2 photo-reduction: insights into CO_2 activation and reaction on surfaces of photocatalysts, Energy Environ. Sci. 9 (2016) 2177–2196, https://doi.org/10.1039/C6EE00383D.

[15] W.-H. Wang, Y. Himeda, J.T. Muckerman, G.F. Manbeck, E. Fujita, CO_2 hydrogenation to formate and methanol as an alternative to photo- and electrochemical CO_2 reduction, Chem. Rev. 115 (2015) 12936–12973, https://doi.org/10.1021/acs.chemrev.5b00197.

[16] R.P. Ye, J. Ding, W. Gong, M.D. Argyle, Q. Zhong, Y. Wang, C.K. Russell, Z. Xu, A. G. Russell, Q. Li, M. Fan, Y.-G. Yao, CO_2 hydrogenation to high-value products via heterogeneous catalysis, Nat. Commun. 10 (2019) 1–15, https://doi.org/10.1038/s41467-019-13638-9.

[17] A. Álvarez, A. Bansode, A. Urakawa, A.V. Bavykina, T.A. Wezendonk, M. Makkee, J. Gascon, F. Kapteijn, Challenges in the greener production of Formates/Formic acid, methanol, and DME by heterogeneously catalyzed CO_2 hydrogenation processes, Chem. Rev. 117 (2017) 9804–9838, https://doi.org/10.1021/acs.chemrev.6b00816.

[18] W. Li, H. Wang, X. Jiang, J. Zhu, Z. Liu, X. Guo, C. Song, A short review of recent advances in CO_2 hydrogenation to hydrocarbons over heterogeneous catalysts, RSC Adv. 8 (2018) 7651–7669, https://doi.org/10.1039/C7RA13546G.

[19] H. Yang, C. Zhang, P. Gao, H. Wang, X. Li, L. Zhong, W. Wei, Y. Sun, A review of the catalytic hydrogenation of carbon dioxide into value-added hydrocarbons, Catal. Sci. Technol. 7 (2017) 4580–4598, https://doi.org/10.1039/C7CY01403A.

[20] S. Dang, H. Yang, P. Gao, H. Wang, X. Li, W. Wei, Y. Sun, A review of research progress on heterogeneous catalysts for methanol synthesis from carbon dioxide hydrogenation, Catal. Today 330 (2019) 61–75, https://doi.org/10.1016/j.cattod.2018.04.021.

[21] J. Qiao, Y. Liu, F. Hong, J. Zhang, A review of catalysts for the electroreduction of carbon dioxide to produce low-carbon fuels, Chem. Soc. Rev. 43 (2013) 631–675, https://doi.org/10.1039/C3CS60323G.

[22] F. Dalena, A. Senatore, M. Basile, S. Knani, A. Basile, A. Iulianelli, Advances in methanol production and utilization, with particular emphasis toward hydrogen generation via membrane reactor technology, Membranes 8 (2018) 98, https://doi.org/10.3390/membranes8040098.

[23] How is methanol produced, Methanol Inst. (n.d.). https://www.methanol.org/methanol-production/ (accessed March 30, 2020).

[24] J. Vancoillie, J. Demuynck, L. Sileghem, M. Van De Ginste, S. Verhelst, Comparison of the renewable transportation fuels, hydrogen and methanol formed from hydrogen, with gasoline-engine efficiency study, Int. J. Hydrog. Energy 37 (2012) 9914–9924, https://doi.org/10.1016/j.ijhydene.2012.03.145.

[25] E. Christensen, J. Yanowitz, M. Ratcliff, R.L. McCormick, Renewable oxygenate blending effects on gasoline properties, Energy Fuels 25 (2011) 4723–4733, https://doi.org/10.1021/ef2010089.

[26] J. Spero, B. Devito, L. Theodore, Regulatory Chemicals Handbook, Marcel Dekker, New York, 2000.

[27] N.S. Hidzir, A. Som, Z. Abdullah, Ethanol production via direct hydration of ethylene: a review, in: Int. Conf. Glob. Sustain. Chem. Eng., ICGSE, 2014, p. 7.

[28] D. Pimentel, T.W. Patzek, Ethanol production using corn, switchgrass, and wood; biodiesel production using soybean and sunflower, Nat. Resour. Res. 14 (2005) 65–76, https://doi.org/10.1007/s11053-005-4679-8.

[29] C.M. Jensen, W.C. Trogler, Catalytic hydration of terminal alkenes to primary alcohols, Science 233 (1986) 1069–1071, https://doi.org/10.1126/science.233.4768.1069.

[30] T. Walther, J.M. François, Microbial production of propanol, Biotechnol. Adv. 34 (2016) 984–996, https://doi.org/10.1016/j.biotechadv.2016.05.011.

[31] P. Dürre, Fermentative butanol production: bulk chemical and biofuel, Ann. N. Y. Acad. Sci. 1125 (2008) 353–362, https://doi.org/10.1196/annals.1419.009.

[32] H. Xu, D. Rebollar, H. He, L. Chong, Y. Liu, C. Liu, C.-J. Sun, T. Li, J.V. Muntean, R.E. Winans, D.-J. Liu, T. Xu, Highly selective electrocatalytic CO_2 reduction to ethanol by metallic clusters dynamically formed from atomically dispersed copper, Nat. Energy 5 (2020) 623–632, https://doi.org/10.1038/s41560-020-0666-x.

[33] W. Ma, S. Xie, T. Liu, Q. Fan, J. Ye, F. Sun, Z. Jiang, Q. Zhang, J. Cheng, Y. Wang, Electrocatalytic reduction of CO_2 to ethylene and ethanol through hydrogen-assisted C–C coupling over fluorine-modified copper, Nat. Catal. 3 (2020) 478–487, https://doi.org/10.1038/s41929-020-0450-0.

[34] H.T. Luk, C. Mondelli, D.C. Ferré, J.A. Stewart, J. Pérez-Ramírez, Status and prospects in higher alcohols synthesis from syngas, Chem. Soc. Rev. 46 (2017) 1358–1426, https://doi.org/10.1039/C6CS00324A.

[35] P.L. Spath, D.C. Dayton, Preliminary Screening – Technical and Economic Assessment of Synthesis Gas to Fuels and Chemicals with Emphasis on the Potential for Biomass-Derived Syngas, 2003, p. 160.

[36] S. Zaman, K.J. Smith, A review of molybdenum catalysts for synthesis gas conversion to alcohols: catalysts, mechanisms and kinetics, Catal. Rev. 54 (2012) 41–132, https://doi.org/10.1080/01614940.2012.627224.

[37] K. Fang, D. Li, M. Lin, M. Xiang, W. Wei, Y. Sun, A short review of heterogeneous catalytic process for mixed alcohols synthesis via syngas, Catal. Today 147 (2009) 133–138, https://doi.org/10.1016/j.cattod.2009.01.038.

[38] M. Gupta, M.L. Smith, J.J. Spivey, Heterogeneous catalytic conversion of dry syngas to ethanol and higher alcohols on Cu-based catalysts, ACS Catal. 1 (2011) 641–656, https://doi.org/10.1021/cs2001048.

[39] M. Ao, G.H. Pham, J. Sunarso, M.O. Tade, S. Liu, Active centers of catalysts for higher alcohol synthesis from syngas: a review, ACS Catal. 8 (2018) 7025–7050, https://doi.org/10.1021/acscatal.8b01391.

[40] P. Forzatti, E. Tronconi, I. Pasquon, Higher alcohol synthesis, Catal. Rev. 33 (1991) 109–168, https://doi.org/10.1080/01614949108020298.

[41] K. Xiao, Z. Bao, X. Qi, X. Wang, L. Zhong, K. Fang, M. Lin, Y. Sun, Advances in bifunctional catalysis for higher alcohol synthesis from syngas, Chin. J. Catal. 34 (2013) 116–129, https://doi.org/10.1016/S1872-2067(11)60496-8.

[42] M.M.J. Li, S.C.E. Tsang, Bimetallic catalysts for green methanol production via CO_2 and renewable hydrogen: a mini-review and prospects, Catal. Sci. Technol. 8 (2018) 3450–3464, https://doi.org/10.1039/C8CY00304A.

[43] O.A. Ojelade, S.F. Zaman, A review on Pd based catalysts for CO_2 hydrogenation to methanol: In-depth activity and DRIFTS mechanistic study, Catal. Surv. Asia 24 (2020) 11–37, https://doi.org/10.1007/s10563-019-09287-z.

[44] X. Nie, W. Li, X. Jiang, X. Guo, C. Song, Recent advances in catalytic CO_2 hydrogenation to alcohols and hydrocarbons. Adv. Catal., Elsevier, 2019, pp. 121–233, https://doi.org/10.1016/bs.acat.2019.10.002.

[45] D. Xu, Y. Wang, M. Ding, X. Hong, G. Liu, S.C.E. Tsang, Advances in higher alcohol synthesis from CO_2 hydrogenation, Chem (2020), https://doi.org/10.1016/j.chempr.2020.10.019.

[46] P. Gao, L. Zhang, S. Li, Z. Zhou, Y. Sun, Novel heterogeneous catalysts for CO_2 hydrogenation to liquid fuels, ACS Cent. Sci. 6 (2020) 1657–1670, https://doi.org/10.1021/acscentsci.0c00976.

[47] X. He, CO_2 hydrogenation for ethanol production: a thermodynamic analysis, Int. J. Oil Gas Coal Eng. 5 (2017) 145, https://doi.org/10.11648/j.ogce.20170506.14.

[48] K. Stangeland, H. Li, Z. Yu, Thermodynamic analysis of chemical and phase equilibria in CO_2 hydrogenation to methanol, dimethyl ether, and higher alcohols, Ind. Eng. Chem. Res. 57 (2018) 4081–4094, https://doi.org/10.1021/acs.iecr.7b04866.

[49] C. Jia, J. Gao, Y. Dai, J. Zhang, Y. Yang, The thermodynamics analysis and experimental validation for complicated systems in CO_2 hydrogenation process, J. Energy Chem. 25 (2016) 1027–1037, https://doi.org/10.1016/j.jechem.2016.10.003.

[50] C. Yang, R. Mu, G. Wang, J. Song, H. Tian, Z.J. Zhao, J. Gong, Hydroxyl-mediated ethanol selectivity of CO_2 hydrogenation, Chem. Sci. 10 (2019) 3161–3167, https://doi.org/10.1039/c8sc05608k.

[51] H. Kusama, K. Okabe, K. Sayama, H. Arakawa, Ethanol synthesis by catalytic hydrogenation of CO_2 over Rh-$FeSiO_2$ catalysts, Energy 22 (1997) 343–348, https://doi.org/10.1016/S0360-5442(96)00095-3.

[52] H. Kusama, K. Okabe, K. Sayama, H. Arakawa, CO_2 hydrogenation to ethanol over promoted Rh/SiO_2 catalysts, Catal. Today 28 (1996) 261–266, https://doi.org/10.1016/0920-5861(95)00246-4.

[53] H. Kusama, K. Okabe, H. Arakawa, Effect of Ce additive on CO_2 hydrogenation over Rh/SiO_2 catalysts, J. Jpn. Pet. Inst. 44 (2001) 384–391, https://doi.org/10.1627/jpi1958.44.384.

[54] M.R. Gogate, R.J. Davis, Comparative study of CO and CO_2 hydrogenation over supported Rh–Fe catalysts, Catal. Commun. 11 (2010) 901–906, https://doi.org/10.1016/j.catcom.2010.03.020.

[55] H. Kusama, K. Okabe, K. Sayama, H. Arakawa, Rhodium catalysts promoted by cerium oxide in the CO_2 hydrogenation to ethanol, J. Jpn. Pet. Inst. 42 (1999) 178–179, https://doi.org/10.1627/jpi1958.42.178.

[56] K. Kitamura Bando, K. Soga, K. Kunimori, H. Arakawa, Effect of Li additive on CO_2 hydrogenation reactivity of zeolite supported Rh catalysts, Appl. Catal. Gen. 175 (1998) 67–81, https://doi.org/10.1016/S0926-860X(98)00202-6.

[57] Y. Izumi, H. Kurakata, K.I. Aika, Ethanol synthesis from carbon dioxide on [$Rh_{10}Se$]/TiO_2 catalyst characterized by X-ray absorption fine structure spectroscopy, J. Catal. 175 (1998) 236–244, https://doi.org/10.1006/jcat.1998.1998.

[58] H. Kusama, K. Okabe, K. Sayama, H. Arakawa, The effect of rhodium precursor on ethanol synthesis by catalytic hydrogenation of carbon dioxide over silica supported rhodium catalysts. Stud. Surf. Sci. Catal., Elsevier, 1998, pp. 431–434, https://doi.org/10.1016/S0167-2991(98)80788-X.

[59] T. Inui, T. Yamamoto, M. Inoue, H. Hara, T. Takeguchi, J.B. Kim, Highly effective synthesis of ethanol by CO_2-hydrogenation on well balanced multi-functional FT-type composite catalysts, Appl. Catal. Gen. 186 (1999) 395–406, https://doi.org/10.1016/S0926-860X(99)00157-X.

[60] T. Inui, T. Yamamoto, Effective synthesis of ethanol from CO_2 on polyfunctional composite catalysts, Catal. Today 45 (1998) 209–214, https://doi.org/10.1016/S0920-5861(98)00217-X.

[61] K.K. Bando, H. Kusama, T. Saito, K. Sato, T. Tanaka, F. Dumeignil, M. Imamura, N. Matsubayashi, H. Shimada, Effect of precursors on structure of Rh nanoparticles on SiO_2 support: in-situ EXAFS observation during CO_2 hydrogenation. Stud. Surf. Sci. Catal., Elsevier, 2001, pp. 737–740, https://doi.org/10.1016/S0167-2991(01)82191-1.

[62] H. Kurakata, Y. Izumi, K.I. Aika, Ethanol synthesis from carbon dioxide on TiO_2-supported [$Rh_{10}Se$] catalyst, Chem. Commun. (1993) 389–390.

[63] T. Inoue, T. Iizuka, K. Tanabe, Hydrogenation of carbon dioxide and carbon monoxide over supported rhodium catalysts under 10 bar pressure, Appl. Catal. 46 (1989) 1–9, https://doi.org/10.1016/S0166-9834(00)81390-1.

[64] J.S. Lee, S. Kim, K.H. Lee, I.S. Nam, J.S. Chung, Y.G. Kim, H.C. Woo, Role of alkali promoters in K/MoS_2 catalysts for CO-H_2 reactions, Appl. Catal. Gen. 110 (1994) 11–25, https://doi.org/10.1016/0926-860X(94)80101-0.

[65] G.J. Millar, C.H. Rochester, K.C. Waugh, An FTIR study of the adsorption of formic acid and formaldehyde on potassium-promoted Cu/SiO_2 catalysts, J. Catal. 155 (1995) 52–58, https://doi.org/10.1006/jcat.1995.1187.

[66] K.K. Bando, N. Ichikuni, H. Arakawa, K. Asakuara, The effect of Li on structure of supported Rh particles in zeolite, Mol. Cryst. Liq. Cryst. Sci. Technol. Sect. Mol. Cryst. Liq. Cryst. 341 (2000) 473–478, https://doi.org/10.1080/10587250008026184.

[67] K.K. Bando, H. Arakawa, N. Ichikuni, K. Asakura, A novel effect of Li additive: dynamic control of Rh mobility during CO_2 hydrogenation reaction, in: A. Corma, F.V. Melo, S. Mendioroz, J.L.G. Fierro (Eds.), Stud. Surf. Sci. Catal., Elsevier, 2000, pp. 3759–3764, https://doi.org/10.1016/S0167-2991(00)80608-4.

[68] C. Yang, C.W. Garl, Infrared studies of carbon monoxide chemisorbed on rhodium, J. Phys. Chem. 61 (1957) 1504–1512, https://doi.org/10.1021/j150557a013.

[69] J.C. Lavalley, J. Saussey, J. Lamotte, Infrared study of carbon monoxide hydrogenation over rhodiumkeria and rhodlum/sfllca catalysts, J. Phys. Chem. 94 (1990) 5941–5947.

[70] A. Kiennemann, R. Breault, J.P. Hindermann, M. Laurin, Ethanol promotion by the addition of cerium to rhodium–silica catalysts, J. Chem. Soc. Faraday Trans. 1 Phys. Chem. Condens. Phases. 83 (1987) 2119, https://doi.org/10.1039/f19878302119.

[71] M. Ichikawa, Catalysis by supported metal crystallites from carbonyl clusters. I. Catalytic methanol synthesis under mild conditions over supported rhodium, platinum, and iridium crystallites prepared from Rh, Pt, and Ir carbonyl cluster compounds deposited on ZnO and MgO, Bull. Chem. Soc. Jpn. 51 (1978) 2268–2272, https://doi.org/10.1246/bcsj.51.2268.

[72] Y. Choi, P. Liu, Mechanism of ethanol synthesis from syngas on Rh(111), J. Am. Chem. Soc. 131 (2009) 13054–13061, https://doi.org/10.1021/ja903013x.

[73] R. Zhang, G. Wang, B. Wang, L. Ling, Insight into the effect of promoter Mn on ethanol formation from syngas on a Mn-promoted MnCu(211) surface: a comparison with a Cu(211) surface, J. Phys. Chem. C 118 (2014) 5243–5254, https://doi.org/10.1021/jp409447u.

[74] R. Zhang, B. Wang, H. Liu, L. Ling, Effect of surface hydroxyls on CO_2 hydrogenation over Cu/γ-Al_2O_3 catalyst: a theoretical study, J. Phys. Chem. C 115 (2011) 19811–19818, https://doi.org/10.1021/jp206065y.

[75] J. Xu, X. Su, H. Duan, B. Hou, Q. Lin, X. Liu, X. Pan, G. Pei, H. Geng, Y. Huang, T. Zhang, Influence of pretreatment temperature on catalytic performance of rutile TiO_2-supported ruthenium catalyst in CO_2 methanation, J. Catal. 333 (2016) 227–237, https://doi.org/10.1016/j.jcat.2015.10.025.

[76] R. Burch, M.J. Hayes, The preparation and characterisation of Fe-promoted Al_2O_3-supported Rh catalysts for the selective production of ethanol from syngas, J. Catal. 165 (1997) 249–261, https://doi.org/10.1006/jcat.1997.1482.

[77] K. Kitamura Bando, K. Soga, K. Kunimori, N. Ichikuni, K. Okabe, H. Kusama, K. Sayama, H. Arakawa, CO_2 hydrogenation activity and surface structure of zeolite-supported Rh catalysts, Appl. Catal. Gen. 173 (1998) 47–60, https://doi.org/10.1016/S0926-860X(98)00143-4.

[78] H. Kusama, K. Okabe, K. Sayama, H. Arakawa, The effect of rhodium particle size on ethanol synthesis by catalytic hydrogenation of carbon dioxide over silica supported Rhodium catalysts, J. Jpn. Pet. Inst. 40 (1997) 415–419, https://doi.org/10.1627/jpi1958.40.415.

[79] T. Iizuka, Y. Tanaka, K. Tanabe, Hydrogenation of carbon monoxide and carbon dioxide over supported rhodium catalysts, J. Mol. Catal. 17 (1982) 381–389, https://doi.org/10.1016/0304-5102(82)85049-9.

[80] T. Iizuka, Y. Tanaka, K. Tanabe, Hydrogenation of CO and CO_2 over rhodium catalysts supported on various metal oxides, J. Catal. 76 (1982) 1–8, https://doi.org/10.1016/0021-9517(82)90230-5.

[81] F. Solymosi, A. Erdőhelyi, T. Bánsági, Methanation of CO_2 on supported rhodium catalyst, J. Catal. 68 (1981) 371–382, https://doi.org/10.1016/S0167-2991(08)64768-0.

[82] Y. Izumi, Selective ethanol synthesis from carbon dioxide, Platin. Met. Rev. 41 (1997) 166–170.

[83] K. Larmier, W.-C. Liao, S. Tada, E. Lam, R. Verel, A. Bansode, A. Urakawa, A. Comas-Vives, C. Copéret, CO_2-to-Methanol Hydrogenation on Zirconia-supported copper nanoparticles: reaction intermediates and the role of the metal–support interface, Angew. Chem. Int. Ed. 56 (2017) 2318–2323, https://doi.org/10.1002/anie.201610166.

[84] S. Kattel, P. Liu, J.G. Chen, Tuning selectivity of CO_2 hydrogenation reactions at the metal/oxide interface, J. Am. Chem. Soc. 139 (2017) 9739–9754, https://doi.org/10.1021/jacs.7b05362.

[85] J. Liu, J. Shi, D. He, Q. Zhang, X. Wu, Y. Liang, Q. Zhu, Surface active structure of ultra-fine Cu/ZrO_2 catalysts used for the CO_2+H_2 to methanol reaction, Appl. Catal. Gen. 218 (2001) 113–119, https://doi.org/10.1016/S0926-860X(01)00625-1.

[86] L. Li, D. Mao, J. Yu, X. Guo, Highly selective hydrogenation of CO_2 to methanol over CuO–ZnO–ZrO_2 catalysts prepared by a surfactant-assisted co-precipitation method, J. Power Sources 279 (2015) 394–404, https://doi.org/10.1016/j.jpowsour.2014.12.142.

[87] G. Bonura, M. Cordaro, C. Cannilla, F. Arena, F. Frusteri, The changing nature of the active site of Cu-Zn-Zr catalysts for the CO_2 hydrogenation reaction to methanol, Appl. Catal. B Environ. 152–153 (2014) 152–161, https://doi.org/10.1016/j.apcatb.2014.01.035.

[88] R. Ladera, F.J. Pérez-Alonso, J.M. González-Carballo, M. Ojeda, S. Rojas, J.L. G. Fierro, Catalytic valorization of CO_2 via methanol synthesis with Ga-promoted Cu–ZnO–ZrO_2 catalysts, Appl. Catal. B Environ. 142–143 (2013) 241–248, https://doi.org/10.1016/j.apcatb.2013.05.019.

[89] F. Arena, G. Mezzatesta, G. Zafarana, G. Trunfio, F. Frusteri, L. Spadaro, Effects of oxide carriers on surface functionality and process performance of the Cu–ZnO system in the synthesis of methanol via CO_2 hydrogenation, J. Catal. 300 (2013) 141–151, https://doi.org/10.1016/j.jcat.2012.12.019.

[90] J. Słoczyński, R. Grabowski, P. Olszewski, A. Kozłowska, J. Stoch, M. Lachowska, J. Skrzypek, Effect of metal oxide additives on the activity and stability of Cu/ZnO/ZrO_2 catalysts in the synthesis of methanol from CO_2 and H_2, Appl. Catal. Gen. 310 (2006) 127–137, https://doi.org/10.1016/j.apcata.2006.05.035.

[91] X. Guo, D. Mao, G. Lu, S. Wang, G. Wu, The influence of La doping on the catalytic behavior of Cu/ZrO_2 for methanol synthesis from CO_2 hydrogenation, J. Mol. Catal. Chem. 345 (2011) 60–68, https://doi.org/10.1016/j.molcata.2011.05.019.

[92] H. dong Zhuang, S. fen Bai, X. mei Liu, Z.F. Yan, Structure and performance of Cu/ZrO_2 catalyst for the synthesis of methanol from CO_2 hydrogenation, J. Fuel Chem. Technol. 38 (2010) 462–467, https://doi.org/10.1016/S1872-5813(10)60041-2.

[93] X. Guo, D. Mao, S. Wang, G. Wu, G. Lu, Combustion synthesis of CuO–ZnO–ZrO_2 catalysts for the hydrogenation of carbon dioxide to methanol, Catal. Commun. 10 (2009) 1661–1664, https://doi.org/10.1016/j.catcom.2009.05.004.

[94] X. Guo, D. Mao, G. Lu, S. Wang, G. Wu, Glycine–nitrate combustion synthesis of CuO–ZnO–ZrO_2 catalysts for methanol synthesis from CO_2 hydrogenation, J. Catal. 271 (2010) 178–185, https://doi.org/10.1016/j.jcat.2010.01.009.

[95] F. Arena, K. Barbera, G. Italiano, G. Bonura, L. Spadaro, F. Frusteri, Synthesis, characterization and activity pattern of Cu–ZnO/ZrO_2 catalysts in the hydrogenation of carbon dioxide to methanol, J. Catal. 249 (2007) 185–194, https://doi.org/10.1016/j.jcat.2007.04.003.

[96] P. Gao, F. Li, N. Zhao, F. Xiao, W. Wei, L. Zhong, Y. Sun, Influence of modifier (Mn, La, Ce, Zr and Y) on the performance of Cu/Zn/Al catalysts via hydrotalcite-like precursors for CO_2 hydrogenation to methanol, Appl. Catal. Gen. 468 (2013) 442–452, https://doi.org/10.1016/j.apcata.2013.09.026.

[97] A. Le Valant, C. Comminges, C. Tisseraud, C. Canaff, L. Pinard, Y. Pouilloux, The Cu–ZnO synergy in methanol synthesis from CO_2, Part 1: origin of active site explained by experimental studies and a sphere contact quantification model on Cu+ZnO mechanical mixtures, J. Catal. 324 (2015) 41–49, https://doi.org/10.1016/j.jcat.2015.01.021.

[98] M.M.J. Li, C. Chen, T. Ayvalı, H. Suo, J. Zheng, I.F. Teixeira, L. Ye, H. Zou, D. O'Hare, S.C.E. Tsang, CO_2 hydrogenation to methanol over catalysts derived from single cationic layer CuZnGa LDH precursors, ACS Catal. 8 (2018) 4390–4401, https://doi.org/10.1021/acscatal.8b00474.

[99] J. Toyir, P.R. de la Piscina, J.L.G. Fierro, N. Homs, Highly effective conversion of CO_2 to methanol over supported and promoted copper-based catalysts: influence of support and promoter, Appl. Catal. B Environ. 29 (2001) 207–215, https://doi.org/10.1016/S0926-3373(00)00205-8.

[100] F. Liao, Y. Huang, J. Ge, W. Zheng, K. Tedsree, P. Collier, X. Hong, S.C. Tsang, Morphology-dependent interactions of ZnO with Cu nanoparticles at the materials' interface in selective hydrogenation of CO_2 to CH_3OH, Angew. Chem. Int. Ed. 50 (2011) 2162–2165, https://doi.org/10.1002/anie.201007108.

[101] M.J.L. Ginés, A.J. Marchi, C.R. Apesteguía, Kinetic study of the reverse water-gas shift reaction over $CuO/ZnO/Al_2O_3$ catalysts, Appl. Catal. Gen. 154 (1997) 155–171, https://doi.org/10.1016/S0926-860X(96)00369-9.

[102] S.-I. Fujita, M. Usui, N. Takezawa, Mechanism of the reverse water gas shift reaction over Cu/ZnO catalyst, J. Catal. 134 (1992) 220–225, https://doi.org/10.1016/0021-9517(92)90223-5.

[103] J.A. Rodriguez, J. Evans, L. Feria, A.B. Vidal, P. Liu, K. Nakamura, F. Illas, CO_2hydrogenation on Au/TiC, Cu/TiC, and Ni/TiC catalysts: Production of CO, methanol, and methane, J. Catal. 307 (2013) 162–169, https://doi.org/10.1016/j.jcat.2013.07.023.

[104] C.S. Chen, W.H. Cheng, S.S. Lin, Mechanism of CO formation in reverse water–gas shift reaction over Cu/Al_2O_3 catalyst, Catal. Lett. 68 (2000) 45–48, https://doi.org/10.1023/A:1019071117449.

[105] C.S. Chen, W.H. Cheng, S.S. Lin, Study of reverse water gas shift reaction by TPD, TPR and CO_2 hydrogenation over potassium-promoted Cu/SiO_2 catalyst, Appl. Catal. Gen. 238 (2003) 55–67, https://doi.org/10.1016/S0926-860X(02)00221-1.

[106] C.S. Chen, J.H. Wu, T.W. Lai, Carbon dioxide hydrogenation on Cu nanoparticles, J. Phys. Chem. C 114 (2010) 15021–15028, https://doi.org/10.1021/jp104890c.

[107] C.S. Chen, W.H. Cheng, Study on the mechanism of CO formation in reverse water gas shift reaction over Cu/SiO_2 catalyst by pulse reaction, TPD and TPR, Catal. Lett. 83 (2002) 121–126, https://doi.org/10.1023/A:1021006718974.

[108] C.S. Chen, W.H. Cheng, S.S. Lin, Enhanced activity and stability of a Cu/SiO_2 catalyst for the reverse water gas shift reaction by an iron promoter, Chem. Commun. (2001) 1770–1771, https://doi.org/10.1039/B104279N.

[109] C.S. Chen, W.H. Cheng, S.S. Lin, Study of iron-promoted Cu/SiO_2 catalyst on high temperature reverse water gas shift reaction, Appl. Catal. Gen. 257 (2004) 97–106, https://doi.org/10.1016/S0926-860X(03)00637-9.

[110] Y.A. Daza, J.N. Kuhn, CO_2 conversion by reverse water gas shift catalysis: comparison of catalysts, mechanisms and their consequences for CO_2 conversion to liquid fuels, RSC Adv. 6 (2016) 49675–49691, https://doi.org/10.1039/C6RA05414E.

[111] S. Li, H. Guo, C. Luo, H. Zhang, L. Xiong, X. Chen, L. Ma, Effect of iron promoter on structure and performance of K/Cu–Zn catalyst for higher alcohols synthesis from CO_2 hydrogenation, Catal. Lett. 143 (2013) 345–355, https://doi.org/10.1007/s10562-013-0977-7.

[112] M. Takagawa, A. Okamoto, H. Fujimura, Y. Izawa, H. Arakawa, Ethanol synthesis from carbon dioxide and hydrogen. Stud. Surf. Sci. Catal., Elsevier, 1998, pp. 525–528, https://doi.org/10.1016/S0167-2991(98)80812-4.

[113] T. Yamamoto, T. Inui, Highly effective synthesis of ethanol from CO_2 on Fe, Cu-based novel catalysts. Stud. Surf. Sci. Catal., Elsevier, 1998, pp. 513–516, https://doi.org/10.1016/S0167-2991(98)80809-4.

[114] W. Guo, W.G. Gao, H. Wang, J.J. Tian, Higher alcohols synthesis from CO_2 hydrogenation over K_2O-modified $CuZnFeZrO_2$ catalysts, Adv. Mater. Res. 827 (2013) 20–24, https://doi.org/10.4028/www.scientific.net/AMR.827.20.

[115] H. Guo, S. Li, F. Peng, H. Zhang, L. Xiong, C. Huang, C. Wang, X. Chen, Roles investigation of promoters in K/Cu–Zn catalyst and higher alcohols synthesis from CO_2 hydrogenation over a novel two-stage bed catalyst combination system, Catal. Lett. 145 (2015) 620–630, https://doi.org/10.1007/s10562-014-1446-7.

[116] B. An, Z. Li, Y. Song, J. Zhang, L. Zeng, C. Wang, W. Lin, Cooperative copper centres in a metal–organic framework for selective conversion of CO_2 to ethanol, Nat. Catal. 2 (2019) 709–717, https://doi.org/10.1038/s41929-019-0308-5.

[117] J.J. Spivey, K.M. Dooley, Promotion effects in Co-based Fischer–Tropsch catalysis. Catalysis, 2006, pp. 1–40, https://doi.org/10.1039/9781847555229-00001.

[118] F. Ding, A. Zhang, M. Liu, Y. Zuo, K. Li, X. Guo, C. Song, CO_2hydrogenation to hydrocarbons over iron-based catalyst: effects of physicochemical properties of Al_2O_3 supports, Ind. Eng. Chem. Res. 53 (2014) 17563–17569, https://doi.org/10.1021/ie5031166.

[119] D.J. Dwyer, G.A. Somorjai, Hydrogenation of CO and CO_2 over iron foils: correlations of rate, product distribution, and surface composition, J. Catal. 52 (1978) 291–301, https://doi.org/10.1016/0021-9517(78)90143-4.

[120] J. Zhang, S. Lu, X. Su, S. Fan, Q. Ma, T. Zhao, Selective formation of light olefins from CO_2 hydrogenation over Fe–Zn–K catalysts, J. CO2 Util. 12 (2015) 95–100, https://doi.org/10.1016/j.jcou.2015.05.004.

[121] N. Meiri, Y. Dinburg, M. Amoyal, V. Koukouliev, R.V. Nehemya, M.V. Landau, M. Herskowitz, Novel process and catalytic materials for converting CO_2 and H_2 containing mixtures to liquid fuels and chemicals, Faraday Discuss. 183 (2015) 197–215, https://doi.org/10.1039/C5FD00039D.

[122] F. Jiang, B. Liu, S. Geng, Y. Xu, X. Liu, Hydrogenation of CO_2 into hydrocarbons: enhanced catalytic activity over Fe-based Fischer–tropsch catalysts, Catal. Sci. Technol. 8 (2018) 4097–4107, https://doi.org/10.1039/C8CY00850G.

[123] J. Liu, A. Zhang, M. Liu, S. Hu, F. Ding, C. Song, X. Guo, Fe-MOF-derived highly active catalysts for carbon dioxide hydrogenation to valuable hydrocarbons, J. CO_2 Util. 21 (2017) 100–107, https://doi.org/10.1016/j.jcou.2017.06.011.

[124] J. Zhang, X. Su, X. Wang, Q. Ma, S. Fan, T.S. Zhao, Promotion effects of Ce added Fe–Zr–K on CO_2 hydrogenation to light olefins, React. Kinet. Mech. Catal. 124 (2018) 575–585, https://doi.org/10.1007/s11144-018-1377-1.

[125] T. Numpilai, T. Witoon, N. Chanlek, W. Limphirat, G. Bonura, M. Chareonpanich, J. Limtrakul, Structure–activity relationships of Fe-Co/K-Al_2O_3 catalysts calcined at different temperatures for CO_2 hydrogenation to light olefins, Appl. Catal. Gen. 547 (2017) 219–229, https://doi.org/10.1016/j.apcata.2017.09.006.

[126] X. Wang, J. Zhang, J. Chen, Q. Ma, S. Fan, T. sheng Zhao, Effect of preparation methods on the structure and catalytic performance of Fe–Zn/K catalysts for CO_2 hydrogenation to light olefins, Chin. J. Chem. Eng. 26 (2018) 761–767, https://doi.org/10.1016/j.cjche.2017.10.013.

[127] J. Wei, Q. Ge, R. Yao, Z. Wen, C. Fang, L. Guo, H. Xu, J. Sun, Directly converting CO_2 into a gasoline fuel, Nat. Commun. 8 (2017) 1–9, https://doi.org/10.1038/ncomms15174.

[128] X. Cui, P. Gao, S. Li, C. Yang, Z. Liu, H. Wang, L. Zhong, Y. Sun, Selective production of aromatics directly from carbon dioxide hydrogenation, ACS Catal. 9 (2019) 3866–3876, https://doi.org/10.1021/acscatal.9b00640.

[129] N. Boreriboon, X. Jiang, C. Song, P. Prasassarakich, Fe-based bimetallic catalysts supported on TiO_2 for selective CO_2 hydrogenation to hydrocarbons, J. CO2 Util. 25 (2018) 330–337, https://doi.org/10.1016/j.jcou.2018.02.014.

[130] Y.H. Choi, E.C. Ra, E.H. Kim, K.Y. Kim, Y.J. Jang, K.-N. Kang, S.H. Choi, J.-H. Jang, J.S. Lee, Sodium-containing spinel zinc ferrite as a catalyst precursor for the selective synthesis of liquid hydrocarbon fuels, ChemSusChem. 10 (2017) 4764–4770, https://doi.org/10.1002/cssc.201701437.

[131] Y. Sun, G. Yang, C. Wen, L. Zhang, Z. Sun, Artificial neural networks with response surface methodology for optimization of selective CO_2 hydrogenation using K-promoted iron catalyst in a microchannel reactor, J. CO2 Util. 24 (2018) 10–21, https://doi.org/10.1016/j.jcou.2017.11.013.

[132] S. Geng, F. Jiang, Y. Xu, X. Liu, Iron-based Fischer–Tropsch synthesis for the efficient conversion of carbon dioxide into isoparaffins, ChemCatChem. 8 (2016) 1303–1307, https://doi.org/10.1002/cctc.201600058.

[133] R. Kieffer, M. Fujiwara, L. Udron, Y. Souma, Hydrogenation of CO and CO_2 toward methanol, alcohols and hydrocarbons on promoted copper-rare earth oxides catalysts, Catal. Today 36 (1997) 15–24, https://doi.org/10.1016/S0920-5861(96)00191-5.

[134] P. Mériaudeau, K. Albano, C. Naccache, Promotion of platinum-based catalysts for methanol synthesis from syngas, J. Chem. Soc. Faraday Trans. 1 Phys. Chem. Condens. Phases. 83 (1987) 2113–2118, https://doi.org/10.1039/F19878302113.

[135] K. Higuchi, Y. Haneda, K. Tabata, Y. Nakahara, M. Takagawa, A study for the durability of catalysts in ethanol synthesis by hydrogenation of carbon dioxide. Stud. Surf. Sci. Catal., Elsevier, 1998, pp. 517–520, https://doi.org/10.1016/S0167-2991(98)80810-0.

[136] P. Gao, S. Li, X. Bu, S. Dang, Z. Liu, H. Wang, L. Zhong, M. Qiu, C. Yang, J. Cai, W. Wei, Y. Sun, Direct conversion of CO_2 into liquid fuels with high selectivity over a bifunctional catalyst, Nat. Chem. 9 (2017) 1019–1024, https://doi.org/10.1038/nchem.2794.

[137] F. Jiao, J. Li, X. Pan, J. Xiao, H. Li, H. Ma, M. Wei, Y. Pan, Z. Zhou, M. Li, S. Miao, J. Li, Y. Zhu, D. Xiao, T. He, J. Yang, F. Qi, Q. Fu, X. Bao, Selective conversion of syngas to light olefins, Science 351 (2016) 1065–1068, https://doi.org/10.1126/science.aaf1835.

[138] K. Cheng, B. Gu, X. Liu, J. Kang, Q. Zhang, Y. Wang, Direct and highly selective conversion of synthesis gas into lower olefins: design of a bifunctional catalyst combining methanol synthesis and carbon–carbon coupling, Angew. Chem. Int. Ed. 55 (2016) 4725–4728, https://doi.org/10.1002/anie.201601208.

[139] H. Guo, S. Li, H. Zhang, F. Peng, L. Xiong, J. Yang, C. Wang, X. Chen, Y. Chen, Reaction condition optimization and lumped kinetics study for lower alcohols synthesis from syngas using a two-stage bed catalyst combination system, Ind. Eng. Chem. Res. 53 (2014) 123–131, https://doi.org/10.1021/ie402422p.

[140] D.L.S. Nieskens, D. Ferrari, Y. Liu, R. Kolonko, The conversion of carbon dioxide and hydrogen into methanol and higher alcohols, Catal. Commun. 14 (2011) 111–113, https://doi.org/10.1016/j.catcom.2011.07.020.

[141] M. Kishida, K. Yamada, H. Nagata, K. Wakabayashi, CO_2 hydrogenation for C_{2+} alcohols synthesis over silica-supported Ir-Mo catalysts, Chem. Lett. 23 (1994) 555–556, https://doi.org/10.1246/cl.1994.555.

[142] S. Liu, H. Zhou, L. Zhang, Z. Ma, Y. Wang, Activated carbon-supported Mo-Co-K sulfide catalysts for synthesizing higher alcohols from CO_2, Chem. Eng. Technol. 42 (2019) 962–970, https://doi.org/10.1002/ceat.201800401.

[143] A. Calafat, F. Vivas, J.L. Brito, Effects of phase composition and of potassium promotion on cobalt molybdate catalysts for the synthesis of alcohols from CO_2 and H_2, Appl. Catal. Gen. 172 (1998) 217–224, https://doi.org/10.1016/S0926-860X(98)00127-6.

[144] W. Xu, P.J. Ramirez, D. Stacchiola, J.A. Rodriguez, Synthesis of α-MoC_{1-x} and β-MoC_y catalysts for CO_2 hydrogenation by thermal carburization of Mo-oxide in hydrocarbon and hydrogen mixtures, Catal. Lett. 144 (2014) 1418–1424, https://doi.org/10.1007/s10562-014-1278-5.

[145] Y. Chen, S. Choi, L.T. Thompson, Low temperature CO_2 hydrogenation to alcohols and hydrocarbons over Mo_2C supported metal catalysts, J. Catal. 343 (2016) 147–156, https://doi.org/10.1016/j.jcat.2016.01.016.

[146] Y. Liu, K. Murata, M. Inaba, Synthesis of mixed alcohols from synthesis gas over alkali and Fischer–Tropsch metals modified MoS_2/Al_2O_3-montmorillonite catalysts, React. Kinet. Mech. Catal. 113 (2014) 187–200, https://doi.org/10.1007/s11144-014-0725-z.

[147] P.E. Boahene, V.R. Surisetty, R. Sammynaiken, A.K. Dalai, Higher alcohol synthesis using K-doped $CoRhMoS_2$/MWCNT catalysts: influence of pelletization, particle size and incorporation of binders, Top. Catal. 57 (2014) 538–549, https://doi.org/10.1007/s11244-013-0210-3.

[148] M. Konarova, F. Tang, J. Chen, G. Wang, V. Rudolph, J. Beltramini, Nano- and microscale engineering of the molybdenum disulfide-based catalysts for syngas to

ethanol conversion, ChemCatChem. 6 (2014) 2394–2402, https://doi.org/10.1002/cctc.201402067.
[149] C.H. Ma, H.Y. Li, G.D. Lin, H.B. Zhang, Ni-decorated carbon nanotube-promoted Ni–Mo–K catalyst for highly efficient synthesis of higher alcohols from syngas, Appl. Catal. B Environ. 100 (2010) 245–253, https://doi.org/10.1016/j.apcatb.2010.07.040.
[150] J.J. Wang, J.R. Xie, Y.H. Huang, B.H. Chen, G.D. Lin, H.B. Zhang, An efficient Ni–Mo–K sulfide catalyst doped with CNTs for conversion of syngas to ethanol and higher alcohols, Appl. Catal. Gen. 468 (2013) 44–51, https://doi.org/10.1016/j.apcata.2013.08.026.
[151] T. Toyoda, T. Minami, E.W. Qian, Mixed alcohol synthesis over sulfided molybdenum-based catalysts, Energy Fuels 27 (2013) 3769–3777, https://doi.org/10.1021/ef400262a.
[152] S.F. Zaman, K.J. Smith, Synthesis gas conversion over a Rh–K–MoP/SiO_2 catalyst, Catal. Today 171 (2011) 266–274, https://doi.org/10.1016/j.cattod.2011.02.017.
[153] C.H. Ma, H.Y. Li, G.D. Lin, H.B. Zhang, MWCNT-supported Ni–Mo–K catalyst for higher alcohol synthesis from syngas, Catal. Lett. 137 (2010) 171–179, https://doi.org/10.1007/s10562-010-0343-y.
[154] F. Zeng, X. Xi, H. Cao, Y. Pei, H.J. Heeres, R. Palkovits, Synthesis of mixed alcohols with enhanced C_{3+} alcohol production by CO hydrogenation over potassium promoted molybdenum sulfide, Appl. Catal. B Environ. 246 (2019) 232–241, https://doi.org/10.1016/j.apcatb.2019.01.063.
[155] M. Nagai, T. Kurakami, Reverse water gas shift reaction over molybdenum carbide, J. Chem. Eng. Jpn. 38 (2005) 807–812, https://doi.org/10.1252/jcej.38.807.
[156] X. Zhang, X. Zhu, L. Lin, S. Yao, M. Zhang, X. Liu, X. Wang, Y.-W. Li, C. Shi, D. Ma, Highly dispersed copper over β-Mo_2C as an efficient and stable catalyst for the reverse water gas shift (RWGS) reaction, ACS Catal. 7 (2017) 912–918, https://doi.org/10.1021/acscatal.6b02991.
[157] A.G. Kharaji, A. Shariati, M.A. Takassi, A novel γ-Alumina supported Fe-Mo bimetallic catalyst for reverse water gas shift reaction, Chin. J. Chem. Eng. 21 (2013) 1007–1014, https://doi.org/10.1016/S1004-9541(13)60573-X.
[158] Y. Ma, Z. Guo, Q. Jiang, K.H. Wu, H. Gong, Y. Liu, Molybdenum carbide clusters for thermal conversion of CO_2 to CO via reverse water-gas shift reaction, J. Energy Chem. (2020), https://doi.org/10.1016/j.jechem.2020.03.012.
[159] J. Gao, Y. Wu, C. Jia, Z. Zhong, F. Gao, Y. Yang, B. Liu, Controllable synthesis of α-MoC_{1-x} and β-Mo_2C nanowires for highly selective CO_2 reduction to CO, Catal. Commun. 84 (2016) 147–150, https://doi.org/10.1016/j.catcom.2016.06.026.
[160] T. Tatsumi, A. Muramats, H.O. Tominaga, Alcohol synthesis from CO_2/H_2 on silica-supported molybdenum catalysts, Chem. Lett. 14 (1985) 593–594, https://doi.org/10.1246/cl.1985.593.
[161] J.L. Dubois, K. Sayama, H. Arakawa, CO_2 hydrogenation over carbide catalysts, Chem. Lett. 21 (1992) 5–8, https://doi.org/10.1246/cl.1992.5.
[162] S. Liu, H. Zhou, Q. Song, Z. Ma, Synthesis of higher alcohols from CO_2 hydrogenation over Mo–Co–K sulfide-based catalysts, J. Taiwan Inst. Chem. Eng. 76 (2017) 18–26, https://doi.org/10.1016/j.jtice.2017.04.007.
[163] T. Tatsumi, A. Muramatsu, H.O. Tominaga, Supported molybdenum catalysts for alcohol synthesis from CO-H_2, Appl. Catal. 34 (1987) 77–88, https://doi.org/10.1016/S0166-9834(00)82447-1.
[164] R.G. dos Santos, A.C. Alencar, Biomass-derived syngas production via gasification process and its catalytic conversion into fuels by Fischer Tropsch synthesis: a review, Int. J. Hydrog. Energy (2019), https://doi.org/10.1016/j.ijhydene.2019.07.133. In press.
[165] M.A. Coronel-García, A.I. Reyes de la Torre, J.A. Melo-Banda, A.L. Martínez-Salazar, R. Silva Rodrigo, N.P. Díaz Zavala, B. Portales Martínez, J.M. Domínguez, Study of Co, Ru/SBA-15 type materials for Fischer–Tropsch synthesis in fixed bed tubular reactor: I. Effect of the high Ru content on the catalytic activity, Int. J. Hydrog. Energy 40 (2015) 17264–17271, https://doi.org/10.1016/j.ijhydene.2015.09.061.
[166] O.L. Eliseev, M.V. Tsapkina, P.E. Davydov, L.D. Dzhukasheva, A.L. Lapidus, Synthesis of hydrocarbons from carbon monoxide and hydrogen in the presence of cobalt catalysts promoted with cerium oxide, Solid Fuel Chem. 51 (2017) 166–169, https://doi.org/10.3103/S036152191703003X.
[167] M.K. Gnanamani, G. Jacobs, W.D. Shafer, B.H. Davis, Fischer–tropsch synthesis: activity of metallic phases of cobalt supported on silica, Catal. Today 215 (2013) 13–17, https://doi.org/10.1016/j.cattod.2013.03.004.
[168] S. Taghavi, A. Tavasoli, A. Asghari, M. Signoretto, Loading and promoter effects on the performance of nitrogen functionalized graphene nanosheets supported cobalt Fischer-Tropsch synthesis catalysts, Int. J. Hydrog. Energy 44 (2019) 10604–10615, https://doi.org/10.1016/j.ijhydene.2019.03.015.
[169] M. Lacroix, L. Dreibine, B. de Tymowski, F. Vigneron, D. Edouard, D. Bégin, P. Nguyen, C. Pham, S. Savin-Poncet, F. Luck, M.J. Ledoux, C. Pham-Huu, Silicon carbide foam composite containing cobalt as a highly selective and re-usable Fischer–Tropsch synthesis catalyst, Appl. Catal. Gen. 397 (2011) 62–72, https://doi.org/10.1016/j.apcata.2011.02.012.
[170] M. Zhao, C. Yan, J. Sun, Q. Zhang, Modified iron catalyst for direct synthesis of light olefin from syngas, Catal. Today 316 (2018) 142–148, https://doi.org/10.1016/j.cattod.2018.05.018.
[171] B. Todic, L. Nowicki, N. Nikacevic, D.B. Bukur, Fischer–tropsch synthesis product selectivity over an industrial iron-based catalyst: effect of process conditions, Catal. Today 261 (2016) 28–39, https://doi.org/10.1016/j.cattod.2015.09.005.
[172] K. Asami, K. Komiyama, K. Yoshida, H. Miyahara, Synthesis of lower olefins from synthesis gas over active carbon-supported iron catalyst, Catal. Today 303 (2018) 117–122, https://doi.org/10.1016/j.cattod.2017.09.010.
[173] H.M. Torres Galvis, K.P. de Jong, Catalysts for production of lower olefins from synthesis gas: a review, ACS Catal. 3 (2013) 2130–2149, https://doi.org/10.1021/cs4003436.
[174] Z.Z. Wang, W.F. Han, H.Z. Liu, Hydrothermal synthesis of sulfur-resistant MoS_2 catalyst for methanation reaction, Catal. Commun. 84 (2016) 120–123, https://doi.org/10.1016/j.catcom.2016.06.016.
[175] A.A. Andreev, V.J. Kafedjiysky, R.M. Edreva-Kardjieva, Active forms for water-gas shift reaction on NiMo-sulfide catalysts, Appl. Catal. Gen. 179 (1999) 223–228, https://doi.org/10.1016/S0926-860X(98)00321-4.
[176] A. Muramatsu, T. Tatsumi, H. Tominaga, Active species of molybdenum for alcohol synthesis from carbon monoxide-hydrogen, J. Phys. Chem. 96 (1992) 1334–1340, https://doi.org/10.1021/j100182a058.
[177] X.M. Wu, Y.Y. Guo, J.M. Zhou, G.D. Lin, X. Dong, H.B. Zhang, Co-decorated carbon nanotubes as a promoter of Co–Mo–K oxide catalyst for synthesis of higher alcohols from syngas, Appl. Catal. Gen. 340 (2008) 87–97, https://doi.org/10.1016/j.apcata.2007.09.051.
[178] Y. Lian, R. Xiao, W. Fang, Y. Yang, Potassium-decorated active carbon supported Co-Mo-based catalyst for water-gas shift reaction, J. Nat. Gas Chem. 20 (2011) 77–83, https://doi.org/10.1016/S1003-9953(10)60154-5.
[179] J. Ye, C. Liu, D. Mei, Q. Ge, Methanol synthesis from CO_2 hydrogenation over a Pd_4/In_2O_3 model catalyst: a combined DFT and kinetic study, J. Catal. 317 (2014) 44–53, https://doi.org/10.1016/j.jcat.2014.06.002.
[180] L.C. Grabow, M. Mavrikakis, Mechanism of methanol synthesis on Cu through CO_2 and CO hydrogenation, ACS Catal. 1 (2011) 365–384, https://doi.org/10.1021/cs200055d.
[181] B.H. Davis, Fischer–tropsch synthesis: reaction mechanisms for iron catalysts, Catal. Today 141 (2009) 25–33, https://doi.org/10.1016/j.cattod.2008.03.005.
[182] J.A. Schaidle, L.T. Thompson, Fischer–tropsch synthesis over early transition metal carbides and nitrides: CO activation and chain growth, J. Catal. 329 (2015) 325–334, https://doi.org/10.1016/j.jcat.2015.05.020.
[183] J.N. Zheng, K. An, J.M. Wang, J. Li, Y. Liu, Direct synthesis of ethanol via CO_2 hydrogenation over the Co/La-Ga-O composite oxide catalyst, J. Fuel Chem. Technol. 47 (2019) 697–708, https://doi.org/10.1016/S1872-5813(19)30031-3.
[184] B. Liu, B. Ouyang, Y. Zhang, K. Lv, Q. Li, Y. Ding, J. Li, Effects of mesoporous structure and Pt promoter on the activity of Co-based catalysts in low-temperature CO_2 hydrogenation for higher alcohol synthesis, J. Catal. 366 (2018) 91–97, https://doi.org/10.1016/j.jcat.2018.07.019.
[185] S. Zhang, X. Liu, Z. Shao, H. Wang, Y. Sun, Direct CO_2 hydrogenation to ethanol over supported Co_2C catalysts: studies on support effects and mechanism, J. Catal. 382 (2020) 86–96, https://doi.org/10.1016/j.jcat.2019.11.038.
[186] B. Ouyang, S. Xiong, Y. Zhang, B. Liu, J. Li, The study of morphology effect of Pt/Co_3O_4 catalysts for higher alcohol synthesis from CO_2 hydrogenation, Appl. Catal. Gen. 543 (2017) 189–195, https://doi.org/10.1016/j.apcata.2017.06.031.
[187] M.K. Gnanamani, H.H. Hamdeh, G. Jacobs, W.D. Shafer, S.D. Hopps, G. A. Thomas, B.H. Davis, Hydrogenation of carbon dioxide over K-promoted FeCo bimetallic catalysts prepared from mixed metal oxalates, ChemCatChem. 9 (2017) 1303–1312, https://doi.org/10.1002/cctc.201601337.
[188] K. Okabe, H. Yamada, T. Hanaoka, T. Matsuzaki, H. Arakawa, Y. Abe, CO_2 hydrogenation to alcohols over highly dispersed Co/SiO_2 catalysts derived from acetate, Chem. Lett. 30 (2001) 904–905, https://doi.org/10.1246/cl.2001.904.
[189] L. Wang, S. He, L. Wang, Y. Lei, X. Meng, F.S. Xiao, Cobalt–nickel catalysts for selective hydrogenation of carbon dioxide into ethanol, ACS Catal. 9 (2019) 11335–11340, https://doi.org/10.1021/acscatal.9b04187.
[190] L. Wang, L. Wang, J. Zhang, X. Liu, H. Wang, W. Zhang, Q. Yang, J. Ma, X. Dong, S.J. Yoo, J.-G. Kim, X. Meng, F.-S. Xiao, Selective hydrogenation of CO_2 to ethanol over cobalt catalysts, Angew. Chem. Int. Ed. 57 (2018) 6104–6108, https://doi.org/10.1002/anie.201800729.
[191] Z. He, Q. Qian, J. Ma, Q. Meng, H. Zhou, J. Song, Z. Liu, B. Han, Water-enhanced synthesis of higher alcohols from CO_2 hydrogenation over a Pt/Co_3O_4 catalyst under milder conditions, Angew. Chem. Int. Ed. 55 (2016) 737–741, https://doi.org/10.1002/anie.201507585.
[192] M. Schubert, S. Pokhrel, A. Thomé, V. Zielasek, T.M. Gesing, F. Roessner, L. Mädler, M. Bäumer, Highly active Co–Al_2O_3-based catalysts for CO_2 methanation with very low platinum promotion prepared by double flame spray pyrolysis, Catal. Sci. Technol. 6 (2016) 7449–7460, https://doi.org/10.1039/C6CY01252C.
[193] T. Das, G. Deo, Synthesis, characterization and in situ DRIFTS during the CO_2 hydrogenation reaction over supported cobalt catalysts, J. Mol. Catal. Chem. 350 (2011) 75–82, https://doi.org/10.1016/j.molcata.2011.09.008.
[194] R.E. Owen, J.P. O'Byrne, D. Mattia, P. Plucinski, S.I. Pascu, M.D. Jones, Cobalt catalysts for the conversion of CO_2 to light hydrocarbons at atmospheric pressure, Chem. Commun. 49 (2013) 11683–11685, https://doi.org/10.1039/C3CC46791K.
[195] M.K. Gnanamani, G. Jacobs, H.H. Hamdeh, W.D. Shafer, F. Liu, S.D. Hopps, G. A. Thomas, B.H. Davis, Hydrogenation of carbon dioxide over Co–Fe bimetallic catalysts, ACS Catal. 6 (2016) 913–927, https://doi.org/10.1021/acscatal.5b01346.
[196] M.K. Gnanamani, G. Jacobs, R.A. Keogh, W.D. Shafer, D.E. Sparks, S.D. Hopps, G. A. Thomas, B.H. Davis, Fischer-Tropsch synthesis: effect of pretreatment conditions of cobalt on activity and selectivity for hydrogenation of carbon dioxide, Appl. Catal. Gen. 499 (2015) 39–46, https://doi.org/10.1016/j.apcata.2015.03.046.
[197] M.L. Smith, N. Kumar, J.J. Spivey, CO adsorption behavior of Cu/SiO_2, Co/SiO_2, and CuCo/SiO_2 catalysts studied by in situ DRIFTS, J. Phys. Chem. C 116 (2012) 7931–7939, https://doi.org/10.1021/jp301197s.

[198] G. Jiao, Y. Ding, H. Zhu, X. Li, J. Li, R. Lin, W. Dong, L. Gong, Y. Pei, Y. Lu, Effect of La_2O_3 doping on syntheses of C_1–C_{18} mixed linear α-alcohols from syngas over the Co/AC catalysts, Appl. Catal. Gen. 364 (2009) 137–142, https://doi.org/10.1016/j.apcata.2009.05.040.

[199] K. Takeuchi, T. Matsuzaki, H. Arakawa, T. Hanaoka, Y. Sugi, Synthesis of C_2-oxygenates from syngas over cobalt catalysts promoted by ruthenium and alkaline earths, Appl. Catal. 48 (1989) 149–157, https://doi.org/10.1016/S0166-9834(00)80272-9.

[200] K. Takeuchi, T. Matsukaki, H. Arakawa, Y. Sugi, Synthesis of ethanol from syngas over Co-Re-Sr/SiO_2 catalysts, Appl. Catal. 18 (1985) 325–334, https://doi.org/10.1016/S0166-9834(00)84010-5.

[201] K. Takeuchi, T. Matsuzaki, T.A. Hanaoka, H. Arakawa, Y. Sugi, K. Wei, Alcohol synthesis from syngas over cobalt catalysts prepared from $Co_2(CO)_8$, J. Mol. Catal. 55 (1989) 361–370, https://doi.org/10.1016/0304-5102(89)80270-6.

[202] T. Matsuzaki, K. Takeuchi, T. Hanaoka, H. Arawaka, Y. Sugi, Effect of transition metals on oxygenates formation from syngas over Co/SiO_2, Appl. Catal. Gen. 105 (1993) 159–184, https://doi.org/10.1016/0926-860X(93)80246-M.

[203] T. Matsuzaki, K. Takeuchi, T. Hanaoka, H. Arakawa, Y. Sugi, Hydrogenation of carbon monoxide over highly dispersed cobalt catalysts derived from cobalt(II) acetate, Catal. Today 28 (1996) 251–259, https://doi.org/10.1016/0920-5861(95)00245-6.

[204] T. Matsuzaki, T. Hanaoka, K. Takeuchi, H. Arakawa, Y. Sugi, K. Wei, T. Dong, M. Reinikainen, Oxygenates from syngas over highly dispersed cobalt catalysts, Catal. Today 36 (1997) 311–324, https://doi.org/10.1016/S0920-5861(96)00224-6.

[205] G. Jacobs, T.K. Das, Y. Zhang, J. Li, G. Racoillet, B.H. Davis, Fischer–tropsch synthesis: support, loading, and promoter effects on the reducibility of cobalt catalysts, Appl. Catal. Gen. 233 (2002) 263–281, https://doi.org/10.1016/S0926-860X(02)00195-3.

[206] R. Zhang, G. Wen, H. Adidharma, A.G. Russell, B. Wang, M. Radosz, M. Fan, C_2oxygenate synthesis via Fischer–Tropsch synthesis on Co_2C and Co/Co_2C interface catalysts: How to control the catalyst crystal facet for optimal selectivity, ACS Catal. 7 (2017) 8285–8295, https://doi.org/10.1021/acscatal.7b02800.

[207] G. Prieto, A. Martínez, P. Concepción, R. Moreno-Tost, Cobalt particle size effects in Fischer–Tropsch synthesis: structural and in situ spectroscopic characterisation on reverse micelle-synthesised Co/ITQ-2 model catalysts, J. Catal. 266 (2009) 129–144, https://doi.org/10.1016/j.jcat.2009.06.001.

[208] G. Zhou, H. Liu, Y. Xing, S. Xu, H. Xie, K. Xiong, CO_2 hydrogenation to methane over mesoporous Co/SiO_2catalysts: Effect of structure, J. CO2 Util. 26 (2018) 221–229, https://doi.org/10.1016/j.jcou.2018.04.023.

[209] J. Graciani, K. Mudiyanselage, F. Xu, A.E. Baber, J. Evans, S.D. Senanayake, D. J. Stacchiola, P. Liu, J. Hrbek, J.F. Sanz, J.A. Rodriguez, Highly active copper-ceria and copper-ceria-titania catalysts for methanol synthesis from CO_2, Science 345 (2014) 546–550, https://doi.org/10.1126/science.1253057.

[210] Y.H. Zhao, K. Sun, X. Ma, J. Liu, D. Sun, H.Y. Su, W.X. Li, Carbon chain growth by formyl insertion on rhodium and cobalt catalysts in syngas conversion, Angew. Chem. Int. Ed. 50 (2011) 5335–5338, https://doi.org/10.1002/anie.201100735.

[211] F.S. Xiao, A. Fukuoka, M. Ichikawa, Mechanism of formation oxygenated compounds from CO+H_2 reaction over SiO_2-supported Ru-Co bimetallic carbonyl cluster-derived catalysts, J. Catal. 138 (1992) 206–222, https://doi.org/10.1016/0021-9517(92)90018-D.

[212] P.Y. Sheng, A. Yee, G.A. Bowmaker, H. Idriss, H_2 production from ethanol over Rh–Pt/CeO_2catalysts: the role of Rh for the efficient dissociation of the carbon–carbon bond, J. Catal. 208 (2002) 393–403, https://doi.org/10.1006/jcat.2002.3576.

[213] Z. He, Q. Qian, Z. Zhang, Q. Meng, H. Zhou, Z. Jiang, B. Han, Synthesis of higher alcohols from CO_2 hydrogenation over a PtRu/Fe_2O_3 catalyst under supercritical condition, Philos. Trans. R. Soc. Math. Phys. Eng. Sci. 373 (2015), 20150006, https://doi.org/10.1098/rsta.2015.0006.

[214] F.J. Caparrós, L. Soler, M.D. Rossell, I. Angurell, L. Piccolo, O. Rossell, J. Llorca, Remarkable carbon dioxide hydrogenation to ethanol on a palladium/iron oxide single-atom catalyst, ChemCatChem. 10 (2018) 2365–2369, https://doi.org/10.1002/cctc.201800362.

[215] R. Bliem, E. McDermott, P. Ferstl, M. Setvin, O. Gamba, J. Pavelec, M. A. Schneider, M. Schmid, U. Diebold, P. Blaha, L. Hammer, G.S. Parkinson, Subsurface cation vacancy stabilization of the magnetite (001) surface, Science 346 (2014) 1215–1218, https://doi.org/10.1126/science.1260556.

[216] S. Bai, Q. Shao, P. Wang, Q. Dai, X. Wang, X. Huang, Highly active and selective hydrogenation of CO_2 to ethanol by ordered Pd–Cu nanoparticles, J. Am. Chem. Soc. 139 (2017) 6827–6830, https://doi.org/10.1021/jacs.7b03101.

[217] D. Wang, Q. Bi, G. Yin, W. Zhao, F. Huang, X. Xie, M. Jiang, Direct synthesis of ethanol via CO_2 hydrogenation using supported gold catalysts, Chem. Commun. 52 (2016) 14226–14229, https://doi.org/10.1039/C6CC08161D.

[218] O.A. Ojelade, S.F. Zaman, M.A. Daous, A.A. Al-Zahrani, A.S. Malik, H. Driss, G. Shterk, J. Gascon, Optimizing Pd:Zn molar ratio in PdZn/CeO_2 for CO_2 hydrogenation to methanol, Appl. Catal. Gen. 584 (2019), 117185, https://doi.org/10.1016/j.apcata.2019.117185.

[219] A.S. Malik, S.F. Zaman, A.A. Al-Zahrani, M.A. Daous, H. Driss, L.A. Petrov, Development of highly selective PdZn/CeO_2 and Ca-doped PdZn/CeO_2 catalysts for methanol synthesis from CO_2 hydrogenation, Appl. Catal. Gen. 560 (2018) 42–53, https://doi.org/10.1016/j.apcata.2018.04.036.

[220] H. Kong, H.-Y. Li, G.-D. Lin, H.-B. Zhang, Pd-decorated CNT-Promoted Pd-Ga_2O_3 catalyst for hydrogenation of CO_2 to methanol, Catal. Lett. 141 (2011) 886, https://doi.org/10.1007/s10562-011-0584-4.

[221] J.J. Strohm, J. Zheng, C. Song, Low-temperature steam reforming of jet fuel in the absence and presence of sulfur over Rh and Rh–Ni catalysts for fuel cells, J. Catal. 238 (2006) 309–320, https://doi.org/10.1016/j.jcat.2005.12.010.

[222] A. Vita, C. Italiano, L. Pino, M. Laganà, V. Recupero, Hydrogen-rich gas production by steam reforming of n-dodecane. Part II: stability, regenerability and sulfur poisoning of low loading Rh-based catalyst, Appl. Catal. B Environ. 218 (2017) 317–326, https://doi.org/10.1016/j.apcatb.2017.06.059.

[223] H.H. Kung, Deactivation of methanol synthesis catalysts - a review, Catal. Today 11 (1992) 443–453, https://doi.org/10.1016/0920-5861(92)80037-N.

[224] A.S. Bambal, V.S. Guggilla, E.L. Kugler, T.H. Gardner, D.B. Dadyburjor, Poisoning of a silica-supported cobalt catalyst due to presence of sulfur impurities in syngas during Fischer–tropsch synthesis: effects of chelating agent, Ind. Eng. Chem. Res. 53 (2014) 5846–5857, https://doi.org/10.1021/ie500243h.

[225] Z. Li, J.-S. Choi, H. Wang, A.W. Lepore, R.M. Connatser, S.A. Lewis, H.M. Meyer, D.M. Santosa, A.H. Zacher, Sulfur-tolerant molybdenum carbide catalysts enabling low-temperature stabilization of fast pyrolysis bio-oil, Energy Fuels 31 (2017) 9585–9594, https://doi.org/10.1021/acs.energyfuels.7b01707.

[226] P.Y. Hou, H. Wise, Kinetic studies with a sulfur-tolerant methanation catalyst, J. Catal. 93 (1985) 409–416, https://doi.org/10.1016/0021-9517(85)90188-5.

[227] X. Jiang, X. Nie, X. Guo, C. Song, J.G. Chen, Recent advances in carbon dioxide hydrogenation to methanol via heterogeneous catalysis, Chem. Rev. 120 (2020) 7984–8034, https://doi.org/10.1021/acs.chemrev.9b00723.

[228] J. Wang, G. Li, Z. Li, C. Tang, Z. Feng, H. An, H. Liu, T. Liu, C. Li, A highly selective and stable ZnO-ZrO_2 solid solution catalyst for CO_2 hydrogenation to methanol, Sci. Adv. 3 (2017), e1701290, https://doi.org/10.1126/sciadv.1701290.

[229] O. Martin, A.J. Martín, C. Mondelli, S. Mitchell, T.F. Segawa, R. Hauert, C. Drouilly, D. Curulla-Ferré, J. Pérez-Ramírez, Indium oxide as a superior catalyst for methanol synthesis by CO2 hydrogenation, Angew. Chem. Int. Ed. 55 (2016) 6261–6265, https://doi.org/10.1002/anie.201600943.

[230] I. Sharafutdinov, C.F. Elkjær, H.W. Pereira de Carvalho, D. Gardini, G. L. Chiarello, C.D. Damsgaard, J.B. Wagner, J.-D. Grunwaldt, S. Dahl, I. Chorkendorff, Intermetallic compounds of Ni and Ga as catalysts for the synthesis of methanol, J. Catal. 320 (2014) 77–88, https://doi.org/10.1016/j.jcat.2014.09.025.